

**Identification of Factors That Establish
Asymmetry and Cell-death Fate
in the NSM lineage
in *Caenorhabditis elegans***

Julia Hatzold

München 2006

**Identification of Factors That Establish
Asymmetry and Cell-death Fate
in the NSM lineage
in *Caenorhabditis elegans***

Dissertation
an der Fakultät für Biologie
der Ludwig-Maximilians-Universität
München

vorgelegt von
Julia Hatzold
aus München

München, den 21. April 2006

Erstgutachter: Prof. Dr. Charles N. David

Zweitgutachter: Prof. Dr. Stefan Jentsch

Tag der mündlichen Prüfung: 30. Mai 2006

Table of Contents

Table of Contents.....	1
1 Abstract.....	5
2 Introduction.....	6
2.1 <i>C. elegans</i> represents an excellent model organism for studying development and programmed cell death.....	7
2.2 Cell death in <i>C.elegans</i>	7
2.3 The specification of cell death in the NSM sister cells.....	9
2.4 Thesis Aims.....	12
3 Material and Methods.....	13
3.1 Materials.....	13
3.1.1 Chemicals.....	13
3.1.2 Devices.....	14
3.1.3 Enzymes, antibodies, and standards.....	15
3.1.4 Kits.....	16
3.1.5 Bacteria strains.....	16
3.1.6 Plasmids and Vectors.....	17
3.1.6.1 Provided vectors and plasmids.....	17
3.1.6.2 Constructed plasmids.....	17
3.1.7 Oligonucleotides.....	19
3.1.8 <i>C. elegans</i> strains.....	21
3.1.8.1 Strains used in this study.....	21
3.1.8.2 Strains constructed in this study.....	23
3.2 Methods.....	26
3.2.1 Molecular biological methods.....	26
3.2.1.1 Protein purification.....	26
3.2.1.2 Electrophoretic mobility shift assays.....	27
3.2.1.3 Immunohistochemistry.....	27
3.2.1.4 RT-PCR analysis of <i>hlh-3</i> transcripts.....	28
3.2.2 Biological examinations of <i>C. elegans</i>	28
3.2.2.1 Generation of transgenic animals.....	28
3.2.2.2 RNAi experiments.....	29

3.2.2.2.1	RNAi by feeding as the method of delivering dsRNA	29
3.2.2.2.2	RNAi by injection as the method of delivering dsRNA	29
3.2.2.3	PCR-Screen for deletion mutants.....	30
3.2.2.4	EMS mutagenesis and <i>hlh-2(bx108)</i> enhancer screen	30
3.2.2.5	SNP mapping	31
3.3.3.6	Estimation of the cell size of NSM and NSM sister cells.....	31
4	Results.....	33
4.1	The NSM sister cell death is specified by asymmetric expression of the cell-death activator gene <i>egl-1</i>	33
4.2	Region B of the <i>egl-1</i> locus is required for <i>egl-1</i> expression in the NSM sister cells.....	35
4.3	Identification of factors that contribute to the killing of the NSM sister cells	37
4.3.1	Candidate gene approach	37
4.3.1.1	The <i>bHLH</i> gene <i>hlh-2</i> is required for the NSM sister cell death	39
4.3.1.2	<i>hlh-2</i> acts synergistically with <i>hlh-3</i> to kill the NSM sister cells	40
4.3.1.2.1	RNAi of <i>achaete-scute</i> -like <i>bHLH</i> genes	40
4.3.1.2.2	Isolation and characterization of <i>hlh-3</i> deletions.....	41
4.3.1.2.3	<i>hlh-2</i> and <i>hlh-3</i> are specifically required for the NSM sister cell death	43
4.3.1.2.4	Are HLH-2 and HLH-3 present in the NSM sister cell at the time it is dying?44	
4.3.1.2.4.1	Co-localization of EGL-1 and HLH-2 using antibody staining	44
4.3.1.2.4.2	The NSM and NSM sister cell can be identified due to their position within the embryo	46
4.3.1.2.4.3	<i>hlh-2::gfp</i> is expressed in the NSM and the NSM sister cell but not in the NSM mother cell.....	49
4.3.1.2.4.4	<i>hlh-3::gfp</i> is expressed in the NSM and the NSM sister cell but not in the NSM mother cell.....	49
4.3.1.2.5	HLH-2 and HLH-3 bind to Region B of the <i>egl-1</i> locus <i>in vitro</i>	50
4.3.1.2.6	HLH-2 and HLH-3 can induce ectopic <i>egl-1</i> expression.....	51
4.3.2	<i>hlh-2</i> enhancer screen	53

4.3.2.1	Summary of candidates.....	55
4.3.2.2	Analysis of the Ces phenotype of the identified mutants	56
4.3.2.3	Linkage analysis and characterization of the candidates.....	59
4.3.2.3.1	<i>bc97</i>	59
4.3.2.3.2	<i>bc211</i>	62
4.3.2.3.3	<i>bc213</i> and <i>bc214</i> represent new alleles of <i>ces-2</i>	63
4.3.2.3.3.1	<i>bc213</i> results in an early stop codon in the <i>ces-2</i> coding region	64
4.3.2.3.4	<i>bc240</i>	65
4.3.2.3.5	<i>bc241</i>	68
4.3.2.3.6	<i>bc242</i>	69
4.3.2.3.7	<i>bc252</i>	74
4.3.2.3.8	<i>bc260</i>	76
4.4	<i>dnj-11</i> is required for the NSM sister cell death.....	76
4.4.1	Cloning of <i>bc212</i> : <i>bc212</i> is a mutation in <i>dnj-11</i>	77
4.4.2	<i>dnj-11(bc212)</i> animals have a pleiotropic phenotype and <i>bc212</i> is most likely a missense mutation.....	83
4.4.2.1	<i>dnj-11(bc212)</i> results in a cold-sensitive NSM sister cell survival phenotype which is suppressed by a loss-of-function mutation in <i>ces-1</i>	84
4.4.2.2	<i>dnj-11</i> is not required for cell death in general.....	85
4.4.2.3	Reduction of <i>dnj-11</i> function results in morphological defects.....	87
4.4.2.4	<i>dnj-11(bc212)</i> causes slow growth and embryonic lethality	89
4.4.2.5	The broodsize of <i>dnj-11(bc212)</i> animals is strongly reduced.....	90
4.4.2.6	$P_{dnj-11}dnj-11::gfp$ is Expressed Ubiquitously, and DNJ-11::GFP Localizes to the Cytosol.....	90
4.4.2.7	<i>dnj-11</i> encodes a protein with a DnaJ domain and two Myb-like DNA binding domains and is a member of the MIDA1-like protein family...	92
4.4.2.8	<i>dnj-11</i> might be involved in establishing asymmetry during the division of the NSM mother cell.....	95
4.4.2.9	Analysis of the domains of DNJ-11 for their functional relevance in the NSM sister cell death.....	99
4.4.2.10	Are Hsp70 proteins involved in establishing the cell death fate of the NSM sister cell?	101
4.5	Identification of factors that repress <i>egl-1</i> expression in the NSMs.....	104

4.5.1	The <i>C. elegans</i> genome encodes two homologs of <i>ces-1</i> , which are candidates factors for acting redundantly with <i>ces-1</i>	104
4.5.2	<i>ces-1</i> might act in conjunction with <i>lin-22</i> , a <i>hairy</i> homolog.....	106
5	Discussion.....	108
5.1	<i>egl-1</i> is regulated at the transcriptional level, a mechanism that is conserved 108	
5.2	<i>hll-2</i> and <i>hll-3</i> are required for the NSM sister cell death.....	109
5.3	A forward genetic screen resulted in the isolation of at least six new genes involved in the cell-death fate of NSM sister cells.....	113
5.4	<i>dnj-11</i> might be required to establish asymmetry during the division of the NSM mother cell.....	114
5.5	CES-1 is involved in establishing asymmetry during the division of the NSM mother cell.....	115
5.6	DNJ-11 might establish asymmetry in the NSM mother cell by regulating CES-1 activity.....	117
6	References.....	122
	Abbreviations.....	129
	CURRICULUM VITAE.....	130

1 Abstract

During the development of a *C. elegans* hermaphrodite, 131 of the 1090 cells generated die due to programmed cell death, an important process conserved throughout the animal kingdom. Although a genetic pathway for programmed cell death has been established in *C. elegans*, not much is known about the signals that trigger cell death in cells destined to die. One particular cell-death event, the death of the NSM sister cell, occurs about 430 min after the first division of the zygote, just 20 min after its progenitor cell has undergone an asymmetric cell division. The sister of the NSM sister cell, the NSM, however, survives and differentiates into a serotonergic neuron located in the pharynx. Here, I show that the cell-death activator *egl-1* is expressed in the NSM sister cell, which is destined to die, but not in the surviving NSM. In addition, using a candidate gene approach, I found that in *hlh-2(bc108lf); hlh-3(bc248lf)* animals, 30% of the NSM sister cells survive. This observation suggests that the NSM sister cell death is at least partially dependent on the activity of *hlh-2* and *hlh-3*, which code for bHLH transcription factors. These and additional results suggest that *egl-1* expression is directly activated in the NSM sister cell by a heterodimer composed of HLH-2 and HLH-3, which binds to a specific *cis*-regulatory region of the *egl-1* locus.

In order to identify additional factors that contribute to the NSM sister cell death, I performed a forward genetic screen. In particular, I screened for mutations that enhance the NSM sister cell survival caused by *hlh-2(bc108)*. This screen resulted in the identification of mutations in at least six genes not previously implicated in this cell-death event. One of these mutations, *bc212*, is a loss-of-function mutation in the gene *dnj-11*. *dnj-11* codes for a protein with a J domain, which is found in chaperones, as well as two SANT domains, which are implicated in transcriptional regulation. *dnj-11* is an essential gene expressed in most if not all cells. Furthermore, it acts in the NSM sister cell death pathway by negatively regulating the activity of the *snail*-like gene *ces-1*. *dnj-11* is required for the ability of the NSM mother cell to divide asymmetrically. I propose that *dnj-11* promotes the death of the NSM sister cell by establishing polarity in the NSM mother cell. Moreover, I present evidence that the *snail*-like *ces-1* gene is involved in establishing polarity in the NSM mother cell as well, revealing a new function of *ces-1* in *C. elegans*.

2 Introduction

A fascinating aspect of animal development is the fact that, starting from one single cell, the zygote, a complex organism is generated with multiple types of cells. One important feature for obtaining cellular diversity is the process of asymmetric cell division, a division of a polar mother cell that creates distinct daughter cells by differential distribution of cell fate determinants. Studies in model systems like *Drosophila* and *Caenorhabditis elegans* have provided many insights into the conserved mechanisms of asymmetric cell division. During the development of the nematode *C. elegans*, already the first division occurs asymmetrically resulting in two different sized cells that are committed to two different fates. Later in the developing embryo, many cell divisions take place that give rise to a neuron or neuronal precursor and a cell that subsequently undergoes programmed cell death. Here, two indispensable developmental processes converge; programmed cell death or apoptosis is a fundamental feature of animal development to eliminate unwanted or potentially dangerous cells. Proper regulation of this physiological process is of crucial importance; lack of cell death can result in cancer and autoimmune diseases, whereas ectopic cell death has been associated with neurodegenerative diseases (Thompson, 1995; Vaux, 1993). The mechanisms of programmed cell death have been conserved through evolution. It is striking that in both invertebrate and vertebrate neurogenesis, superfluous neurons are removed by programmed cell death; for example, more than 50% of all neurons formed by neurogenesis in vertebrates are removed by programmed cell death before adulthood (reviewed by Oppenheim, 1991). On the other hand, during the development of a *C. elegans* hermaphrodite, 131 somatic cells die by programmed cell death, of which 105 are sisters of cells that differentiate into neurons. When prevented from dying, these cells can adopt a neuronal fate. Considering that the nervous system of a *C. elegans* hermaphrodite is composed of only 302 neurons, more than a quarter of the cells generated during development that have the potential to form neurons undergo programmed cell death.

2.1 *C. elegans* represents an excellent model organism for studying development and programmed cell death

The nematode *Caenorhabditis elegans* has been proven to be a suitable model organism for studying a great range of different biological processes. Besides the fact that it is easy and inexpensive to maintain in the laboratory, the only 1 mm long worm can be grown on agar plates with *E. coli* as food source, its short generation time of only 3 days and a broodsize of up to 300 make it a convenient model organism. *C. elegans* individuals are mainly hermaphrodites (XX animals), which can reproduce by self-fertilization; however, at low frequency, a spontaneous loss of the X chromosome at meiosis can result in XO males, which can fertilize hermaphrodites and therefore allow crosses between different strains. *C. elegans* is transparent making it possible to follow development at the cellular level even in the living individual (Wood, 1988). This is very suitable for studying programmed cell death; dying cells can be observed directly using Differential Interference Contrast (DIC) microscopy (Nomarski Optics) due to distinct morphological changes. The anatomical simplicity of this organism is another advantage: during the development of a *C. elegans* hermaphrodite exactly 1090 somatic cells are generated, of which 131 are determined to die and subsequently undergo programmed cell death. This lineage is essentially invariant, and therefore makes it possible to predict which cell is going to die at what time and position (Sulston and Horvitz, 1977; Sulston et al., 1983). Programmed cell death is not essential for the viability of *C. elegans*, unlike in many other animals (Ellis and Horvitz, 1986), which allowed the isolation and analysis of various cell death mutants.

2.2 Cell death in *C. elegans*

A major step towards our understanding about the mechanisms of programmed cell death has been made by genetic analyses in *C. elegans* (reviewed by (Horvitz, 1999)). A central cell death pathway has been established that is required for the killing of all cells destined to die during development. It is composed of four genes, namely *egl-1* (*egl*, egg-laying defective), *ced-9* (*ced*, cell-death defective), *ced-4* and *ced-3*. These four genes play a role in activating the apoptotic program in a cell that is destined to die, and they act in a simple genetic pathway, in which *egl-1* negatively regulates *ced-9*, *ced-9* negatively

regulates *ced-4*, and *ced-4* positively regulates *ced-3*, the activity of which is required for programmed cell death. These genes, when mutated, can block all cell death events taking place during development and therefore cause a Ced phenotype (Ced, cell-death defective). Interestingly, these genes are highly conserved throughout evolution, and their gene products fulfill similar functions in cell death in organisms as different as worms and humans.

The *ced-3* gene encodes a pro-caspase, *ced-4* an Apaf1-like adaptor, *ced-9* a Bcl-2-like cell-death inhibitor, and *egl-1* a pro-apoptotic member of the Bcl-2 family, a BH3-only protein. Based on genetic and cell biological observations, a model of how these factors interact, has been established. It suggests that CED-9, CED-4 and proCED-3 proteins are present in most if not all cells during *C. elegans* embryogenesis. The anti apoptotic CED-9 has been proposed to block the activity of the pro apoptotic CED-4 in cells that live, and it has been shown that CED-9 and CED-4 co-localize at the surface of mitochondria (Chen et al., 2000). In cells destined to die, EGL-1 is proposed to negatively regulate CED-9 by binding to CED-9 and thereby inducing a major conformational change of CED-9 (Yan et al., 2004), which in turn results in the release of CED-4 (Conradt and Horvitz, 1998; del Peso et al., 1998; Parrish et al., 2000). CED-4 then is proposed to mediate the self activation of the pro caspase CED-3 leading to cell death. Recently, a fifth gene, *drp-1* (*drp*, dynamin-related protein), has been identified that is involved in the activation of programmed cell death in *C. elegans*. *drp-1* codes for a dynamin-related protein and is required for mitochondrial fragmentation induced by the EGL-1/CED-9 heterodimer. Mitochondrial fragmentation has been suggested to enhance the pro-apoptotic activity of CED-4 and CED-3 (Jagasia et al., 2005). In mammals, mitochondria are known to be involved in the activation of caspases, and this work provided the first evidence that mitochondria play an important role in cell death also in the worm.

The active core machinery initiates the “execution phase”, in which the dying cell disassembles and gets phagocytosed by neighboring cells. DNA degradation has been shown to be important for the progression of the apoptotic process, and to date ten genes have been identified of being involved in the degradation of the DNA of an apoptotic cell. Apoptotic cells expose “eat-me” signals, which are recognized by neighboring cells to trigger phagocytosis. Two different pathways have been shown to promote the

engulfment of a dying cell. One pathway is defined by the genes *ced-1*, *ced-6*, and *ced-7*, which are acting most likely in the recognition of the cell corpse. Interestingly, only *ced-7* has been shown to be required in both dying and engulfing cell, whereas the other genes function in the engulfing cell. The second pathway consists of the genes *ced-2*, *ced-5*, *ced-10*, *ced-12*, and *psr-1*, regulating actin cytoskeleton rearrangement.

2.3 The specification of cell death in the NSM sister cells

To date, only little is known about how specific cells are instructed to die. It is of particular interest how the most upstream component of the central cell-death pathway, the BH3-only protein EGL-1, is regulated in particular cells that are destined to die. No factors have been identified that act upstream of *egl-1* being required for cell death in general; however, mutations in genes have been isolated that only affect specific cell deaths. For example, a mutation in the gene *tra-1* (*tra*, transformer) results in the block of the hermaphrodite-specific neurons (HSNs) in males (Conradt and Horvitz, 1999). The *tra-1* gene not only plays a role in cell death; *tra-1* functions as the terminal regulator of all somatic sexual fates in *C. elegans* (reviewed by (Goodwin and Ellis, 2002)). The *tra-1* gene product TRA-1A, a zinc-finger DNA-binding protein, has been shown to directly repress the transcription of *egl-1* in the HSNs of hermaphrodites but not in the HSNs of males. This shows that the activity of EGL-1 is regulated at the transcriptional level, at least in the case of the HSNs, in which the life-versus-death decision is determined by somatic sex (Conradt and Horvitz, 1999).

The majority of cell deaths occurring during *C. elegans* development, however, is not regulated by the somatic sex, but appears to be determined solely by the invariant cell lineage (Figure 2-1). One example is the cell-death event occurring in the NSM lineage. At about 410 min after the first division, the NSM mother cell divides asymmetrically and gives rise to two daughter cells; one differentiates into the NSM, a serotonergic motoneuron located in the anterior bulb of the pharynx, the NSM sister, on the other hand, undergoes programmed cell death shortly after the division (Figure 2-1). The two genes *ces-1* and *ces-2* (*ces*, cell death specification) have been identified that, when mutated, can block specifically the death of the NSM sister cells (Ellis and Horvitz, 1991). Genetically, *ces-1* and *ces-2* function upstream of *egl-1*. A loss-of-function (lf)

mutation in *ces-2* results in the survival of the NSM sister cells. On the contrary, this cell death is blocked by a gain-of-function (gf) mutation in *ces-1* suggesting that *ces-1* can act in preventing cells from undergoing cell death. A *ces-1(lf)* mutation causes no obvious phenotype; however, it suppresses the ability of the *ces-2(lf)* mutation to block the death of the NSM sister cells, from which can be concluded that *ces-2* causes the NSM sister cells to die by negatively regulating *ces-1*. Both genes encode transcription factors; CES-1 is a member of the Snail family of zinc-finger transcription factors (Metzstein and Horvitz, 1999), whereas the *ces-2* gene product is a DNA-binding protein most closely related to the proline- and acid-rich (PAR) subfamily of basic leucine-zipper (bZIP) transcription factors of vertebrates (Metzstein et al., 1996). Interestingly, *cis*-regulatory regions upstream of the *ces-1* transcription unit include a potential CES-2 binding site, which suggests that CES-2 might be a direct, negative regulator of *ces-1* transcription. Since the *ces-1(gf)* mutation is located adjacent to this potential CES-2 binding site, it might result overexpression of *ces-1* in NSM sister cells and thereby result in the negative regulation of *egl-1*. This hypothesis is supported by the observation that overexpression of *ces-1* from extrachromosomal arrays carrying the wild-type *ces-1* locus causes NSM sister cell survival (Metzstein and Horvitz, 1999).

Members of the Snail family of zinc-finger DNA-binding proteins act predominantly as repressors of transcription (reviewed by (Hemavathy et al., 2000)). An interesting candidate for a gene repressed by *ces-1* is therefore *egl-1*, the most upstream component of the central cell death pathway. Indeed, Snail-binding sites have been found in the *egl-1* regulatory region, to which CES-1 has been shown to bind *in vitro* and it has been proposed that the NSM sister cells die in *ces-1(gf)* mutants because ectopic CES-1 represses *egl-1* transcription (Thellmann et al., 2003).

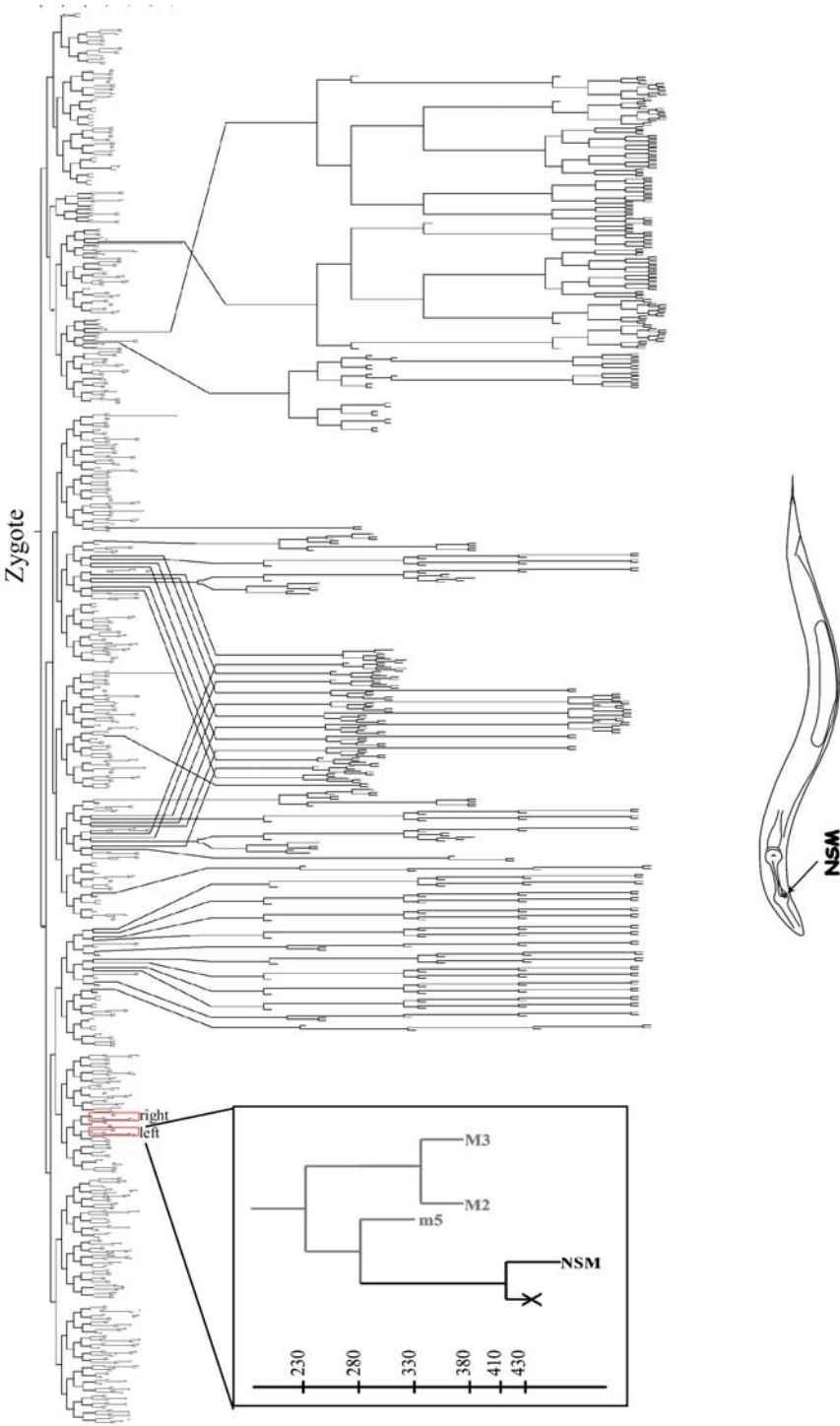


Figure 2-1 Schematic representation of the invariant cell lineage of a *C. elegans* hermaphrodite.

2.4 Thesis Aims

As described above, not much is known about the mechanisms that establish the cell death fate of the NSM sister cell. Here, different approaches are undertaken to gain information about factors that are required for the activation of the cell death machinery specifically in the NSMs. Of interest was how *egl-1*, the most upstream component of the central cell death pathway, is regulated; and the analysis of candidate genes allowed establishing a model of its activation. Furthermore, a forward genetic screen was performed to identify genes required for the NSM sister cell death. Candidates isolated in that screen might have mutation in genes required for the direct activation of *egl-1*, as well as genes required upstream, for example acting in establishing asymmetry during the division of the NSM mother cell.

Taken together, the aim of the thesis was to obtain insights about how an asymmetric cell division is created that results in one cell destined to survive and one cell subsequently undergoing cell death on the example of the NSM and NSM sister cell.

3 Material and Methods

3.1 Materials

3.1.1 Chemicals

Chemicals used in this study are listed in Table 3-1.

Table 3-1 Chemicals used in this study

Chemical	Company	Chemical	Company
2-Mercaptoethanol	Sigma	DMSO	Fisher
2-Propanol	Fisher	DNase	Roche
Acetic Acid, Glacial	Fisher	DTT (Dithiothreitol)	Sigma
Acetone	Fisher	ECL developing solution	Amersham Pharmacia
Acrylamide	Bio-Rad	EDTA di-Sodiumsalt	Fisher
Agar	Sigma	EMS	
Ammoniumchloride	Fisher	Ethidiumbromide	Fisher
Ammoniumpersulfate	Fisher	Ethyl Alcohol 95%	Aaper
Ammoniumsulfate	Fisher	Ethyl Alcohol absolute	Aaper
Ampicillin	Cellgro	Formide	Stkrm
Boric Acid		Gelatin	Fisher
Brilliant Blue R	Sigma	Glycerin	Fisher
BSA	Sigma	Glycine	Fisher
Calciumchloride	Fisher	Halocarbon Oil 700	Sigma
Chloroform	Fisher	Heparin Sodium	Acros
Cholesterol	Sigma	Hepes	Roche
Cholesterol	Sigma	Hydrochloric Acid 1N	Fisher
Citric Acid	Fisher	Hydrogen Peroxide 30%	Fisher
DAPI	Sigma	Imidazol	Qiagen
Dextrose	Fisher	IPEGAL CA360	Sigma
di-Potassium-hydrogen-phosphate	Sigma	IPTG	Roche Sigma

Chemical	Company	Chemical	Company
Kanamycine	Sigma	Potassiumacetat	Fisher
L-Leucine	Sigma	Potassiumchloride	Fisher
Lysozyme	Sigma	Potassiumdihydrogen-phosphate	Sigma
Lyticase	Sigma	Potassiumhydroxide Pellets	Fisher
Magnesiumchloride	Fisher	TEMED	Eurobio
Magnesiumsulfate	Fisher	Tetracylin	Eurobio
Methanol	Fisher	Triton X 100	Roth
Mineral Oil	Sigma	Trizol	
Nonidet P40	Sigma	Trypton	Difco
ONPG	Sigma	Tween 20	Sigma
Paraformaldehyde	Sigma	VectaShield	
Peptone	Fisher	X-Gal	Invitrogen
Phenol:Chloroform:Iso-amylalcohol (25:24:1)	Amresco	Yeast Extract	Fisher
Poly-L-lysine	Sigma	β -Mercaptoethanol	Sigma

3.1.2 Devices

In Table 3-2, important devices used in this study are listed.

Table 3-2 Devices

Devices	Company
Fluorescence- and light microscope, Axioskop 2,	Carl Zeiss
Light microscope Axiovert S100	Carl Zeiss
Stereo microscope MS5	Leica
stereo microscope with epifluorescence	Olympus
CCD Camera	Visitron
TCS NT confocal microscope	Leica

3.1.3 Enzymes, antibodies, and standards

Table 3-3 Enzymes

Enzymes	Company
Restriction enzymes	New England BioLabs
<i>T4</i> -Ligase	New England BioLabs
Alkaline Phosphatase	New England BioLabs
<i>Taq</i> -Polymerase	MBI Fermentas
Herculase	Stratagene Cloning Systems
Native <i>Pfu</i> -Polymerase	Stratagene Cloning Systems
Lysozym	Fisher Scientific
RNase	Boehringer
Proteinase K	Boehringer
Klenow	New England BioLabs
T7 RNA polymerase	New England BioLabs
T3 RNA polymeras	New England BioLabs

Table 3-4 Standards

Standards	Company
DNA-Standard 1kb DNA Ladder	GIBCO BRL Life Technologies
Kaleidoscope Prestained Standard	Bio-Rad
Prestained SDS-PAGE Standards Broad Range	Bio-Rad

Table 3-5 Antibodies

Antibodies	Host	Company, Reference
HIS (H-15)	Rabbit	Santa Cruz
GAM-HRP	Goat	Bio-Rad
alpha GFP	Mouse	Clontech
GAM-FITC	Goat	Clontech
GAR-Cy3	Goat	Dianova
HLH-2	Rabbit	(Krause et al., 1997)

3.1.4 Kits

Table 3-6 Kits used in this study

Kit	Company
Plasmid Kits	Qiagen
QIAquick Gel Extraction Kit	Qiagen
Ni-NTA Spin Kit	Qiagen
Bio-Rad protein assay	Bio-Rad
SuperScript TM III First Strand Synthesis System for RT-PCR	Invitrogen
DNeasy Tissue Kit	Qiagen

3.1.5 Bacteria strains

Table 3-7 Bacteria strains

Strain	Genotype	Reference
DH5	$\langle F^-$, <i>endA1</i> , <i>gyrA96</i> , <i>thi-1</i> , <i>hsdR17(rK-,mK+)</i> , <i>supE44</i> , <i>relA1</i> , λ 80d <i>lacZ</i> \square M15, \square (<i>lacZYA-argF</i>), U169	(Hanahan, 1985)
Epicurion Coli BL21Codon Plus TM (DE3)-RIL	B F^- <i>omp T</i> <i>hsdS</i> (rB- mB-) <i>dcm</i> +Tetr <i>gal</i> \square (DE3) <i>endA</i> Hte [<i>argU ileY leuW Camr</i>]	Stratagene, Amsterdam, Niederlande
HT115(DE3)	F^- , <i>mrcA</i> , <i>mrcB</i> , IN(<i>rrnDrrnE</i>) 1, <i>lambda-</i> , <i>rnc14::Tr10</i> (DE3 lysogen: <i>lavUV5 promoter - T7 polymerase</i>) (<i>RNAseIII minus</i>)	((Timmons et al., 2001)
OP50	<i>ura-</i>	(Brenner, 1974)
HB101	F^- Δ (<i>gpt-proA</i>)62 <i>leuB6</i> <i>glnV44</i> <i>ara-14</i> <i>galK2</i> <i>lacY1</i> Δ (<i>mcrC-mrr</i>) <i>rpsL20</i> (Strr) <i>xyl-5</i> <i>mtl-1</i> <i>recA13</i>	(Sambrook et al., 1989)

3.1.6 Plasmids and Vectors

3.1.6.1 Provided vectors and plasmids

The following vectors and plasmids were used in this thesis.

Table 3-8 Plasmids used in this study.

name	Description	reference	used for
pBC528	<i>dnj-11</i> minimal rescuing fragment with H129Q mutation and <i>gfp</i> inserted at <i>BsmI</i> site	Barbara Conradt	rescue experiments
pBC529	<i>dnj-11</i> minimal rescuing fragment with W456G mutation and <i>gfp</i> inserted at <i>BsmI</i> site	Barbara Conradt	rescue experiments
pBluescript KS+	II	Stratagene	plasmid construction
pRF4	contains the dominant <i>rol-6(su1006)</i> allele		co-injection marker
pKM1195	<i>hll-3</i> cDNA with His-tag	(Krause et al., 1997)	protein purification
pKM1199	<i>hll-2</i> cDNA with His-tag	(Krause et al., 1997)	protein purification
ppD95.02	open-ended <i>gfp</i> cassette (<i>unc-54</i> promoter)	Andy Fire	PCR template
ppD49.78	contains <i>hsp16-2</i> promoter	Andy Fire	plasmid construction
ppD93.97	$P_{myo-3gfp}$	Andy Fire	co-injection marker

3.1.6.2 Constructed plasmids

The following plasmids were constructed in this work.

Table 3-9 Plasmids constructed in this study.

name	cloning	used for
pBC123A	<i>Bam</i> HI fragment including <i>hll-2</i> cDNA (1.2 kB) of pKM 1199 subcloned into <i>Bam</i> HI site of pPD129.36	RNAi by feeding
pBC124A	<i>Bam</i> HI fragment including <i>hll-3</i> cDNA (869 kB) of pKM 1195 subcloned into <i>Bam</i> HI site of pPD129.36	RNAi by feeding
pBC188	456bp PCR-product of <i>hll-4</i> , with <i>Bam</i> HI ends	RNAi by feeding

name	cloning	used for
	(805 to 1260 of wormbase sequence), cloned into <i>Bam</i> HI sites of pPD129.36	
pBC189	343bp PCR-product of <i>hllh-6</i> with <i>Bam</i> HI ends (371 to 713 of wormbase sequence), cloned into <i>Bam</i> HI sites of pPD129.36	RNAi by feeding
pBC190	270bp PCR-product of <i>hllh-12</i> with <i>Bam</i> HI ends (525 to 794 of wormbase sequence), cloned into <i>Bam</i> HI sites of pPD129.36	RNAi by feeding
pBC191	304bp PCR-product of <i>hllh-14</i> with <i>Bam</i> HI ends (7 to 310 of wormbase sequence), cloned into <i>Bam</i> HI sites of pPD129.36	RNAi by feeding
pBC226	<i>hllh-3</i> <i>Bam</i> HI-fragment of pBC124A cloned into <i>Bam</i> HI site of pBS KSII+	in vitro transcription of RNA
pBC227	<i>hllh-4</i> <i>Bam</i> HI-fragment of pBC188 cloned into <i>Bam</i> HI site of pBS KSII+	in vitro transcription of RNA
pBC228	<i>hllh-6</i> <i>Bam</i> HI-fragment of pBC189 cloned into <i>Bam</i> HI site of pBS KSII+	in vitro transcription of RNA
pBC229	<i>hllh-12</i> <i>Bam</i> HI-fragment of pBC190 cloned into <i>Bam</i> HI site of pBS KSII+	in vitro transcription of RNA
pBC230	<i>hllh-14</i> <i>Bam</i> HI-fragment of pBC191 cloned into <i>Bam</i> HI site of pBS KSII+	in vitro transcription of RNA
pBC296	<i>hllh-2</i> cDNA in pPD49.78	generation of transgenic worms with heat shock inducible expression of <i>hllh-2</i>
pBC297	<i>Nhe</i> I/ <i>Sac</i> I fragment of <i>hllh-3</i> cDNA from pKM1199 cloned into <i>Nhe</i> I/ <i>Sac</i> I site of pPD49.78	generation of transgenic worms with heat shock inducible expression of <i>hllh-3</i>
pBC466	<i>Pvu</i> II <i>Bgl</i> II fragment of cosmid F38A4, containing the <i>dnj-11</i> locus, blunted, inserted into <i>Eco</i> RV site of pBS KSII+	transformation rescue experiments
pBC479	<i>gfp</i> coding region amplified by PCR with <i>Bsm</i> Igfp sense and antisense from pPD95.02; cloned into <i>Eco</i> RV site	plasmid construction
pBC484	<i>Eco</i> RV- <i>Hinc</i> II fragment was cut out of pBC466, remaining plasmid was religated	transformation rescue experiments
pBC486	PCR fragment containing the <i>bc212</i> mutation, amplified by <i>dnj-11</i> <i>Nco</i> I and <i>dnj-11</i> cDNA antisense1 from <i>bc212 bcIs25</i> worm lysis, cloned into <i>Eco</i> RV site of pBS KSII+	plasmid construction

name	cloning	used for
pBC503	PvuII/ <i>Nco</i> I fragment from pBC486 (contains <i>bc212</i>) and PvuII/ <i>Bsm</i> I fragment from pBC484 cloned into <i>Bsm</i> I/ <i>Nco</i> I backbone of pBC484	plasmid construction
pBC507	<i>Bsm</i> I fragment from pBC479 containing <i>gfp</i> cloned in frame into <i>Bsm</i> I site of pBC484	transformation rescue experiments
pBC508	<i>Bsm</i> I fragment from pBC479 containing <i>gfp</i> cloned in frame into <i>Bsm</i> I site of pBC503	transformation rescue experiments
pBC524	<i>gfp</i> fragment amplified by PCR from pPD95.02 with F548G <i>gfp</i> and <i>Bsm</i> Iantisense cloned into <i>Eco</i> RV site	plasmid construction
pBC530	<i>Bsm</i> I fragment containign <i>gfp</i> + F578G mutation in DNJ-11 (from pBC524) was cloned into <i>Bsm</i> I site of pBC484	transformation rescue experiments

3.1.7 Oligonucleotides

Oligonucleotides were designed with Vector NTI and ordered from Metabion, Martinsried, Germany, and IDT, Coralville, IA, respectively.

Table 3-10 Oligonucleotides

Oligo	Target	Sequence	used for
hllh-4sense	<i>hllh-4</i>	gaagggatcctgttctgaacaacatcttccaacg	plasmid construction
hllh-4antisense	<i>hllh-4</i>	gaagggatcccagttgatggtgatagaaatag	plasmid construction
hllh-6sense	<i>hllh-6</i>	gaagggatccaattccacattccaactcc	plasmid construction
hllh-6antisense	<i>hllh-6</i>	gaagggatcccaactgatgagctgaaaatt	plasmid construction
hllh-12sense	<i>hllh-12</i>	gaagggatccgccacctttacataattc	plasmid construction
hllh-12antisense	<i>hllh-12</i>	gaagggatccatataaacattggtttgggg	plasmid construction
hllh-14sense	<i>hllh-14</i>	gaagggatccctgagctcagattttcag	plasmid construction
hllh-14antisense	<i>hllh-14</i>	gaagggatcctgcgttctctctcatttctg	plasmid construction
ces-2antisense	<i>ces-2</i>	tgcaaaatattacaaagtgggttacag	sequencing of the <i>ces-2</i> locus
ces-2sense1	<i>ces-2</i>	tggactttcatagagcactatcgg	sequencing of the <i>ces-2</i> locus
ces-2sense2	<i>ces-2</i>	gatagtgtgaaagtaactagattaacgc	sequencing of the <i>ces-2</i> locus
ces-2sense3	<i>ces-2</i>	ccagtgcgaaatggccaatatcatag	sequencing of the <i>ces-2</i> locus
ces-2sense4	<i>ces-2</i>	agcaattctagtcaaaatagtcgccg	sequencing of the <i>ces-2</i> locus
ces-2sense5	<i>ces-2</i>	caacaaaagatacagaacagtcataac	sequencing of the <i>ces-2</i> locus
hllh-3A304	<i>hllh-3</i>	tgcggttgattataggggtttg	genotyping of <i>hllh-3(bc248)</i>
hllh-3antisense	<i>hllh-3</i>	gaattggatcacccgattattg	genotyping of <i>hllh-3(bc248)</i>
hllh-3sense1	<i>hllh-3</i>	atttctgaactcaagctcctgaaag	genotyping of <i>hllh-3(bc248)</i>
bx108sense	<i>hllh-2</i>	acaaggccctccatctctg	sequencing of <i>hllh-2(bc208)</i>
bx108antisense	<i>hllh-2</i>	acagcagtcgaacaattgcc	sequencing of <i>hllh-2(bc208)</i>
Y38H8.5sense	<i>Y38H8.5</i>	gaagggatcctcaaaactacggaacaaacg	SNP mapping
Y38H8.5antisense	<i>Y38H8.5</i>	gaagggatcctttctgatcctcgtgagtc	SNP mapping

Oligo	Target	Sequence	used for
C55C2.1sense	<i>C55C2.1</i>	gaagggatccctaccatagggcaatgtc	SNP mapping
C55C2.1antisense	<i>C55C2.1</i>	gaagggatccctgagtgagttggatggtg	SNP mapping
K02D7.2sense	<i>K02D7.2</i>	gaagggatccctaaaaacacattctctcc	SNP mapping
K02D7.2antisense	<i>K02D7.2</i>	gaagggatccctcgtaaagagattttgtgc	SNP mapping
C17H12antisense	<i>cosmid C17H12</i>	tgggacaagcgacgttgttg	SNP mapping
C17H12antisense2	<i>cosmid C17H12</i>	atatcccaaacacgcttttc	SNP mapping
C17H12sense	<i>cosmid C17H12</i>	cagcgacaacgacgttcagaag	SNP mapping
C17H12sense2	<i>cosmid C17H12</i>	tgtagtatttatatgtagcaaccg	SNP mapping
C17H12sense3	<i>cosmid C17H12</i>	aatatttacgtgagcctagc	SNP mapping
C01B10sense	<i>cosmid C01B10</i>	ttccgatttgcgattatttg	SNP mapping
C01B10antisense	<i>cosmid C01B10</i>	atatcccaaacacgcttttc	SNP mapping
C01B10sense2	<i>cosmid C01B10</i>	ccgatgaagtatttggtaac	SNP mapping
T22D1snpantisense	SNP <i>T22D1::35967</i>	tcacgcgatcacaaatattg	SNP mapping
T22D1snpsense	SNP <i>T22D1::35967</i>	caaaagtcgacattcaaatcc	SNP mapping
C43G2 snpantisense	SNP <i>C43G2::22057</i>	tcaatggcatttttagtactg	SNP mapping
C43G2 snpsense	SNP <i>C43G2::22057</i>	gggtatttttattatgtgttc	SNP mapping
K08B4antisense	SNP <i>K08B4::2299</i>	gtattccaatggcatatcga	SNP mapping
K08B4antisense2	SNP <i>K08B4::2299</i>	gttagctcagaaatcgactg	SNP mapping
K08B4sense	SNP <i>K08B4::2299</i>	ttccaattaatcccctcac	SNP mapping
K08B4sense2	SNP <i>K08B4::2299</i>	taacagcaggagtaccatc	SNP mapping
dele43antisense	<i>egl-1, region B</i>	ttgctgcaacatcatcac	genotyping of <i>egl-1(bc274)</i>
dele43sense	<i>egl-1, region B</i>	gaaaatttaggtggtggaag	genotyping of <i>egl-1(bc274)</i>
dele43wt	<i>egl-1, region B</i>	gttcaaaattggttcacag	genotyping of <i>egl-1(bc274)</i>
ZK381antisense	SNP <i>ZK381::5047</i>	tggctatttgcacatttacc	SNP mapping
ZK381sense	SNP <i>ZK381::5047</i>	agttatacctgtcagggttttac	SNP mapping
Y73antisense	SNPY73B6BR::24 51	gagaaaacacattgaaactc	SNP mapping
Y73sense	SNPY73B6BR::24 51	caacgagttctttattgtc	SNP mapping
R05G6antisense	SNP <i>R05G6::2917</i>	tttgacggatagctacatacg	SNP mapping
R05G6sense	SNP <i>R05G6::2917</i>	gggttcaaacatcgagc	SNP mapping
ok1228wt	<i>C55C2.1</i>	tgcaacgcatagtaagttg	genotyping of <i>C55C2.1(ok1228)</i>
hlh3cDNAantisense2	<i>hlh-3</i>	cctggcagtgagctgtgctg	<i>hlh-3</i> RT-PCR
hlh3cDNAsense2	<i>hlh-3</i>	gatcgttctggcaccatgtgac	<i>hlh-3</i> RT-PCR
BsmIgfantisense	<i>gfp of pPD95.02</i>	gaaggaatgcatcattttagtattcatcca	plasmid construction
BsmIgfpsense	<i>gfp of pPD95.02</i>	agcctgcattcgtcttcaagtatctcgttcaaatgagtaaag gagaagaac	plasmid construction
dnj-11antisense	<i>dnj-11</i>	tatttctcagattatgtccc	sequencing the of <i>dnj-11</i> locus
dnj-11cDNAantisense	<i>dnj-11 cDNA</i>	tcatttcttttttaacca	<i>dnj-11</i> RT-PCR
dnj-11cDNAantisense1	<i>dnj-11 cDNA</i>	aacgaatttctgcagatgtagc	<i>dnj-11</i> RT-PCR
dnj-11cDNAsense	<i>dnj-11 cDNA</i>	atgactacgggcaatttacaag	<i>dnj-11</i> RT-PCR
dnj-11NcoI	<i>dnj-11 locus</i>	atgttgtgactgcgtttaaacc	plasmid construction
dnj-11sense	<i>dnj-11</i>	taacgagcctaaatgtgatg	sequencing the of <i>dnj-11</i> locus
dnj-11seq1	<i>dnj-11</i>	cggcttcttttctttttttgtt	sequencing the of <i>dnj-11</i> locus
dnj-11seq2	<i>dnj-11</i>	ggatccttagcataagctatatca	sequencing the of <i>dnj-11</i> locus

Oligo	Target	Sequence	used for
ok1228sense	<i>C55C2.1</i>	tgtaattgggtgagagcag	genotyping of <i>C55C2.1(ok1228)</i>
ok1228antisense	<i>C55C2.1</i>	ttggcgttttgtgtctctg	genotyping of <i>C55C2.1(ok1228)</i>
C49H3sense	<i>C49H3</i>	ttgcagttcggagtgtcttatg	SNP mapping
C49H3antisense	<i>C49H3</i>	tggctcgggtgcaagtctattg	SNP mapping
C28C12sense	<i>C28C12</i>	cagaacaatgaccgagtcgag	SNP mapping SNP mapping
C28C12antisense	<i>C28C12</i>	agatttgccaattccaagtagc	SNP mapping SNP mapping
hlh3exon1antisense	<i>hlh-3</i>	gactgaacttttcagattgtctttg	<i>hlh-3</i> RT-PCR
F548Ggfp	<i>gfp</i>	agcctgcattctcgtggaagtagtctctggtcaaatgagtaaa ggagaagaac	plasmid construction
Y59H11ARantisense	<i>Y59H11AR</i>	cctagcgtttacagagaag	SNP mapping
Y59H11ARsense	<i>Y59H11AR</i>	ggacagtcgagagaagctag	SNP mapping
Y17G7B_3antisense	<i>Y17G7B.3</i>	gaaggatccttctctcaattggc	plasmid construction
Y17G7B_3sense	<i>Y17G7B.3</i>	gaaggatccataaaatgtctaccactcc	plasmid construction
F11F1_1antisense	<i>F11F1.1</i>	gaaggatccttcaatctctgaccgcc	plasmid construction
F11F1_1sense	<i>F11F1.1</i>	gaaggatccacgttaaacaataattggac	plasmid construction
F54C9_2antisense	<i>F54C9.2</i>	gaaggatccccgactgtttgagattaag	plasmid construction
F54C9_2sense	<i>F54C9.2</i>	gaaggatccaagaacgtatctctgaag	plasmid construction
T24H7_2antisense	<i>T24H7.2</i>	gaaggatccatctctcatgagcactctc	plasmid construction
T24H7_2sense	<i>T24H7.2</i>	gaaggatccccgagaaagctatacagttg	plasmid construction
T14G8_3antisense	<i>T14G8.3</i>	gaaggatccatctcagaagcttcacaac	plasmid construction
T14G8_3RNAisense	<i>T14G8.3</i>	gaaggatccccgtgaaggactctttatg	plasmid construction
F20C5antisense	<i>snp in F20C5</i>	gccttctcccgtgaaatc	plasmid construction
F20C5sense	<i>snp in F20C5</i>	tgctgagggttcatccaacatg	plasmid construction

3.1.8 *C. elegans* strains

C. elegans was cultured and maintained as described on NGM medium at 20°C unless otherwise noted (Brenner, 1974). The Bristol strain N2 was used as the standard wild-type strain.

3.1.8.1 Strains used in this study

Mutations used in this study are listed below and are described by (Riddle et al., 1997), except where noted otherwise. Strains were obtained from the „*C. elegans* Genetic Center“, University of Minnesota, USA, or obtained directly from the laboratory of their origin.

Table 3-11 *C. elegans* strains used in this study.

Strain	Genotype	Reference
CB3497	<i>dpy-25(e817sd)</i>	JHT
CB1259	<i>dpy-19(e1259ts,mat)</i>	DR
CB1275	<i>lin-1(e1275)</i>	

Strain	Genotype	Reference
MT8704	<i>ces-1(n703sd) ces-1(n1434)</i>	Mark Metzstein
MT8033	<i>unc-87(e1216) ces-1(n703sd)</i>	Mark Metzstein
MD122	<i>him-5(e1490)</i>	B. Conradt
MD165	<i>bcIs1; ced-3(n717)</i>	Sibylle Jäger
MT8738	<i>egl-1(n1084sd) egl-1(n3082) unc-76(e911)</i>	Barbara Conradt
MD436	<i>lin-15(n765ts) bcIs30</i>	Marion Thellmann
MD494	<i>ces-1(n703sd); bcIs25</i>	Marion Thellmann
MT372	<i>lin-22(n372)</i>	B. Horvitz
MD545	<i>ced-3(n717); bcIs37; lin-15(n765ts)</i>	B. Conradt
MD548	<i>unc-87(e1216) ces-1(n703sd); bcIs1</i>	B. Conradt
EM496	<i>hlh-2(bx108); him-5(e1490); lin-32(e1926)</i>	Doug Portman
EM497	<i>hlh-2(bx108); him-5(e1490)</i>	Doug Portman
MD1220	<i>egl-41(n1077cs,sd); bcIs9</i>	Stefanie Löser
MD1221	<i>ced-6(n2095); unc-42(e270) bcIs39</i>	Claus Schertel
MD1222	<i>ced-6(n2095); unc-42(e270) bcIs39; bc190</i>	Claus Schertel
MD1223	<i>dpy-5(e61); ced-6(n2095); bcIs39; bc202</i>	Claus Schertel
CB2167	<i>dpy-5(e61) unc-13(e1091am)</i>	
MT1374	<i>dpy-5(e61) unc-29(e1072am)</i>	CF
MT1748	<i>unc-26(e205) dpy-4(e1166sd)</i>	HE
CB2139	<i>dpy-10(e128) unc-4(e120)</i>	DR
MT5053	<i>ces-3(n1952)</i>	RE
MT8033	<i>unc-87(e1216) ces-1(n703sd)</i>	Mark Metzstein
MD165	<i>bcIs1; ced-3(n717)</i>	Sibylle Jäger
CB4856	Hawaii isolate	
AL103	<i>icIs103</i>	Ryan Doonan
RB1179	<i>C55C2.1(ok1228)</i>	OMRF Knockout Group / CGC
ZB137	<i>nIs83</i>	Monica Driscoll
MT1748	<i>unc-26(e205) dpy-4(e1166sd)</i>	HE
CB262	<i>unc-37(e262)</i>	
MT9657	<i>nIs97dm</i>	Mark Metzstein
MD1402	<i>egl-1(bc274)</i>	Gaby Sowa
MT10430	<i>lin-35(n745)</i>	Xiaowei Lu
OD58	<i>bcIs57</i>	Jon Audhya, UCSD

3.1.8.2 Strains constructed in this study

Table 3-12 *C. elegans* strains constructed in this study.

Strain name	genotype	constructed from
MD499	<i>unc-29(e193)</i> ; <i>bcIs30</i>	CB193 and MD436
MD512	<i>unc-5(e53)</i> <i>bcIs25</i>	MD422 and CB2223
MD527	<i>unc-29(e193)</i> ; <i>bcIs25</i>	CB193 and MD422
MD528	<i>ced-4(n1162)</i> ; <i>bcIs30</i>	MD436 and MT2547
MD530	<i>ces-1(n703sd)</i> <i>ces-1(n1434)</i> ; <i>bcIs30</i>	MD436 and MT8704
MD539	<i>ces-1(n703sd)</i> <i>ces-1(n1434)</i> ; <i>bcIs25</i>	MD422 and MT8704
MD583	<i>lin-1(e1275ts)</i> ; <i>bcIs30</i>	CB1275 and MD436
MD656	<i>hlh-2(bx108)</i> ; <i>bcIs25</i> ; <i>him-5(e1490)</i> ; <i>lin-32(e1926)</i>	EM496 and MD655
MD658	<i>hlh-2(bx108)</i> ; <i>bcIs25</i> ; <i>him-5(e1490)</i>	EM497 and MD656
MD661	<i>lin-22(n372)</i> ; <i>bcIs30</i>	MT372 and MD583
MD787	<i>unc-87(e1216)</i> <i>ces-1(n703sd)</i> ; <i>ced-3(n717)</i> ; <i>bcIs37</i> ; <i>lin-15(n765ts)</i>	MD545 and MT8033
MD896	<i>hlh-2(bx108)</i> ; <i>bcIs25</i>	MD658 and MD527
MD898	<i>dpy-19(e1259ts,mat)</i> ; <i>bcIs25</i>	MD422 and CB1259
MD899	<i>unc-29(e193)</i> ; <i>bcIs25</i> ; <i>dpy-11(e224)</i>	MD469 and MD527
MD1013	<i>unc-29(e193)</i> ; <i>dpy-20(e1282ts)</i> <i>bcIs25</i>	MD527 and MD466
MD1014	<i>unc-29(e193)</i> ; <i>dpy-25(e817sd)</i> ; <i>bcIs25</i>	CB3497 abd MD527
MD1015	<i>hlh-2(bx108)</i> ; <i>bcIs25</i> ; <i>dpy-11(e224)</i>	MD899 and MD896
MD1016	<i>hlh-2(bx108)</i> ; <i>dpy-20(e1282ts)</i> <i>bcIs25</i>	MD896 and MD1013
MD1017	<i>hlh-2(bx108)</i> ; <i>dpy-25(e817sd)</i> ; <i>bcIs25</i>	MD896 and MD1014
MD1018	<i>hlh-2(bx108)</i> ; <i>dpy-19(e1259ts,mat)</i> ; <i>bcIs25</i>	MD898 and MD896
MD1019	<i>rrf-3(pk1426)</i> ; <i>bcIs25</i>	MD465 and MD929
MD1020	<i>unc-87(e1216)</i> <i>ces-1(n703sd)</i> ; <i>bcIs1</i> ; <i>ced-3(n717)</i>	MD165 and MD548
MD1021	<i>hlh-2(bx108)</i> ; <i>bcIs25</i> ; <i>him-5(e1490)</i> ; <i>bc97</i>	MD658
MD1022	<i>hlh-2(bx108)</i> ; <i>bcIs25</i> ; <i>bc211</i>	MD896
MD1023	<i>hlh-2(bx108)</i> ; <i>bcIs25</i> <i>bc212</i>	MD896
MD1024	<i>hlh-2(bx108)</i> ; <i>bcIs25</i> ; <i>bc213</i>	MD896
MD1025	<i>hlh-2(bx108)</i> ; <i>bcIs25</i> ; <i>bc214</i>	MD896
MD1029	<i>hlh-2(bx108)</i> ; <i>unc-4(e120)</i> ; <i>bcIs25</i>	MD465 and MD896
MD1100	<i>dpy-10(e128)</i> <i>unc-4(e120)</i> ; <i>bcIs25</i>	CB2139 and MD422
MD1101	<i>hlh-2(bx108)</i> ; <i>bcIs25</i> ; <i>lon-2(e678)</i> <i>lin-15(n765ts)</i>	MD467 and MD896
MD1102	<i>unc-29(e193)</i> ; <i>lin-1(e1275ts)</i>	MD527 and MD583
MD1103	<i>unc-29(e193)</i> ; <i>bcIs25</i> ; <i>bc214</i>	MD1025 and MD527
MD1104	<i>bcIs25</i> ; <i>bc214</i>	MD1103 and MD422
MD1021	<i>hlh-2(bx108)</i> ; <i>bcIs25</i> ; <i>him-5(e1490)</i> ; <i>bc97</i>	MD658

Strain name	genotype	constructed from
MD1204	<i>bcIs1; ced-3(n717); bcEx279</i>	MD165
MD1224	<i>hlh-2(bx108); dpy-20(e1282ts) bcIs25; bc213</i>	MD1016 and MD1024
MD1225	<i>hlh-2(bx108); bcIs25; dpy-11(e224); bc211</i>	MD1015 and MD1022
MD1227	<i>hlh-2(bx108); bcIs25; dpy-11(e224); bc212</i>	MD1015 and MD1023
MD1228	<i>hlh-2(bx108); unc-4(e120); bcIs25; bc212</i>	MD1029 and MD1023
MD1233	<i>unc-29(e193); bcIs25; bc212</i>	MD527 and MD1023
MD1234	<i>hlh-2(bx108); bcIs25; dpy-11(e224); bc214</i>	MD1015 and MD1025
MD1236	<i>hlh-2(bx108); dpy-10(e128) unc-4(e120); bcIs25</i>	MD110 and MD896
MD1253	<i>hlh-3(bc248)</i>	N2
MD1410	<i>dpy-5(e61) hlh-2(bx108); bcIs25</i>	MD1235 and MD896
MD1411	<i>hlh-3(bc248); bcIs25</i>	MD422 and MD1253
MD1810	<i>K02D7.2(bc366) bcIs25</i>	MD422 and MD1812
MD1812	<i>K02D7.2(bc366)</i>	
MD1813	<i>hlh-2(bx108); unc-5(e53) dpy-20(e1282ts) bcIs25</i>	MD896 and MD1335
MD1814	<i>dpy-5(e61) unc-13(e1091am); bc212 bcIs25</i>	MD1407 and CB2167
MD1815	<i>hlh-2(bx108); unc-5(e53) bcIs25 bc242</i>	MD1813 and MD1208
MD1816	<i>hlh-2(bx108); dpy-20(e1282ts) bcIs25 bc242</i>	MD1813 and MD1208
MD1235	<i>dpy-5(e61) unc-29(e1072am); bcIs25</i>	MT1374 and MD422
MD1428	<i>hlh-2(bx108); bc97 ; bcIs25</i>	MD1021 and MD896
MD1412	<i>hlh-2(bx108); bcIs25; bc252</i>	MD896
MD1023	<i>hlh-2(bx108); bcIs25; bc212</i>	MD896
MD1413	<i>hlh-2(bx108); bcIs25; bc260</i>	MD896
MD1404	<i>hlh-2(bx108); bcIs25 bc212</i>	MD896 and MD1023
MD1226	<i>hlh-2(bx108); dpy-19(e1259ts,mat)</i>	
MD1405	<i>ces-2(bc213) ; bcIs25</i>	MD422 and MD1403
MD1468	<i>bcIs25</i>	MD422 and CB4856
MD1461	<i>unc-29(e193); lin-22(n372); bcIs30</i>	MD661 and MD1102
MD1467	<i>ces-1(n703sd) ces-1(n1434); lin-1(e1275ts); bcIs30</i>	MD530 and MD1102
MD1463	<i>dpy-5(e61) hlh-2(bx108); bcIs25; bc242</i>	MD1410 and MD1208
MD1466	<i>dpy-5(e61) hlh-2(bx108); bcIs25; bc252</i>	MD1410 and MD1412
MD1406	<i>unc-29(e193); bcIs25; bc212</i>	MD527 and MD1023
MD1407	<i>bcIs25; bc212</i>	MD422 and MD1406
MD1423	<i>bcIs25 unc-5(e53) bc212 dpy-20(e1282ts)</i>	MD1409 and MD1016
MD1427	<i>hlh-2(bx108); bcIs25; him-5(e1490); bc211</i>	MD1022 and MD658
MD1462	<i>hlh-2(bx108); hlh-3(bc248); bcIs25</i>	MD896 and MD1411
MD1464	<i>dpy-5(e61) hlh-2(bx108); bcIs25; bc240</i>	MD1410 and MD1206
MD1465	<i>hlh-2(bx108); bcIs25 unc-5(e53) dpy-20(e1282ts)</i>	MD896 and MD1423
MD1881	<i>hlh-3(bc277)</i>	MD1481 and N2
MD1882	<i>hlh-3(bc277); bcIs25</i>	MD422 and

Strain name	genotype	constructed from
MD1900	<i>hlh-2(bx108); unc-26(e205) bc240 bcIs25</i>	MD1206 and MT1748
MD1901	<i>hlh-2(bx108); bcIs25 bc240</i>	MD896 and MD1206
MD1902	<i>hlh-2(bx108); bcIs25 bc242</i>	MD896 and MD1208
MD1904	<i>dpy-5(e61) unc-13(e1091am); K02D7.2(bc366) bcIs25</i>	MD1810 and CB2167
MD1905	<i>hlh-2(bx108); unc-26(e205) bc240 bcIs25 dpy-4(e1166sd) IV</i>	MD1900 & MD1910
MD1906	<i>hlh-2(bx108); unc-30(e191) bcIs25 dpy-4(e1166sd)</i>	MD896 and MD1907
MD1907	<i>unc-30(e191) bcIs25 dpy-4(e1166sd)</i>	MD498 and MD507
MD1908	<i>ces-1(n703sd) ces-1(n1434); K02D7.2(bc366) bcIs25</i>	MD539 and MD1904
MD1909	<i>C55C2.1(ok1228); bcIs25</i>	MD422 and RB1179
MD1910	<i>hlh-2(bx108); bc240 bcIs25 dpy-4(e1166sd)</i>	MD1206 and MT1748
MD1888	<i>unc-29(e193); bcIs25; bc211</i>	MD1022 and MD527
MD1889	<i>hlh-2(bx108); bcIs25; dpy-11(e224); bc260</i>	MD1413 and MD1015
MD1890	<i>bcIs25; bc211</i>	MD422 and MD1888
MD1892	<i>bcIs25; egl-1(bc274)</i>	MD1402, N2 and MD422
MD1894	<i>egl-1(bc274)</i>	MD1402 and N2
MD1896	<i>hlh-2(bx108); unc-5(e53) bc240 bcIs25</i>	MD1813 and MD1901
MD1898	<i>hlh-2(bx108); bcIs25; bc241</i>	MD1207 and MD896
MD1911	<i>hlh-2(bx108); unc-4(e120); bcIs25; bc260</i>	MD1029 and MD1413
MD1912	<i>hlh-3(bc248); bc212 bcIs25</i>	MD1407 and MD1411
MD1914	<i>dpy-5(e61) hlh-2(bx108); bcIs25; bc241</i>	MD1410 and
MD1915	<i>dpy-5(e61) hlh-2(bx108); bcIs25; bc97</i>	MD1410 and MD1428
MD2098	<i>hlh-2(bx108); unc-26(e205) dpy-4(e1166sd)</i>	MT1748 and MD986
MD2157	<i>ces-1(n703sd) ces-1(n1434); bc212 bcIs25</i>	MD1814 and MD539
MD2158	<i>ces-1(n703sd) ces-1(n1434) C55C2.1(ok1228); bcIs25</i>	MD539 and
MD2159	<i>unc-5(e53) bc212</i>	MD1423 and N2
MD2161	<i>unc-37(e262); bcIs25</i>	CB262 and MD422
MD2162	<i>unc-29(e1072am) dpy-5(e61) C55C2.1(ok1228); bcIs25</i>	MD1235 and MD1909
MD2165	<i>hlh-2(bx108) C55C2.1(ok1228); bcIs25</i>	MD896 and MD2162
MD2166	<i>hlh-2(bx108); unc-5(e53) bc242 dpy-20(e1282ts) bcIs25</i>	MD1815 and MD1816
MD2169	<i>hlh-2(bx108); hlh-3(bc277); bcIs25</i>	MD896 and MD1882
MD2184	<i>dpy-9(e12) unc-17(e245) bcIs25</i>	MT628 and MD422
MD2187	<i>ced-4(n1162); unc-5(e53) dnj-11(bc212)</i>	MD1602 and MD2159
MD2189	<i>lin-35(n745); bcIs25</i>	MT10430 and MD1235
MD2204	<i>C55C2.1(ok1228); bcIs25</i>	N2, MD422 and RB1179

Strain name	genotype	constructed from
MD2218	<i>bcIs57; dnj-11(bc212) bcIs25</i>	MD1407 and OD58
MD2219	<i>dnj-11(bc212) bcIs25 / nT1</i>	MD1407 and MT13172
MD2221	<i>dnj-11(bc212) bcIs25; dtIs372</i>	MD1407 and IN373
MD2222	<i>ces-1(n703sd); bcIs57</i>	MT1507 and OD58
MD2223	<i>dnj-11(bc212) bcIs25; nIs106</i>	MT9970 and MD1407
MD2224	<i>dnj-11(bc212) bcIs25; bcEx512</i>	MD1407
MD2225	<i>bcEx512</i>	N2 and MD2224

3.2 Methods

3.2.1 Molecular biological methods

Standard molecular biology protocols were performed as essentially described in (Sambrook et al., 1989).

3.2.1.1 Protein purification

Expression plasmids for His₆-HLH-2 (pKM1199) and His₆-HLH-3 (pKM1195) fusion proteins were provided by M. Krause (Krause et al., 1997). His₆-HLH-2 and His₆-HLH-3 fusion proteins were produced in *E. coli* strain BL21-CodonPlus(DE3)-RIL (Stratagene). The cells were induced with 0.5 mM IPTG at the OD₆₀₀ of ~ 0.4. After 2.5 h at 37°C, cells were harvested. Proteins were purified under native conditions using the Qiagen Ni-NTA Spin Kit following the manufacturers instructions for soluble proteins. 5.0 ng and 3.2 ng of His₆-HLH-2 and His₆-HLH-3 fusion protein, respectively, represents 1×10⁻¹³ mol. The purity and concentration of the fusion proteins were assessed by SDS-PAGE and the BioRad protein assay (BioRad). The protein solution was dialysed into Buffer B.

Buffer B

25 mM HEPES (pH 7.5)

20 mM KCl

1 mM DTT

6 mM MgCl₂

10% Glycerol

1 mM EDTA

3.2.1.2 Electrophoretic mobility shift assays

DNA probes were generated by PCR amplification in the presence of 10 μ Ci [32 P]-dATP using the primers 5'-aac tca tcc acg tca cca aa-3' and 5'-ttg tcc act cgt tta cca ca-3' and plasmids pBC08 (wild-type), pBC181 (Snail-/E-box-) or pBC182 (Snail-/E-box+) as templates. The labeled PCR products were purified on a 6% acrylamide/TBE gel. EMSAs were performed as described by Krause et al., 1997).

Binding was quantified using a phosphoimager (Fujifilm BAS-2500) and appropriate software (Aida Image Analyzer V. 3.21).

3.2.1.3 Immunohistochemistry

Embryos were prepared in 10 μ l H₂O on polyL-Lysine coated slides and allowed to develop until the 1.5 fold stage in a moist chamber. They were fixed in 10 μ l of 5% PFA with a cover slip placed on top, incubated for 20 minutes in a moist chamber and frozen in liquid N₂. The cover slip was removed and the slides were incubated in -20°C methanol for 10 min. The specimens were re-hydrated to 1xTTBS (100mM Tris, pH7.5, 0.9% NaCl, 0.1% Tween-29) through a step-wise series of room-temperated methanol:TTBS (9:1, 7:3, 1:1 and 1:4 for 10 min each). The slides were incubated overnight with a 1:500 dilution of antibody in TTBS (rabbit α HLH-2, (Krause et al., 1997)) and a 1:100 dilution (mouse α GFP (Clontech), respectively. After washing them three times with TTBS at 37°C, they were incubated with a 1:200 dilution of secondary antibody Cy3 (donkey against rabbit) and FITC (goat α mouse) for 2 hours in the dark. Afterwards they were washed again three times with TTBS at 37°C and subsequently stained with 1 μ g/ml DAPI (in PBS), 1:1 diluted with vectashield. The slides were sealed and analyzed using a Leica TCS NT confocal microscope.

Poly-L-Lysin

heat 50 ml dH₂O to 60°C

add 100 mg gelatine

cool down to 40°C

add 10 mg CrK(SO₄)₂·12H₂O (Sigma, C-5926)

Take 10 ml of this solution (discard the rest) and add 10 mg Poly-L-Lysin

Put the solution in the fridge overnight and use it the next day. Stable for add 5 ml 10 x PBS about 2 months @ 4°C.

Fixative (5% paraformaldehyde in 0.5 x PBS)

5 g PFA
 add 50 ml ddH₂O
 add 1 ml 1 M NaOH
 stir on heating block (~65°C) until PFA is dissolved
 adjust to pH 7.4 with 1 M HCl (~1 ml)
 adjust to 100 ml with ddH₂O
 filter through a 0.45 µm pore filter
 store aliquots at -20°C

3.2.1.4 RT-PCR analysis of *hllh-3* transcripts

Total RNA was isolated from embryos of the indicated genotype, using the standard TRIZOL method (Burdine and Stern 1996). cDNA was made using the Invitrogen SuperScriptTMIII First Strand Synthesis System for RT-PCR. cDNA was used as a template for a PCR reaction with the appropriate primers.

3.2.2 Biological examinations of *C. elegans***3.2.2.1 Generation of transgenic animals**

Germline transformation was performed as described by (Mello and Fire, 1995). Cosmids and plasmids were injected in the appropriate strain with a concentration shown in Table 3-13.

Table 3-13 Generation of transgenic animals

Plasmid/Cosmid	Concentration	Co injection marker	Concentration	injected strain
pBC296, pBC297	50 ng/µl each	pRF4 (<i>rol-6(su1006)</i>)	50 ng/µl	<i>bcIs1; ced-3(n717)</i>
Y37B6	50 ng/µl	pPD93.97 (<i>P_{myo-3gfp}</i>)	50 ng/µl	<i>bc212 bcIs25</i>
C43G2	10 ng/µl	pPD93.97 (<i>P_{myo-3gfp}</i>)	50 ng/µl	<i>bc212 bcIs25</i>
F38A5	10 ng/µl	pPD93.97 (<i>P_{myo-3gfp}</i>)	50 ng/µl	<i>bc212 bcIs25</i>
F15B10	10 ng/µl	pPD93.97 (<i>P_{myo-3gfp}</i>)	50 ng/µl	<i>bc212 bcIs25</i>
C01B10	10 ng/µl	pPD93.97 (<i>P_{myo-3gfp}</i>)	50 ng/µl	<i>bc212 bcIs25</i>
pBC466	10 ng/µl	pPD93.97 (<i>P_{myo-3gfp}</i>)	50 ng/µl	<i>bc212 bcIs25</i>
pBC484	10 ng/µl	pRF4	50 ng/µl	<i>bc212 bcIs25</i>
pBC508	10 ng/µl	pRF4	50 ng/µl	<i>bc212 bcIs25</i>

Plasmid/Cosmid	Concentration	Co injection marker	Concentration	injected strain
pBC507	10 ng/μl	pRF4	50 ng/μl	<i>bc212 bcIs25</i>
pBC528	10 ng/μl	pRF4	50 ng/μl	<i>bc212 bcIs25/nT1</i>
pBC529	10 ng/μl	pRF4	50 ng/μl	<i>bc212 bcIs25/nT1</i>
pBC530	10 ng/μl	pRF4	50 ng/μl	<i>bc212 bcIs25/nT1</i>

3.2.2.2 RNAi experiments

3.2.2.2.1 RNAi by feeding as the method of delivering dsRNA

Plasmids containing the sequence of interest flanked by two *T7*-promoters were transformed into the *E. coli* strain HT115 (Timmons et al., 2001). NGM plates containing 6 mM IPTG, 50 μg/ml ampicillin and 12.5 μg/ml tetracycline were inoculated with transformed HT115 bacteria. The expression of dsRNA was induced overnight at room temperature. The plates were subsequently inoculated with L4 larvae. Animals were cultured at the specific temperature and their progeny was analyzed.

3.2.2.2.2 RNAi by injection as the method of delivering dsRNA

The sequences of interest were cloned into the pBluescript vector to create a sequence flanked by the *T3* and *T7* promoter. The fragments were amplified by PCR using the primers M13/20 and M13/rev. 20% of the PCR products were used as templates for *in vitro* transcription using the *T3* and *T7* polymerases. Reactions contained 100 U *T3* or *T7* polymerase, 2 mM each rATP, rCTP, rGTP, rUTP, 10 mM DTT in a final volume of 100 μl in DEPC-H₂O buffered with transcription buffer. After incubating for 2 hours at 37°C, five units DNase were added and the reaction incubated for another 20 minutes at 37°C. The RNA was purified by phenol/chloroform extraction and resuspended in 20 μl DEPC-H₂O.

Single stranded RNA obtained through *T7 in vitro* transcription was annealed with an equal amount of the corresponding *T3* RNA at 37°C for 20 minutes, centrifuged at 4°C for 10 minutes and injected into the gonad of young adult worms. The progeny was analyzed for NSM sister cell survival.

3.2.2.3 PCR-Screen for deletion mutants

Genomic DNA pools from mutagenized animals were screened for deletions as described by (Jansen et al., 1997). Deletion mutants were identified by nested PCR. Candidates were thawed from frozen stocks, and surviving animals were picked at the L3 – L4 stage into 50 µl of S-Basal with 0.5% HB101 bacteria in 96 well plates. 96 well plates were incubated in a moist chamber at 20°C. After they had been starved, 12.5 µl worm suspension was added to 12.5 µl 2X Worm Lysis Buffer in 96 well plates. Worm lysis was performed at 60°C for 2 h and subsequently 90°C for 20 min. 0.5 µl template was used for a nested PCR reaction to identify the deletion. Mutants were outcrossed to N2 at least four times prior to use.

2X Worm Lysis Buffer

100 mM KCl

20 mM Tris pH8.2

5 mM MgCl₂

0.9% IGEPAL

0.9% Tween 20

0.02 % gelatin

before use: 9 µl/ml of 20 mg/ml proteinase K was added

3.2.2.4 EMS mutagenesis and *hlh-2(bx108)* enhancer screen

100 to 200 L4 larva with the genotype *hlh-2(bx108); bcIs25* were washed off a medium plate and resuspended in 3 ml M9 buffer in a 15ml canonical tube. In an additional tube, 10 –20 µl EMS (23,5 – 47 mM) were mixed with 1 ml M9. The EMS solution was added to the worms. Worms were incubated for 4 h. Afterwards worms were washed 2x with each 4 ml M9 and transferred to a new plate inoculated with bacteria. The animals were allowed to recover over night. Each 10 mutagenized animals were transferred to a large plate and cultured at 15°C or 20°C. The F1 L4 larvae were transferred clonally to small plates and cultured at 25°C. The F2 progeny was allowed to develop until the adult stage, in which animals form “bags”. “Bags” containing the F3 progeny were mounted on agarose-coated slides and screened for F3 populations with an enhanced NSM sister cell survival phenotype using a epifluorescence microscope. Candidate bags were recovered on small plates.

M9 buffer

3.2.2.5 SNP mapping

N2 animals were crossed with Hawaii males. In the F2 generation, recombinants were isolated and homozygosed for the recombinant chromosome. SNPs (single nucleotide polymorphism) between the Bristol isolate (N2) and the Hawaii isolate are reported in the database http://genome.wustl.edu/gsc/Projects/C_elegans/SNP/. SNPs can alter restriction enzyme sites and can be easily detected using PCR amplification and subsequent restriction digestion. SNPs that do not alter restriction enzyme sites were detected by sequencing. DNA was isolated from animals by worm lysis and used as a template to amplify PCR fragments. SNPs used in this study are listed in Table 3-14.

Table 3-14 SNPs between the Bristol and Hawaii isolate of *C. elegans* used in this study.

SNP	map position	restriction enzyme	digest in
C31H1 at position 4110	2.36	<i>HpyCH4IV</i>	Hawaii
K08B4 at position 2299	2.98	<i>PfFI</i>	Hawaii
Y73B6BR at position 2451	3.21	<i>DraI</i>	N2
F38A5 at position 19715	3.21	<i>XbaI</i>	Hawaii
C43G2 at position 22057	3.21	SNP was identified by sequencing	
C17H12 at position 33927	3.24	SNP was identified by sequencing	
T22D1 at position 35967	3.25	SNP was identified by sequencing	
ZK381 at position 5047	3.26	<i>PvuII</i>	Hawaii
R05G6 at position 2917	3.34	<i>PstI</i>	Hawaii
C49H3 at position 3770	3.49	<i>DraI</i>	N2
C28C12 at position 30229	3.85	<i>MboI</i>	Hawaii
Y59H11AR at position 5541	3.90	<i>RsaI</i>	Hawaii
F20C5 at position 24865	3.96	<i>SfaNI</i>	N2
C01F6 at position 7442	4.06	<i>NsiI</i>	Hawaii

3.3.3.6 Estimation of the cell size of NSM and NSM sister cells

The outline of cells was identified using an integrated *gfp* marker that labels cell membranes (*bcIs57*). Epifluorescence was detected using a Fluorescence- and light microscope (Zeiss) with a CCD camera (Visitron). The NSM mother cell in an embryo was identified by position. About 10 to 15 minutes after it started dividing, the NSM and NSM sister cell can be detected. A stack through the embryo was taken with a Z distance of 0.25 μm between different focal planes. The area of the NSM and the NSM sister cell was determined in each plane by circling the outline of the cell as

detected with epifluorescence. The size of the area was measured using the Metamorph program. The areas of each plane were added. The sum of the NSM sister cell area was divided by the sum of the NSM area, in order to determine the ratio between the two cells.

4 Results

During the development of a *C. elegans* hermaphrodite, at about 420 minutes after the first cleavage, one particular cell division takes place in the left as well as in the right NSM lineage, which is asymmetric. Each of the two cell divisions gives rise to two daughter cells, one of them differentiates into a pharyngeal neurosecretory motorneuron, the NSM, the other cell, the NSM sister cell, dies about 20 minutes later due to programmed cell death (Sulston et al., 1983).

4.1 The NSM sister cell death is specified by asymmetric expression of the cell-death activator gene *egl-1*

The cell death of the NSM sister cells is dependent on the central cell death pathway. So far, not much is known about how the central cell death pathway is activated in specific cells. In the case of the hermaphrodite-specific neurons (HSNs), which specifically die in males but not in hermaphrodites, it has been shown that *egl-1* transcription is repressed in hermaphrodites but not in males. Therefore, the activity of the most upstream component of the central cell death pathway is regulated at the transcriptional level (Conradt and Horvitz, 1999).

It was of great interest to determine whether *egl-1* is transcriptionally regulated also in the NSMs and NSM sister cells. An integrated transgene (*bcIs37* [$P_{egl-1}his24-gfp$]) was used that drives the expression of a fusion of the green fluorescence protein (GFP) with the HIS-24 protein under the *cis*-regulatory regions of the *egl-1* locus (Thellmann et al., 2003). This transgene allows identifying cells that express *egl-1* by looking for GFP positive cells.

The cell death of the NSM sister cells occurs at the so called 1.5 –fold stage of embryogenesis. At this stage, the embryo consists of more than 500 nuclei, which are densely orientated. Therefore, it is rather difficult to identify specific cells due to their position within the embryo. Moreover, no marker is available to identify the NSMs and NSM sister cells at this time. Therefore, the expression of *egl-1* was analyzed in a *ced-3(n717lf)* background. A loss-of-function (lf) mutation in *ced-3* results in a general block in cell death, including the death of the NSM sister cells. Since *ced-3* acts downstream of *egl-1*, a *ced-3*(lf) mutation should not interfere with the expression of the *P_{egl-1}his24-gfp* transgene. Therefore, I was able to analyze ‘undead’

NSM sister cells, which could be identified in the anterior pharynx in early L1 larvae (the first larval stage, shortly after they hatch) using Nomarski microscopy due to their position. GFP could be detected in 88% of the NSM sister cells, which are destined to die, but 0% of the NSMs (n=51), which are destined to survive (Figure 4-1). This indicates that *egl-1* is regulated at the transcriptional level in the NSM lineage.

It has been shown that a gain-of-function (gf) mutation in *ces-1*, *n703*, a gene that acts upstream of *egl-1* and that regulates the NSM sister cell death, results in their inappropriate survival (Ellis and Horvitz, 1991). I analyzed the expression of *P_{egl-1his24-gfp}* in a *ces-1(n703gf)* background. In this mutant background, only 2% of the NSM sister cells are GFP positive (n=51), indicating that *ces-1(n703gf)* causes the NSM sisters to survive by repressing *egl-1* expression.

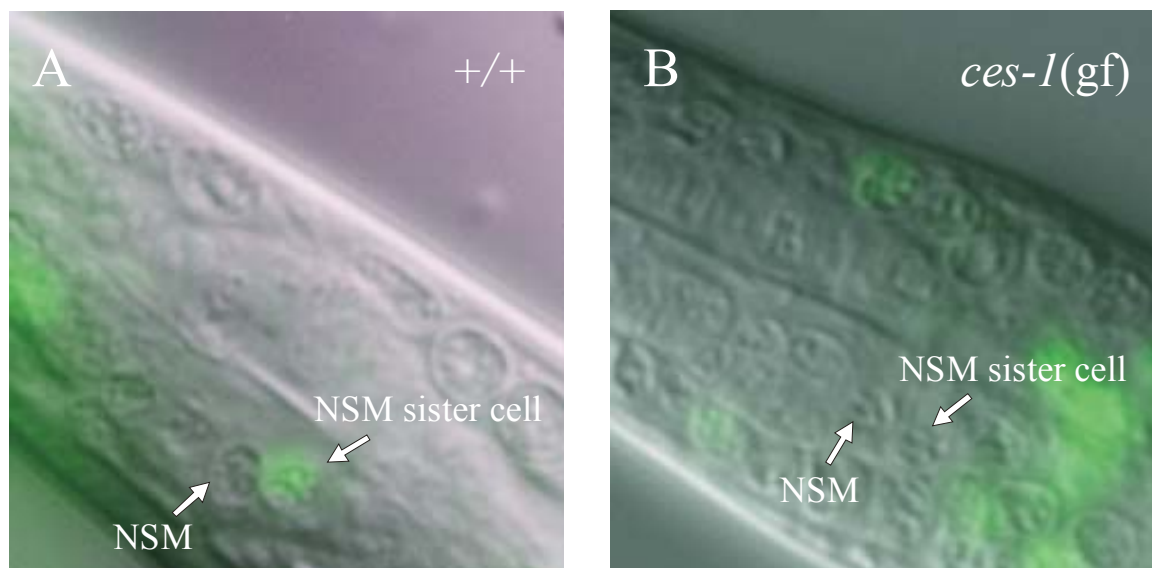


Figure 4-1 *egl-1* is regulated at the transcriptional level in the NSMs and NSM sister cells and its expression is blocked in the NSM sister cells by a *ces-1(gf)* mutation.

A. Merged Nomarski and epifluorescence image of the anterior bulb of the pharynx of a L1 larvae. GFP driven by the *egl-1* promoter can be detected in the NSM sister cell but not in the NSM. The genotype is *ced-3(n717); bclIs37*.

B. Merged Nomarski and epifluorescence image of the anterior bulb of the pharynx of a L1 larvae. No GFP can be detected in the NSM sister cell. The genotype is *unc-87(e1216) ces-1(n703gf); ced-3(n7170); bclIs37*.

4.2 Region B of the *egl-1* locus is required for *egl-1* expression in the NSM sister cells

As shown above, the NSM sister cell death is specified by the transcriptional regulation of *egl-1*. Therefore, it was of interest to determine how *egl-1* transcription is regulated. The *egl-1* locus is a rather complex locus with regulatory regions upstream and downstream of the coding sequence (Conradt and Horvitz, 1998). *cis*-regulatory regions in the locus are highly conserved between *C. elegans* and *C. briggsae* (see Figure 4-2) implying a functional relevance (Heschl and Baillie, 1990). Transformation rescue experiments have shown that the NSM sister cell survival caused by a *lf* mutation of *egl-1* can be rescued by introducing the wild-type *egl-1* locus. The *egl-1* locus lacking a specific region, the so called Region B, however, fails to rescue the NSM sister cell survival indicating that Region B contains the *cis*-regulatory regions necessary for *egl-1* transcription in the NSM sister cells (Thellmann et al., 2003). Region B is located 3' of the *egl-1* coding region. In our lab, a mutant (*egl-1(bc274)*) was isolated that has a deletion of 1510 bp in the *egl-1* 3' regulatory regions including Region B (see Figure 4-2).

In order to easily identify the NSMs and undead NSM sister cells, the $P_{tph-1gfp}$ reporter (*bcIs25*) is used. $P_{tph-1gfp}$ is expressed in serotonergic neurons, including the NSMs and undead NSM sister cells, and allows to quantify NSM sister cell survival by scoring GFP positive cells (Sze et al., 2000; Thellmann et al., 2003). To determine the effect of *bc274* on the survival of the NSM sisters, $P_{tph-1gfp}$ (*bcIs25*) was introduced into the *egl-1(bc274)* strain. As shown in Table 4-1, in *bcIs25*; *egl-1(bc274)* animals, the NSM sister cells survive with a frequency of up to 66%, depending on the temperature at which the animals were cultured. This result strengthens the conclusion that Region B is required for *egl-1* expression in the NSM sister cells. However, the deletion of Region B does not seem to completely eliminate EGL-1 activity in the NSM sister cells, because a third of the NSM sister cells still dies compared to only 4% NSM sister cell death in an *egl-1* null mutant. To determine if the cell-death defect of *egl-1(bc274)* animals is a cell-death-specific (Ces) phenotype or if *egl-1(bc274)* results in a general block in cell death, other cell death events were analyzed. In the anterior pharynx, 16 cells undergo programmed cell death in wild-type; when cell death is blocked by mutations in the central cell death pathway such as *gf* mutations in *ced-9* or *lf* mutations in *ced-3*, *ced-4*, or *egl-1*, 11-12

extra cells can be detected in the anterior pharynx using Nomarski microscopy (Conradt and Horvitz, 1998; Ellis and Horvitz, 1986; Hengartner et al., 1992). In *egl-1(bc274)* mutants, 3.8 extra cells were scored in the anterior pharynx on average (n=19), mainly NSM sister cells (1.5) and I2 sister cells (1.6), moreover, 0.2 I2 nieces, 0.2 m2 sister cells, 0.1 e1 sister cells, and 0.5 m1 sister cells were identified by position. The *egl-1(bc274)* mutation did not block cell death events in other lineages such as the M4 lineage or I1 lineage. This indicates that *egl-1(bc274)* results in a Ces phenotype, and that a functional *egl-1* gene product is still made in other cells.

Table 4-1 A deletion in the *egl-1* 3' regulatory region that includes Region B results in NSM sister cell survival in a cold-sensitive manner.

genotype	NSM sister cell survival [%] (n)		
	15°C	20°C	25°C
+/+	0 (416)	0 (414)	0 (408)
<i>egl-1(bc274)</i>	66 (86)	66 (202)	49 (308)
<i>egl-1(n1084n3082)</i>	n.d.	96 (120)	n.d.

The completed genotype was *bcIs25, bcIss25; egl-1(bc274)*, and *bcIs25; egl-1(n1084n3082)*.

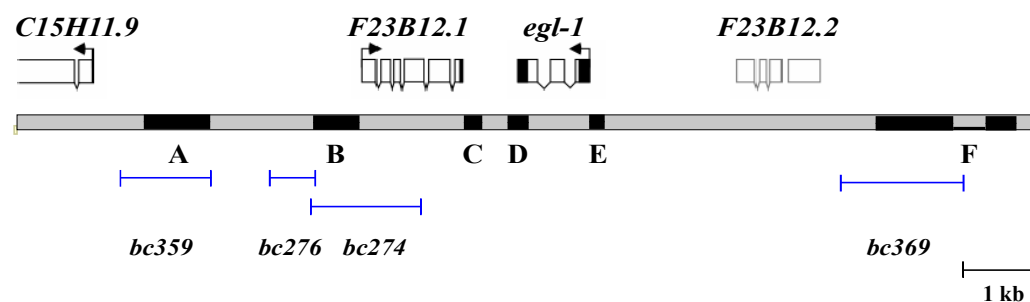


Figure 4-2 Schematic representation of the *C. elegans egl-1* locus. In black, regions are indicated that are highly conserved in *C. briggsae*. Blue bars indicate deletions in the different deletion strains.

In our lab, three other mutants were available with deletions in different parts of the *egl-1* locus (see Figure 4-2, Table 4-2). These mutants were analysed for NSM sister cell survival using Nomarski optics. Neither *bc359* nor *bc276* showed any NSM sister cell survival. Also no other extra cells in the anterior pharynx were observed. Preliminary results suggest that *bc369* causes a weak NSM sister cell survival phenotype (10%). Other pharyngeal cells survived with a higher frequency, as 5.1 extra cells were scored in total, with 0.5 I2-like cells (25% survival), 1.7 extra m2-

like cells (85% survival), 1.1 extra m1-like cells (55% survival), 1.1 extra I1-like cell (55% survival), and 0.6 extra M4 sister cells (60% survival) (n=10). This indicates that Region F seems to be required for different cell death events; yet for the death of the NSM sister cells, Region F is not as important for *egl-1* expression as Region B.

Table 4-2 NSM sister cell survival in different *egl-1* deletion mutants.

Genotype	Deletion	NSM sister cell survival [%] (n)
<i>bc359</i>	Region A	0 (30)
<i>bc276</i>	region between Region A and B	0 (40)
<i>bc274</i>	Region B	66 (202)
<i>bc369</i>	Region F	10 (20)

The NSM sister cell survival was scored using Nomarski microscopy except for *bc274*, which had *bcIs25* in the background and therefore was scored using epifluorescence. Experiments were performed at 20°C. *bc369* was not outcrossed.

4.3 Identification of factors that contribute to the killing of the NSM sister cells

The death of the NSM sister cell is determined by lineage; the NSM mother cell divides asymmetrically to give rise to the anterior daughter, which subsequently differentiates into the NSM, and the posterior daughter, which dies about 20 minutes after the division. The cell death is dependent on the central cell death pathway, and, as shown above, it seems to be initiated by the transcription of its most upstream component, *egl-1*; however, nothing is known about factors that activate the transcription of *egl-1*. Two different approaches were followed to identify these activators; candidate genes, based on previous data, were analyzed, and additionally, a forward genetic screen was performed.

4.3.1 Candidate gene approach

The previous data suggest that the NSM sister cell dies because *egl-1* is transcriptionally activated in this cell, and that this transcriptional activation is mainly mediated by a specific regulatory region of the *egl-1* locus, Region B (4.2). Therefore, I sought to identify activators of *egl-1* expression that function through Region B.

Region B is highly conserved between *C. elegans* and *C. briggsae*, as shown in Figure 4-3 (Thellmann et al., 2003). It contains four E-boxes, which represent binding sites

for bHLH transcription factors. It has been shown that these E-boxes are required for rescuing the NSM sister cell death in an *egl-1(lf)* mutant (Thellmann et al., 2003). Therefore these E-boxes are likely to be required for *egl-1* expression in the NSM sister cells. E-boxes are binding motifs for members of the family of basic helix-loop-helix (bHLH) transcription factors. bHLH proteins can function as transcriptional activators, and they function as dimers, with the basic region binding DNA and the helix-loop-helix domain mediating dimerization between two proteins (reviewed by (Massari and Murre, 2000)). Moreover, the E-boxes in Region B also represent binding sites for Snail-like proteins (Hemavathy et al., 2000). CES-1, a member of the Snail family of transcriptional repressors (Metzstein and Horvitz, 1999), has been shown to bind to these sites *in vitro* (Thellmann et al., 2003). In addition, a *ces-1(gf)* mutation blocks *egl-1* expression in the NSM sister cells (4.1), indicating that CES-1 binds directly to Region B *in vivo*. In different systems, it has been suggested that members of the Snail family of transcription factors can functionally antagonize bHLH proteins by competing for the binding to Snail-binding sites/E-boxes ((Fuse et al., 1994; Kataoka et al., 2000; Nakayama et al., 1998). Therefore, it is possible that *C. elegans* bHLH proteins are involved in the specification of the NSM sister cell death *in vivo*. Of particular interest are the *C. elegans* homologues of neuronal bHLH proteins, which can be divided into two families: the Achaete-Scute complex-related proteins and the Atonal-related proteins (reviewed by (Hassan and Bellen, 2000; Lee, 1997). Tissue-specific bHLH proteins often form DNA-binding heterodimers with ubiquitously expressed E or Daughterless-like proteins. For this reason, the only *C. elegans* daughterless-like gene, *hlh-2*, is a very interesting candidate gene.

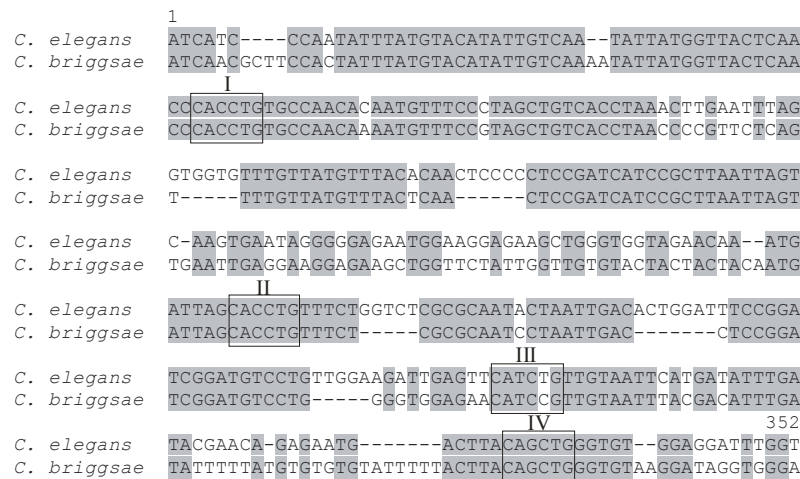


Figure 4-3 Alignment of the sequence of Region B of the *C. elegans egl-1* locus with the corresponding sequence of the *C. briggsae egl-1* locus. Black boxes indicate Snail-binding sites/E-box motifs, the binding sites for bHLH proteins.

4.3.1.1 The *bHLH* gene *hll-2* is required for the NSM sister cell death

So far, *hll-2* has only been defined by weak *lf* mutations, such as *bx108*, which were identified in a screen for enhancers of the phenotype caused by a weak *lf* mutation of *lin-32*, the only *C. elegans atonal*-like gene (Portman and Emmons, 2000). To this point, *bx108* has not been shown to cause a phenotype in an otherwise wild-type background. Reducing the activity of *hll-2* by RNA-mediated interference (RNAi) results in embryonic lethality, indicating that *hll-2* is essential for development (Krause et al., 1997). Escapers of *hll-2(RNAi)* were analyzed for NSM sister cell survival using the $P_{tph-1gfp}$ reporter. It was observed that 15% of the NSM sister cells survived in *hll-2(RNAi)* embryos that escaped early developmental arrest and developed to a stage at which the $P_{tph-1gfp}$ reporter is expressed (Table 4-3).

Moreover, in *hll-2(bx108)* animals 5% of the NSM sister cells survived at 25°C (Table 4-3).

Table 4-3 Reducing the activity of *hll-2* results in NSM sister cell survival.

genotype	NSM sister cell survival [%] (n)		
	15°C	20°C	25°C
+/+	0 (416)	0 (414)	0 (408)
<i>hll-2(bx108)</i>	1 (350)	4 (400)	5 (410)
<i>hll-2(RNAi)</i>	15 (130)	n.d.	n.d.

All animals carried *bcIs25* in the background.

4.3.1.2 *hlh-2* acts synergistically with *hlh-3* to kill the NSM sister cells

The results above suggest that *hlh-2* is required for the death of the NSM sister cells. *hlh-2* encodes a bHLH transcription factor that is thought to function as heterodimer with other bHLH transcription factors, and therefore, it is likely that another bHLH protein acts together with HLH-2 to induce *egl-1* expression.

4.3.1.2.1 RNAi of *achaete-scute*-like *bHLH* genes

Of great interest as possible heterodimerization partners of HLH-2 in the NSM sister cells are Achaete-Scute-like proteins, as their homologs in other species have been shown to compete with Snail-like proteins for the same binding sites (Fuse et al., 1994; Kataoka et al., 2000; Nakayama et al., 1998). Four of the five *C. elegans* *achaete-scute*-like genes (*hlh-3*, *hlh-4*, *hlh-6*, and *hlh-12*) have so far not been defined by mutations. The fifth gene, *hlh-14*, has been identified in a screen for mutants lacking HSNs. *hlh-14* has been shown to promote neuronal fate. In particular, *hlh-14* is required for the asymmetric cell division that gives rise to the PVQ/HSN/PHB neuroblasts (Frank et al., 2003). To analyze the potential role of *Achaete-Scute*-like genes in the specification of the NSM sister cell death, RNAi was used to reduce their activity. A standard method of dsRNA delivery is the method of feeding the worms with bacteria that express dsRNA of the gene of interest (Timmons and Fire, 1998). RNAi by feeding does not work for all genes and in all tissues; especially the nervous system is more resistant to RNAi. No effect of any *Achaete-Scute* gene was observed using RNAi by feeding. dsRNA can also be introduced by injecting animals. With that method, no effect on NSM sister cell survival was observed in *hlh-4(RNAi)*, *hlh-6(RNAi)*, *hlh-12(RNAi)* or *hlh-14(RNAi)* animals (Table 4-4). *hlh-3(RNAi)*, however, caused 7% of the NSM sister cells to survive (n=178) at 25°C, indicating that *hlh-3* is at least partially required for the death of the NSM sister cells (Table 4-4). Moreover, *hlh-3(RNAi)* increased the NSM sister cell survival in *hlh-2(bx108)* animals from 4% to 30%. *hlh-2* and *hlh-3* therefore might act synergistically to cause the death of the NSM sister cells.

Table 4-4 *hlh-3(RNAi)* causes NSM sister cells to survive and enhances the NSM sister cell survival phenotype caused by *hlh-2(bx108)*.

Genotype	NSM sister cell survival [%] (n)		
	20°C		<i>hlh-2(bx108)</i>
	+/+	+/+	
<i>hlh-3(RNAi)</i>	0 (158)	7 +/- 3 (178)	30 +/- 11 (140)
<i>hlh-4(RNAi)</i>	0 (90)	2 +/- 3 (116)	3 +/- 3 (177)
<i>hlh-6(RNAi)</i>	0 (68)	0 +/- 0 (136)	3 +/- 2 (176)
<i>hlh-12(RNAi)</i>	0 (52)	1 +/- 1 (102)	6 +/- 5 (92)
<i>hlh-14(RNAi)</i>	0 (92)	3 +/- 2 (180)	7 +/- 3 (134)

The complete genotype of animals was *hlh-3(RNAi); bcIs25*, *hlh-4(RNAi); bcIs25*, *hlh-6(RNAi); bcIs25*, *hlh-12(RNAi); bcIs25*, and *hlh-14(RNAi); bcIs25*. RNAi was performed by injecting dsRNA.

4.3.1.2.2 Isolation and characterization of *hlh-3* deletions

Since *hlh-3* was not yet defined by a mutation, two deletion mutations in the *hlh-3* gene, *bc248* and *bc277*, were isolated from our deletion library. *bc277* is a 664 bp deletion, removing sequences 35,379 to 36,042 of cosmid T24B8. *bc248* is a 815 bp deletion, removing sequences 35,791 to 36,605 of T24B8. The predicted *hlh-3* locus consists of three exons. *bc277* deletes exon 1 and 188 bp 5' of the predicted ATG. *bc277* does not result in a frame shift. *bc248* deletes exon 2 and also causes no frame shift, but amino acids 33 to 98 are missing and therefore most of the functional domain is not present in the mutant protein (see Figure 4-4).

In order to identify the *hlh-3* mRNA product, RT-PCR was performed. I was unable to amplify a specific product by RT-PCR, using wild-type cDNA and a sense primer in exon 1; however, exon 2 and exon 3 could be amplified using SL1 and SL2 as a sense primer. It is consistent with previous reports that exon 2 and exon 3 are transcribed and *trans*-spliced to both SL1 and SL2 (Krause et al., 1997) (see Figure 4-4). Sequencing of the PCR product revealed that SL1 and SL2 were spliced to the first codon of exon 2. The second codon of exon 2 is an ATG, and conclusively, the *hlh-3* open reading frame starts here in exon 2, and not in exon 1 as annotated in wormbase (www.wormbase.org, the *C. elegans* genome database). This mRNA is also made in *bc277* mutants. In *bc248* mutants, however, an mRNA product is made consisting of exon 1 spliced to exon 3. Since most of the functional domain is

encoded by exon 2, *bc248* represents a strong loss-of-function mutation of *hlh-3*. *bc277* might affect 5' regulatory regions. However, since mRNA is still made, *bc277* might represent a weaker *hlh-3* loss-of-function mutation.

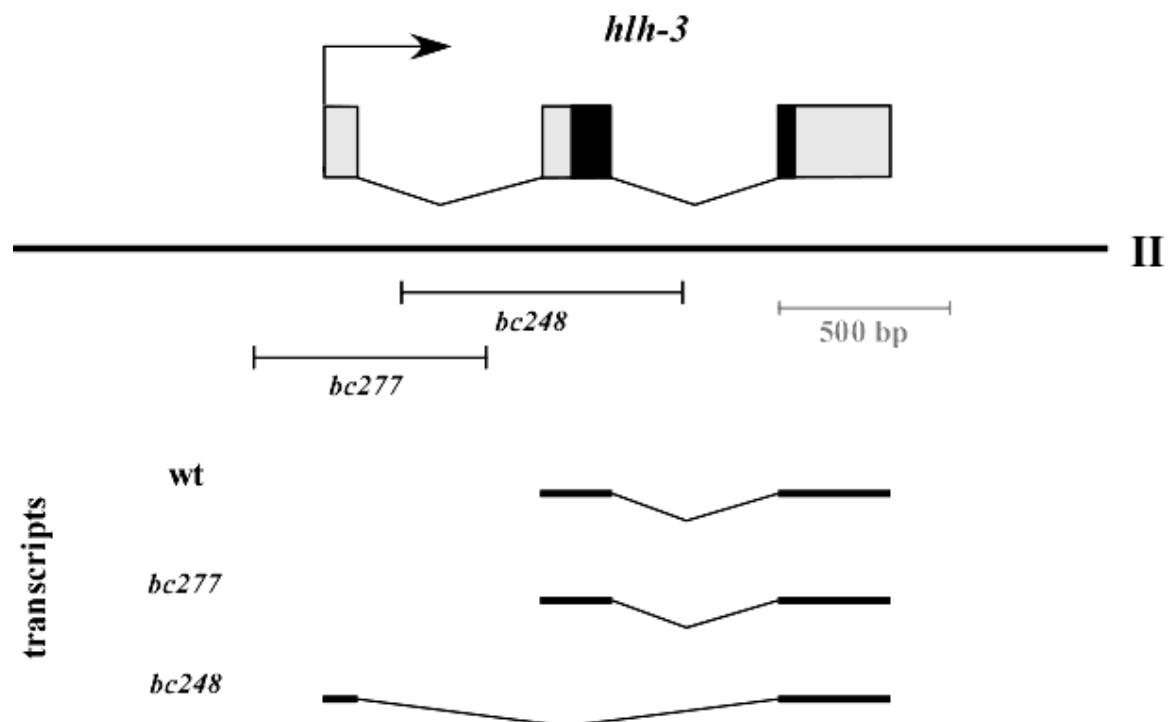


Figure 4-4 Schematic representation of the *hlh-3* locus. In black, the part of the sequence is indicated that codes for the bHLH domain. Black bars represent the deletion mutations.

bc248 and *bc277* animals are viable and don't exhibit any obvious phenotypes. However, *bc248* animals are egg-laying defective as a result of defective pathfinding of the HSN axons (R. Doonan et al., in prep). Both mutants were analyzed for NSM sister cell survival using the $P_{tph-1gfp}$ reporter. *bc248* results in a weak NSM sister cell survival in a temperature sensitive manner, which is similar to that observed in *hlh-3(RNAi)* animals. Moreover, *bc248* and *bc277* strongly enhance the NSM sister cell survival of *hlh-2(bx108)* animals to 31 % and 27%, respectively (Table 4-5). Two observations confirm that *bc248* is a strong *lf* mutation if not null mutation. First, the phenotype of *bc248* was not enhanced by *hlh-3(RNAi)* (Table 4-5). Second, neither the phenotype of *bc248* animals *in trans* to a deficiency that removes the *hlh-3* locus was enhanced (Table 4-5).

In summary, the analysis of *hlh-3* deletion mutants confirms the observation that *hlh-3* is at least partially required for NSM sister cell survival, and that *hlh-3* acts together with *hlh-2* in this process. Since the phenotype of *hlh-3(bc248)* mutants is very weak although most of the functional domain is missing and *bc248* seems to be a

strong *lf* mutation, it seems likely that *hlh-3* function is redundant in specifying the NSM sister cell death.

Table 4-5 *hlh-3* is required for NSM sister cell survival and acts synergistically with *hlh-2*.

Genotype	NSM sister cell survival [%]			
	20°C	n	25°C	n
+/+	0	414	0	408
<i>hlh-3(RNAi)</i>	0	158	7	178
<i>hlh-3(bc248)</i>	2	296	4	412
<i>hlh-3(bc277)</i>	0	232	2	260
<i>hlh-2(bx108); hlh-3(bc248)</i>	19	352	31	72
<i>hlh-2(bx108); hlh-3(bc277)</i>	11	238	27	200
<i>hlh-3(bc248) hlh-3(RNAi)</i>	N.D.		4.2 +/-2.9	188
<i>mnDf69/hlh-3(bc248) *</i>	1.5	260	N.D.	

All strains additionally carried the NSM reporter *bcIs25*. * Animals shown here represent F1 males from a cross of *unc-4(e120) mnDf69/mnC1 dpy-10(e128) unc-52(e444)* males with *hlh-3(bc248); bcIs25* hermaphrodites; 50% of these males theoretically have the genotype *unc-4(e120) mnDf69/hlh-3(bc248)*, whereas the remaining 50% are *mnC1/hlh-3(bc248)*.

4.3.1.2.3 *hlh-2* and *hlh-3* are specifically required for the NSM sister cell death

To determine if *hlh-2* and *hlh-3* are required for programmed cell death in general or if they function specifically in the death of the NSM sister cells, other cell deaths in the anterior pharynx were analyzed in *hlh-2(bx108); hlh-3(bc248); bcIs25* animals using Nomarski microscopy. *hlh-2(bx108); hlh-3(bc248)* animals have on average 1 extra cell (n=12). More than 90% of these cells are NSM sister cells, the remaining cells were most likely m2 sister cells, as determined by the position of their nuclei (Table 4-6). Therefore, reducing the activity of *hlh-2* and *hlh-3* results specifically in the survival of the NSM sister cells. *hlh-2* and *hlh-3* therefore might encode potential direct activators of *egl* expression specific to the NSM sister cells.

Table 4-6 Reducing the activity *hlh-2* and *hlh-3* specifically results in the survival of the NSM sister cells.

Genotype	extra cells	NSM sisters	m2 sisters	n
+/+	0	0	0	9
<i>hlh-2(bx108)</i>	0.4	0.1	0.3	27
<i>hlh-2(bx108); hlh-3(bc248)</i>	1.0	0.9	0.1	12

The anterior pharynx of animals was analysed for extra cells using Nomarski optics. Undead NSM sister cells were identified by position and expression of $P_{ph-1}gfp$. Undead m2 sister cells were identified by position. All animals additionally carried *bcIs25*.

4.3.1.2.4 Are HLH-2 and HLH-3 present in the NSM sister cell at the time it is dying?

If HLH-2 and HLH-3 act as a direct activators of *egl-1* transcription, both proteins are expected to be present in the NSM sister cells at the time their cell-death fate is specified, i.e. in the NSM sister cells of embryos at the 1.5-fold stage of development (about 400-430 minutes after the first cell division).

HLH-2 has been shown to be broadly distributed throughout the embryo during the proliferative phase of embryogenesis (until about 350 minutes). During later stages of embryogenesis, the distribution of HLH-2 becomes more restricted (Krause et al., 1997). The expression of a *hlh-3::GFP* reporter gene overlaps considerably with the distribution of HLH-2, mostly in neurons, another indication that HLH-2 and HLH-3 act together (Krause et al., 1997). An antibody specific for HLH-2 is available (Krause et al., 1997) for detecting HLH-2. In fixed 1.5-fold stage embryos, however, it is impossible to detect NSMs and NSM sister cells based on their position, and, moreover, no marker for the early NSM lineage is available. Therefore it is not possible to determine whether the HLH-2-positive cells include the NSM sister cells.

4.3.1.2.4.1 Co-localization of EGL-1 and HLH-2 using antibody staining

To circumvent the problem of detecting NSMs and NSM sister cells, the following approach was undertaken. *egl-1* appears to be specifically expressed in cells destined to die during embryogenesis (R. Schnabel and B. Conradt, unpublished), including, as

shown above, the NSM sister cells (4.1). In a wild-type background, about 98 cells have undergone programmed cell death by the time an embryo reaches the 1.5-fold stage (Sulston et al., 1983). In a *ced-3(n717)* background, most if not all of these 98 cells survive (Ellis and Horvitz, 1986). *egl-1* expression can be monitored by an integrated $P_{egl-1}gfp$ transgene, which expresses the *gfp* gene under the control of the *cis*-regulatory regions of *egl-1*. As *egl-1* acts upstream of *ced-3*, *ced-3(n717)* does not interfere with the expression of $P_{egl-1}gfp$. $P_{egl-1}gfp$; *ced-3(n717)* embryos were stained with antibodies for both HLH-2 and GFP. In a $P_{egl-1}gfp$; *ced-3(n717)* embryo at the 1.5-fold stage, a large number of undead, GFP-positive cells can therefore be detected (Figure 4-5). I found that a total of four cells expressed $P_{egl-1}gfp$ and were positive for HLH-2 (Figure 4-5). All four cells are located in the head region where the developing pharynx is found. To determine whether two of these four cells may represent the NSM sister cells, embryos of genotype *ces-1(n703gf)*; $P_{egl-1}gfp$; *ced-3(n717)* were stained. As shown above, *ces-1(n703gf)* prevents the deaths of the NSM sister cells by blocking the expression of *egl-1* in these cells. In a *ces-1(n703gf)*; *ced-3(n717)* background, the distribution of HLH-2 and the expression of $P_{egl-1}gfp$ in 1.5-fold stage embryos was overall unchanged; however, a total of only two cells expressed $P_{egl-1}gfp$ and were positive for HLH-2 (Figure 4-5). It is very likely that the two cells that are still positive for HLH-2 but no longer express $P_{egl-1}gfp$ are the NSM sister cells. This result suggests that HLH-2 is most probably present in the NSM sister cells at the time their cell-death fate is determined.

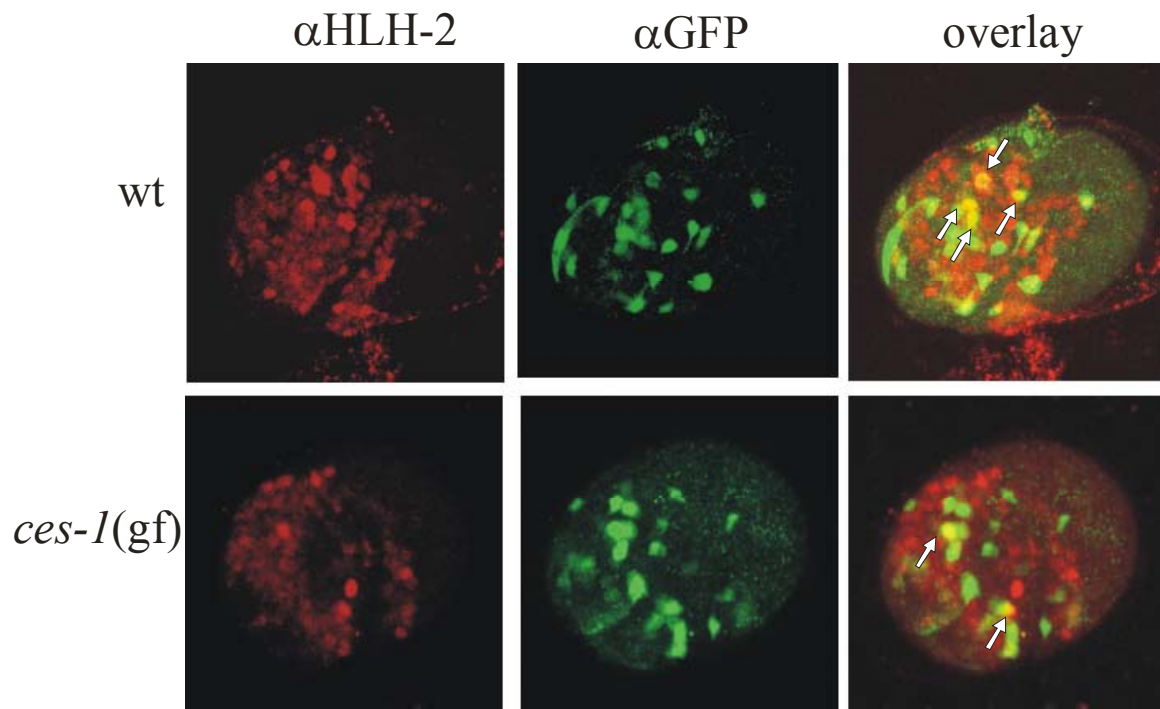


Figure 4-5 HLH-2 is most probably present in the NSM sister cells. Anti-HLH-2 and anti-GFP immunofluorescence staining and overlay of 1.5-fold embryos of the genotype *bcls1; ced-3(n717)* (wt) and *unc-87(e1216) ces-1(n703gf); bcls1; ced-3(n717)* (*ces-1(gf)*). The images represent a projection of stacks of a confocal series through an entire embryo. Double positive cells are indicated by arrows.

4.3.1.2.4.2 The NSM and NSM sister cell can be identified due to their position within the embryo

The experimental set up described above (4.3.1.2.4.1) allowed circumventing the problem of directly identifying the NSM sister cells by position, and gave insight about the presence of HLH-2 in the NSM sister cell. This method, however, does not solve questions about HLH-2 presence in the NSM and the NSM mother cell. It is of great interest to follow the NSM mother cell division and determine the localization of factors that trigger cell death, like HLH-2 and HLH-3, in the mother cell as well as NSM and NSM sister. Using Nomarski microscopy, these cells can be detected due to their position relative to surrounding cells. The nucleus of the NSM mother cell can be detected between the comma and the 1.5 fold stage of embryonic development relative to the position of surrounding cells. It is located above the characteristically ‘round’ nuclei of m6VL and m7VL, while the ‘round’ nucleus of m5L is located to the right, and the rather ‘oval’ and small nuclei of MCL and M3L are located to the left (Figure 4-6D). Shortly before the cell starts dividing, the punctuated structure of

the nucleus starts appearing smoother and finally vanishes. After ten to fifteen minutes two new nuclei can be observed, the nucleus of the NSM on the left side (Figure 4-6E), and the nucleus of the NSM sister cell on the right side. Shortly after that, the NSM sister cell starts to undergo morphological changes typically for dying cells (Sulston and Horvitz, 1977): it becomes highly refractile and turns into a flat, round disk (Figure 4-6F).

Figure 4-6 (see next page) The NSM mother cell, the NSM, and the NSM sister cell can be detected in living embryos by their position using Nomarski optics.

A. Schematic representation of an embryo 430 min after first cleavage (from (Sulston et al., 1983)). In red, NSM and NSM sister cell are circled. They are positioned in a distinct pattern relative to surrounding cells (blue arrow heads).

B. Nomarski image of an embryo about 430 min after first cleavage.

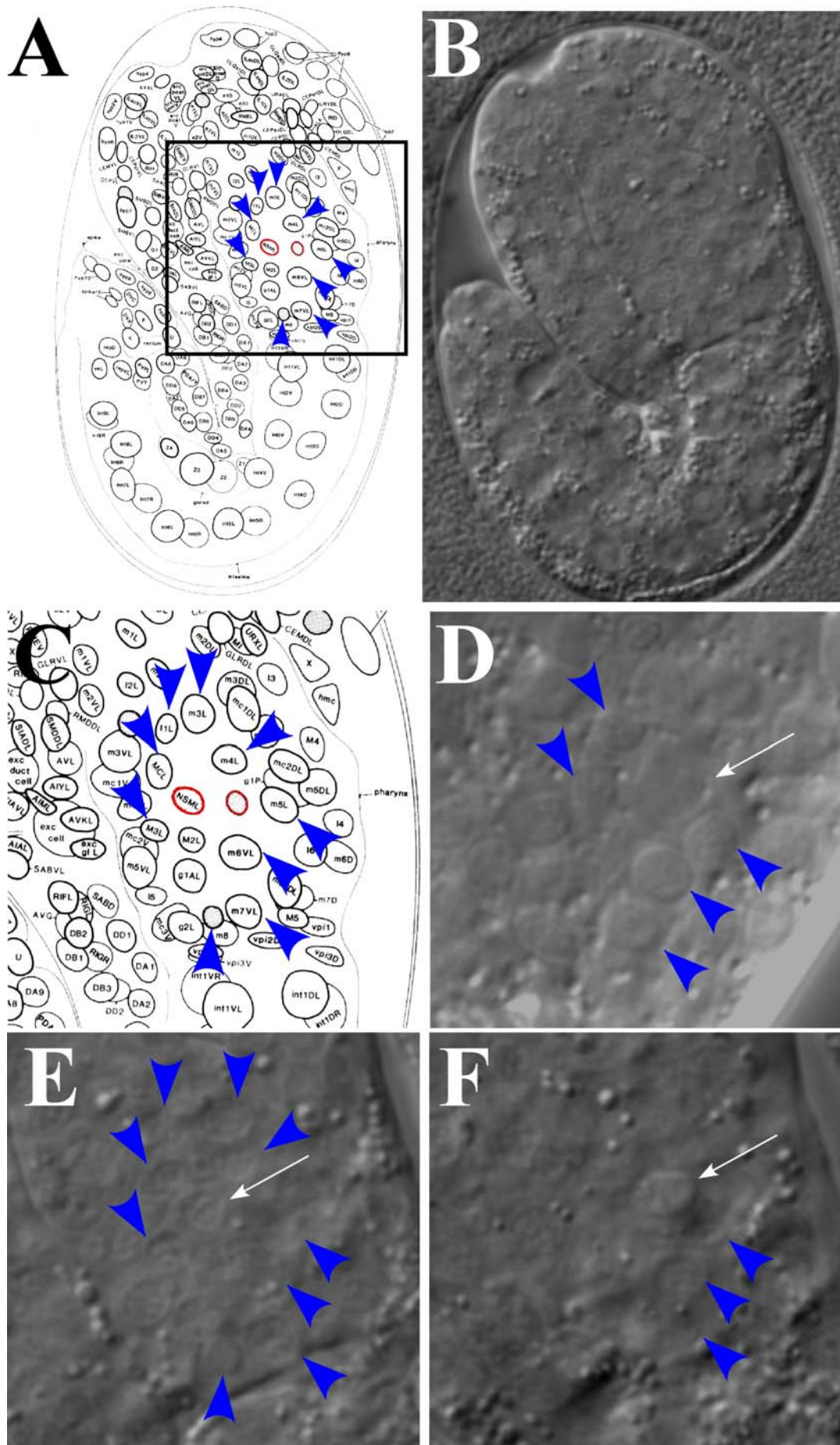
C. Blow up of A.

D. The nucleus of NSM mother cell (white arrow) shortly before the division will take place already started to change morphologically.

E. The nucleus of the NSM (white arrow) shortly after the cell division.

F. The NSM sister cell started already to die as can be determined by its refractile button-like structure.

In F a different focal plane is shown from the same embryo at the same time as in E.



4.3.1.2.4.3 *hlh-2::gfp* is expressed in the NSM and the NSM sister cell but not in the NSM mother cell

Using an integrated *hlh-2::gfp* reporter (Krause et al., 1997), *hlh-2* expression could be monitored in living embryos. As shown in Figure 4-7, GFP was not detected in the NSM mother cell before it divided. However, shortly after the division, weak *gfp* expression was observed in the NSM as well as in the NSM sister cell (n>5).

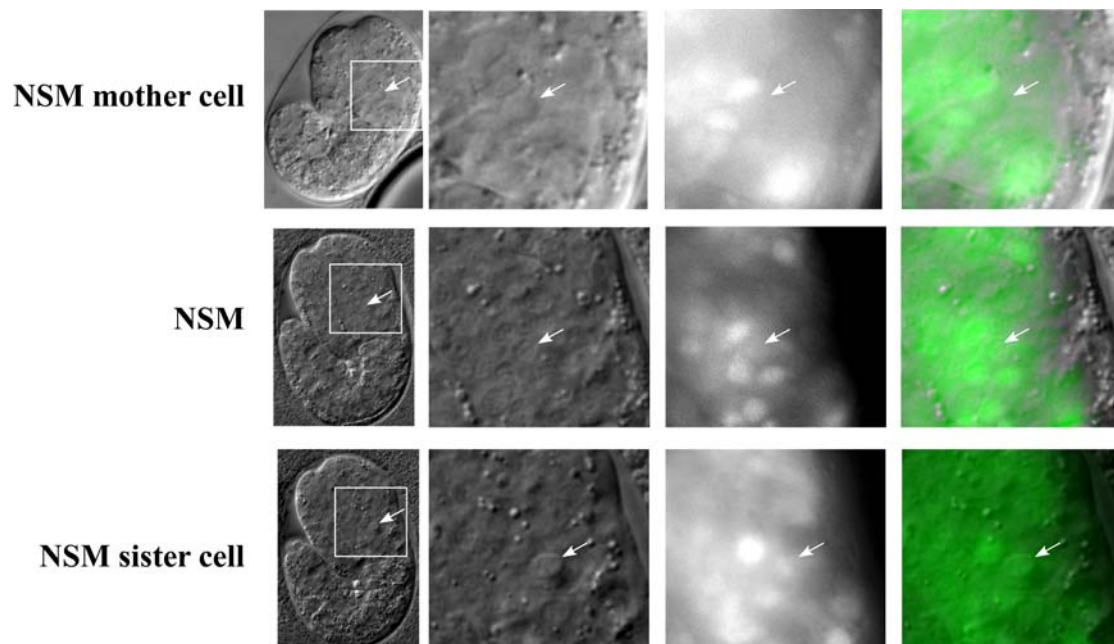


Figure 4-7 *hlh-2* is expressed in the NSM and NSM sister cell, but not in the NSM mother cell.

4.3.1.2.4.4 *hlh-3::gfp* is expressed in the NSM and the NSM sister cell but not in the NSM mother cell

To analyze *hlh-3* expression in the NSMs and NSM sister cells, an integrated *hlh-3::gfp* reporter was used (Krause et al., 1997). A similar pattern as for *hlh-2::gfp* expression was observed: GFP was not detected in the NSM mother cell. However, very weak expression was observed in the NSM as well as in the NSM sister cell. GFP was very faint in both cells, so it was not possible to take pictures.

Taken together, HLH-2 and HLH-3 are present in the NSM sister cell at the time it starts to die, but also in the NSM, which survives.

4.3.1.2.5 HLH-2 and HLH-3 bind to Region B of the *egl-1* locus *in vitro*

hlh-2 and *hlh-3* are required for the NSM sister cell death and act synergistically with each other. The fact that their gene products are actually present in the NSM sister cell at the time it is dying, suggests that they act cell autonomously. Moreover, *hlh-2* and *hlh-3* encode for bHLH proteins that can act as transcriptional activators by binding to E-box motifs. Four conserved E-boxes are present in the *cis* regulatory region of the *egl-1* locus, which is required for the NSM sister cell death, Region B. To determine whether HLH-2 and HLH-3 can bind to these E-boxes in Region B I performed electro mobility shift assays (electro mobility shift assay, EMSA), using bacterially produced, affinity purified His-tagged HLH-2 and HLH-3 fusion proteins. As a probe, the 390 bp DNA fragment consisting of the wild-type Region B, including all four E-boxes was used. As shown in Figure 4-8, homodimers of HLH-2 and heterodimers of HLH-2 and HLH-3 but not homodimers of HLH-3 could bind and shift the probe. Using various fragments of Region B, I could determine that HLH-2/HLH-3 heterodimers can bind to at least three of the four Snail-binding sites/E-boxes *in vitro* (data not shown). To determine if the binding to Region B is specific to the E-boxes, a DNA fragment consisting of mutant Region B, in which the four E-boxes had been mutated (5'-CACCTG-3' to 5'-CATATA-3') was used as a probe. Using amounts of HLH-2/HLH-3 that are sufficient to bind 50% of the wild-type probe (100% binding), binding to mutant Region B was strongly reduced to on average only 4% ($n=3$). HLH-2/HLH-3 binding to Region B *in vitro* therefore is dependent on functional E-boxes. These results suggest that HLH-2 and HLH-3 might cause the NSM sister cells to die by acting as a direct activator of *egl-1* transcription in the NSM sister cells.

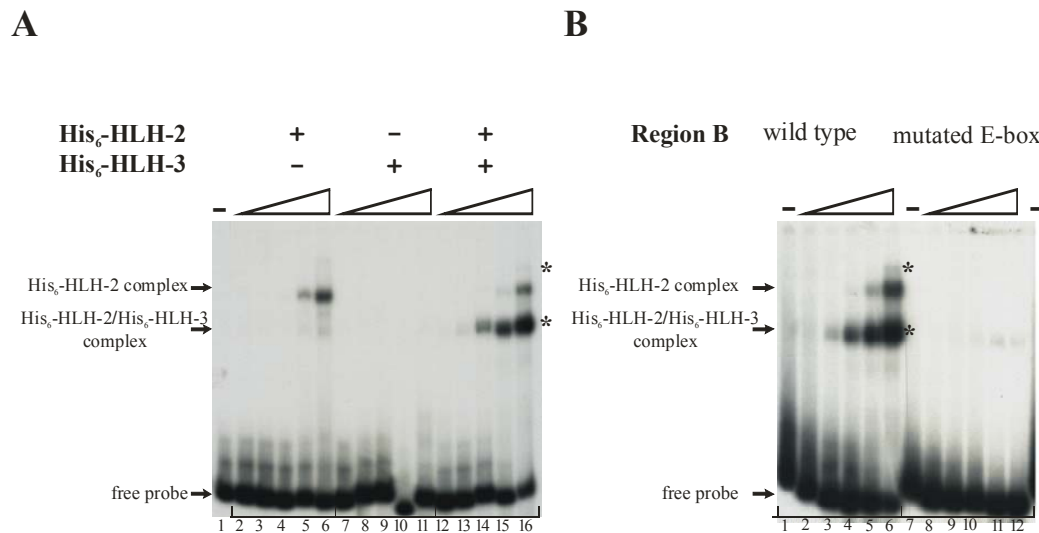


Figure 4-8 HLH-2/HLH-3 binds to the Snail-binding sites/E-boxes in Region B of the *egl-1* locus *in vitro*.

A. A HLH-2 homodimer and a HLH-2/HLH-3 heterodimer bind to wild-type Region B *in vitro*. Increasing amounts of bacterially expressed, affinity-purified His₆-tagged HLH-2 (lanes 2-6), HLH-3 (lanes 7-11) or both HLH-2 and HLH-3 (lanes 12-16) fusion proteins [0 mol (lane 1), 8×10⁻¹⁴ mol (lanes 2, 7 and 12), 2×10⁻¹³ mol (lanes 3, 8 and 13), 4×10⁻¹³ mol (lanes 4, 9 and 14), 8×10⁻¹³ mol (lanes 5, 10 and 15), 2×10⁻¹² mol (lanes 6, 11 and 16)] were incubated with 7 ng of radioactively labeled wild-type Region B. Asterisks indicate a DNA-protein complex with one or two heterodimers bound to Region B.

B. A HLH-2/HLH-3 heterodimer does not bind to mutated E-boxes in Region B. Increasing amounts of both His₆-tagged HLH-2 and HLH-3 [0 mol (lane 1 and 7), 8×10⁻¹⁴ mol (lanes 2 and 8), 2×10⁻¹³ mol (lanes 3 and 9), 4×10⁻¹³ mol (lanes 4 and 10), 8×10⁻¹³ mol (lanes 5 and 11), 2×10⁻¹² mol (lanes 6 and 12)] were incubated with 7 ng of radioactively labeled wild-type Region B with four intact Snail-binding sites (lanes 1-6), or mutant Region B with all four E-boxes mutated (lanes 7-12).

4.3.1.2.6 HLH-2 and HLH-3 can induce ectopic *egl-1* expression

The *in vivo* and *in vitro* data suggest that the NSM sister cells die because a heterodimer composed of HLH-2 and HLH-3 directly activates *egl-1* transcription in these particular cells. It was of interest if these proteins can ectopically induce *egl-1* expression in other cells when overexpressed. The two plasmids pBC296 and pBC297, which express the *hlh-2* and *hlh-3* cDNA, respectively, under the control of the *hsp16-2* heat shock promoter, were injected into *ced-3(n717)* animals carrying an integrated *gfp* reporter under the control of the *egl-1* promoter (*P_{egl-1}gfp (bcIs1)*). This experimental set up allows identifying cells that express *egl-1*, but that fail to die

because cell death is blocked downstream. Transgenic lines were obtained that expressed both plasmids. Transgenic adult animals were allowed to lay eggs for three hours. Afterwards, the eggs were exposed to a 33°C heat shock for 30 minutes and then returned to 20°C. The eggs were subsequently analysed for *gfp* expression. About two hours after the heat shock, a phenotype was observed. Heat shocked wild-type embryos (*bcl-1; ced-3(n717)*) express *gfp* in only a few cells in a symmetric pattern during gastrulation, the stage where the first cell death events occur (Figure 4-9). In heat shocked animals transgenic for *hsp16-2::hlh-2* and *hsp16-2::hlh-3* (*bcEx279*), however, more cells express *gfp* (Figure 4-9) indicating that HLH-2 and HLH-3 can induce ectopic *egl-1* expression when overexpressed. The transgenic embryos eventually arrest after being heat shocked suggesting a lethal effect of ectopically expressed *hlh-2* and *hlh-3*. However, this experiment was done in a *ced-3(lf)* background, in which programmed cell death is blocked. Therefore, the overexpression of *hlh-2* and *hlh-3* results in lethality that is not related to increased programmed cell death.

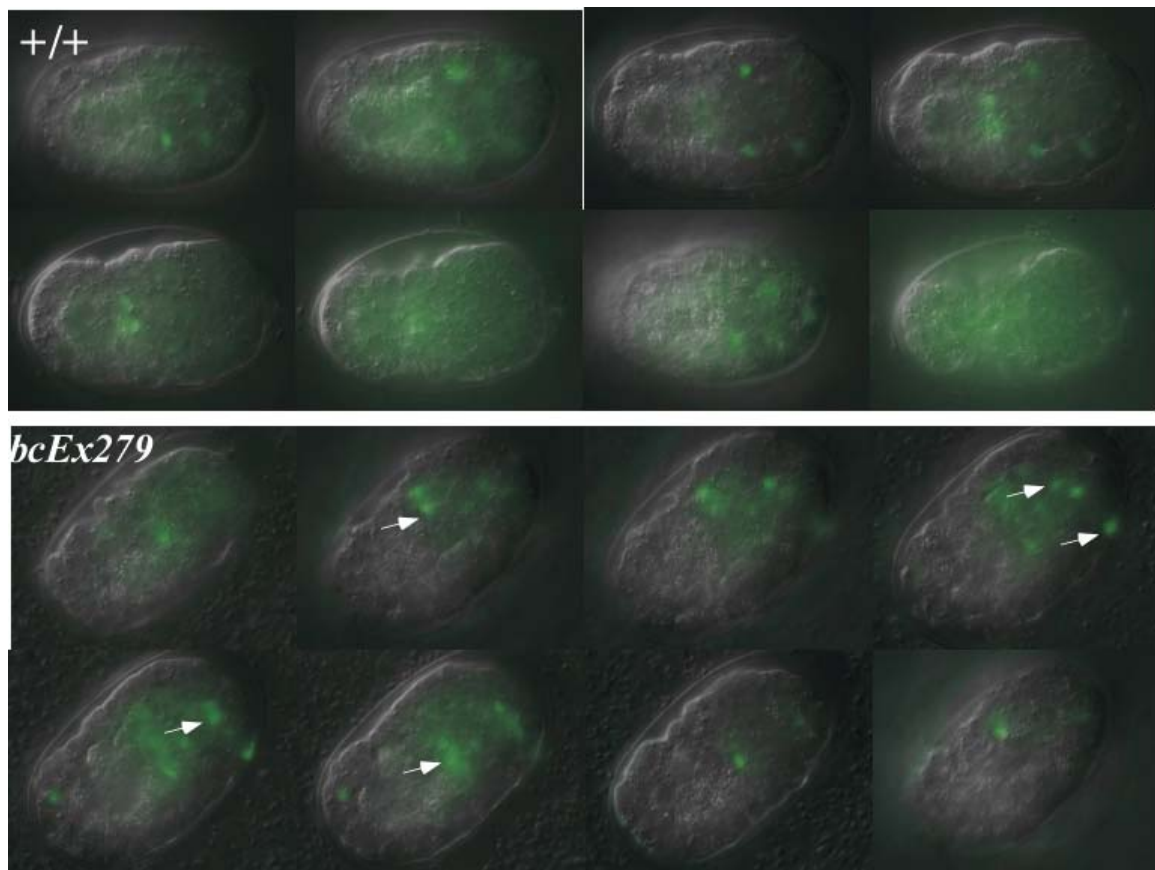


Figure 4-9 Ectopic *egl-1* expression can be induced by overexpression of HLH-2 and HLH-3.

The strains had the genotype *bcIs1; ced-3(n717)* and *ced-3(n717); bcEx279*, respectively. The images represent different focal planes through a stack of an embryo 2h after a 30 min heat shock at 33°C. *egl-1* expression was monitored by detecting GFP positive cells. Arrows point to some ectopic *gfp* expression.

4.3.2 *hlh-2* enhancer screen

A weak *lf* mutation in *hlh-2*, *bx108*, the only *daughterless*-like gene in *C. elegans*, results in the survival of the NSM sister cells with a frequency of only 5% (4.3.1.1). Similarly, *hlh-3(bc248)* causes a weak survival phenotype of 4%. However, *hlh-3(bc248)* increases the NSM sister cell survival phenotype of *hlh-2(bx108)* animals to 31 % (4.3.1.2.2). Considering that *hlh-3(bc248)* is most likely a strong *lf* mutation, *hlh-3* probably acts redundantly together with another factor. On the other hand, the *bx108* mutation in *hlh-2* is of very weak character; it results in an amino acid change from an R to an H in the first helix of the HLH domain, the domain that is important for the protein-protein interaction. This amino acid change does not dramatically change the character and therefore is thought to reduce but not abolish the affinity to dimerize (Portman and Emmons, 2000). To identify factors that act

with HLH-2 to activate *egl-1* transcription, a screen was performed to isolate mutations that enhance the weak NSM sister cell survival observed in *hlh-2(bx108)* mutants.

For this purpose, *hlh-2(bx108); bcIs25* animals were mutagenized with ethyl methanesulfonate (EMS). The F1 generation was isolated clonally. Random EMS-induced mutations in genes required for the death of the NSM sister cells are heterozygous in the F1 generation. However, most of them are recessive. Mutants with recessive mutations will exhibit a phenotype only when homozygous for the mutation. Mutants can be homozygous for a mutation earliest in the F2 generation. In order to identify F2 animals that are homozygous for a mutation that results in a higher frequency of surviving NSM sister cells than 5 % , the F3 generation has to be screened (Figure 4-10).

hlh-2(bx108) hermaphrodites develop into “bags”: since *hlh-2(bx108)* hermaphrodites are egg-laying defective (Egl), the larvae hatch within the worm, which results in animals filled with larvae (see Figure 4-10). That allows screening F3 animals within the F2. About 8 -10 F2 bags per F1 were scored. NSMs and NSM sister cells were detected using epifluorescence. The screen was performed at 25°C, which on the one hand allows identifying temperature-sensitive mutations, and also enhances the bag phenotype.

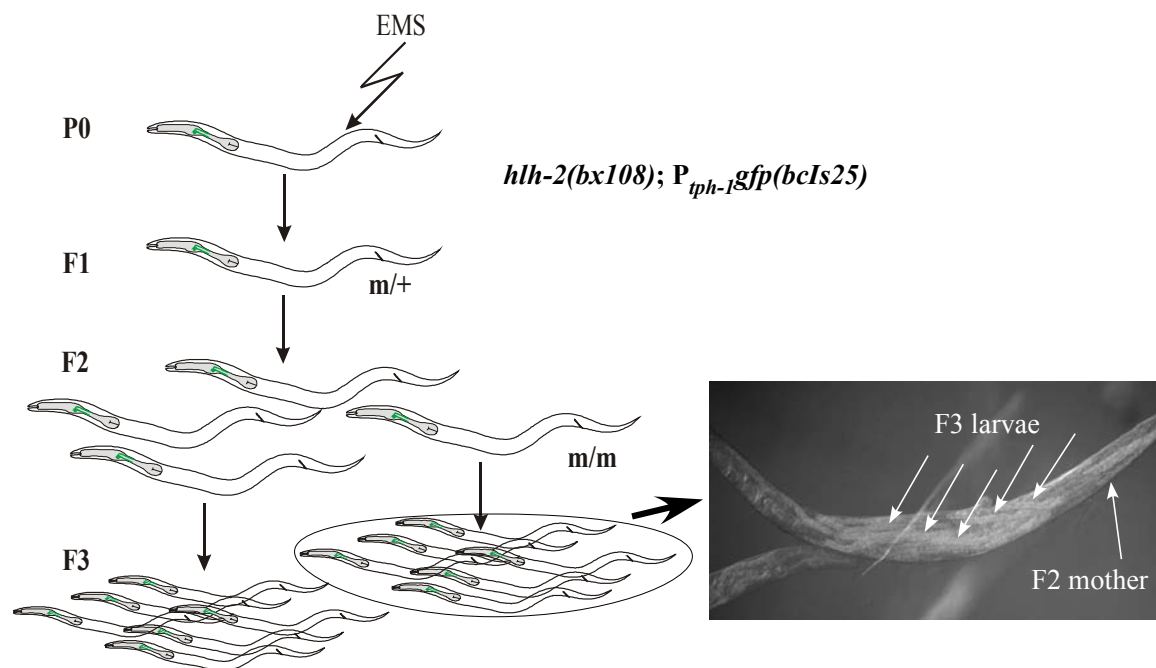


Figure 4-10 The setup of the screen for enhancers of the NSM sister cell survival caused by *hlh-2(bx108)*.

Animals with the genotype *hlh-2(bx108); bcIs25* were mutagenized. F1 animals were isolated clonally, and F2 animals that developed “bags” were scored for populations of F3 larvae with more than 5% NSM sister cell survival by detecting GFP positive cells.

In total, about 2000 haploid genomes were screened, which correspond to more than 8000 “bags”. 14 candidates were isolated that showed enhanced NSM sister cell survival. Mutations were expected that either block cell death in general (Ced phenotype) or that block only specific cell death events (Ces phenotype). To determine whether the 14 candidate mutations cause a Ced or a Ces phenotype, the anterior pharynx of the newly identified mutants was examined for extra cells (4.2). Four mutants (*bc244*, *bc245*, *bc246*, and *bc247*) showed additional extra cells in the pharynx, which indicates that they exhibit a Ced phenotype and are likely to affect genes in the central cell death pathway. These mutations were not of interest for cell-specific activators of *egl-1*. The remaining ten candidates, however, had mutations that only affected specific cell death events (see below).

4.3.2.1 Summary of candidates

Ten candidates were isolated (4.3.2) that specifically enhance the NSM sister cell survival phenotype caused by *hlh-2(bx108)*. These candidates were back crossed to

hllh-2(bx108); bcIs25 animals in order to eliminate background mutations, and analyzed for NSM sister cell survival at 20°C as well as at 25°C. A summary of the data is shown in Table 4-7.

Table 4-7 Summary of mutants isolated in a screen for enhancers of the NSM sister cell survival caused by *hllh-2(bx108)*.

Candidate	NSM sister cell survival		
	[%] (n)		
	20°C	25°C	out crossed
<i>hllh-2(bx108); +/+</i>	4 (414)	5 (408)	
<i>hllh-2(bx108); bc97</i>	15 (136)	9 (76)	4
<i>hllh-2(bx108); bc211</i>	20 (134)	18 (130)	3
<i>hllh-2(bx108); bc212</i>	60 (134)	32 (152)	5
<i>hllh-2(bx108); bc213</i>	91 (100)	87 (30)	3
<i>hllh-2(bx108); bc214</i>	85 (100)	n.d.	3
<i>hllh-2(bx108); bc240</i>	29 (118)	25 (92)	4
<i>hllh-2(bx108); bc241</i>	2 (108)	26 (50)	1
<i>hllh-2(bx108); bc242</i>	22 (130)	48 (120)	3
<i>hllh-2(bx108); bc252</i>	2 (46)	15 (102)	1
<i>hllh-2(bx108); bc260</i>	9 (68)	21 (48)	1

All strains carried *bcIs25*.

4.3.2.2 Analysis of the *Ces* phenotype of the identified mutants

Two genes, which, when mutated, cause the NSM sisters to survive have already been described, namely *ces-1* and *ces-2* (Ellis and Horvitz, 1991 {Metzstein, 1996 #392; Metzstein and Horvitz, 1999}). A *ces-1(gf)* mutation not only results in the survival of the NSM sisters but also causes the I2 sisters, which normally die, to survive. However, a *ces-2(lf)* mutation only interferes with the NSM sister cell death, but not the I2 sister cell death (see Figure 4-11).

sister cell survival. The NSM sisters of *hlh-2(bx108); bcIs25; bc241* L4 larvae that were shifted from 25°C to 20°C as L2/L3 larvae survived with a frequency of 16% (n=84) whereas the control animals that stayed at 25°C showed a survival rate of 20% (n=190). A similar result was observed for *hlh-2(bx108); bcIs25; bc252* animals with 16% NSM sister cell survival (n=86) versus 15% (n=102). As it was much easier to count extra cells in animals grown at 20°C for a certain period of time, this experimental procedure was used to analyze the effect of *bc241* and *bc252* on the survival of certain cells in the anterior pharynx.

Table 4-8 Candidates have different Ces phenotypes.

genotype	extra cells	NSM	I2	m2	other	n
		sister cells	sister cells	sister cells		
+/+	0	0	0	0	0	9
<i>hlh-2(bx108)</i>	0.4	0.05	0	0.3	0.05	27
<i>ces-1(n703)</i>	3.8	1.9	1.6	0	0.3	9
<i>ces-2(n732)</i>	0.4	0.3	0	0	0.1	15
<i>hlh-2(bx108); bc211</i>	1.8	0.8	0.4	0.4	0.2	17
<i>hlh-2(bx108); bc212</i>	1.5	1.2	0	0.3	0	6
<i>bc213</i>	2	1.9	0	0	0.1	8
<i>bc214</i>	1.5	1.5	0	0	0	10
<i>hlh-2(bx108); bc240</i>	1.6	0.6	0.6	0.2	0.2	37
<i>hlh-2(bx108); bc241</i>	1.3	0.4	0.4	0.3	0.1	18
<i>hlh-2(bx108); bc242</i>	1.6	0.7	0.3	0.5	0.1	11
<i>hlh-2(bx108); bc252</i>	0.5	0.2	0.2	0.1	0	13

The anterior pharynx was analyzed for extra cells using Nomarski optics. Cells were identified by their position. All strains additionally carried *bcIs25*. Animals were raised at 20°C except *bc241* and *bc252*

4.3.2.3 Linkage analysis and characterization of the candidates

The ten candidates were further characterized, and linkage experiments were performed to determine on which chromosome these mutations are located. The analysis of *bc212* is described in a separate chapter (4.4).

4.3.2.3.1 *bc97*

The NSM sister cell survival caused by *bc97* in an *hlh-2(bx108)* background is cold sensitive (see Table 4-9). However, although the NSM sister cell survival phenotype is stronger at 20°C (15%) than at 25°C (9%), animals kept at 25°C grow slower and appear sicker than animals grown at 20°C.

hllh-2(bx108); bc97/+ animals did not have any surviving NSM sister cells (n=30), which indicates that *bc97* is a recessive mutation.

The screen was performed in a *hllh-2(bx108)* background, and for that reason, it is possible that the phenotype caused by *bc97* is dependent on *hllh-2(bx108)*. In order to remove the *hllh-2(bx108)* mutation, the strain was crossed with *unc-29(e193); bcIs25* mutant animals. *unc-29* (at 3.28) is located close to *hllh-2* (at 1.84), and *e193* is a recessive If mutation of *unc-29*. Thus, F2 animals that show uncoordinated movement or and Unc (Unc, uncoordinated) phenotype and for this reason are homozygous for *unc-29(e193)* should be wild-type for *hllh-2*. 20 F2 Unc animals were picked clonally and their progeny was scored for NSM sister cell survival. The progeny of 16 F2s showed no NSM sister cell survival, whereas the progeny of four F2s exhibited a very weak phenotype with an average NSM sister cell survival of 3% (n=62-100). Therefore, it is very likely that these animals present *bcIs25; bc97* animals. This result suggests that *hllh-2(bx108)* enhances the phenotype. Also, these results indicate that *bc97* segregates independently from *unc-29* and therefore is not linked to Chromosome I. Further linkage analysis was carried out in a *hllh-2(bx108)* mutant background with different strains each with a phenotypic marker on a specific chromosome. As phenotypic markers recessive mutations were used that either cause a Unc phenotype, a Dpy phenotype (Dpy, Dumpy, animals are shorter and fat), or a Lon phenotype (lon, long.) *hllh-2(bx108); bcIs25; him-5(e1490); bc97* animals were crossed with the marker strains (see Table 4-9). The F2 Unc, Dpy, and Lon animals, respectively, were plated clonally, and their progeny was scored for the *bc97* phenotype. Results are shown in Table 4-9. Since no homozygous *dpy-25(e817)* animal was isolated that is also homozygous for *bc97*, *bc97* is very likely linked to *dpy-25* and therefore located on linkage group II. This linkage is furthermore supported strengthened by the fact that *bc97* segregates independently from *dpy-19* on III, *dpy-20* on IV, *dpy-11* on V, and *lon-2* on X.

Table 4-9 *bc97* is linked to Chromosome II.

marker	LG	F2 homozygous for the phenotypic marker		
		<i>bc97/bc97</i>	<i>bc97/+</i> +/+	and % <i>bc97/bc97</i>
<i>dpy-25</i>	II	0	24	0
<i>dpy-19</i>	III	7	13	35
<i>dpy-20</i>	IV	6	10	38
<i>dpy-11</i>	V	2	8	20
<i>lon-2</i>	X	3	13	19

hlh-2(bx108); bcIs25; him-5(e1490); bc97 animals were crossed with *hlh-2(bx108); dpy-25(e817); bcIs25, hlh-2(bx108); dpy-19(e1259); bcIs25, hlh-2(bx108); dpy-20(e1282) bcIs25, hlh-2(bx108); bcIs25; dpy-11(e224), hlh-2(bx108); bcIs2;* *lon-2(e678)*, respectively. F2 animals homozygous for the markers were isolated clonally, and their progeny was analysed for the *bc97* phenotype.

To map *bc97* on Chromosome II, a three-factor mapping experiment was performed with *dpy-10(e128)* and *unc-4(e120)*. *hlh-2(bx108); bc97; bcIs25; him-5(e1490)* animals were crossed with *hlh-2(bx108); dpy-10(e128) unc-4(e120); bcIs25* animals and the recombinant F2 Dpy non-Uncs and Unc non-Dpys were isolated, homozygosed for the recombinant chromosome, and analyzed for NSM sister cell survival. Three out of five *hlh-2(bx108); dpy-10(e128)* animals had the *bc97* phenotype, but only one of eleven *hlh-2(bx108); unc-4(e120)* animals also carried *bc97*. This suggests that *bc97* might be located between *dpy-10* and *unc-4* and closer to *unc-4*.

Interestingly, as shown in Figure 4-12, *hlh-3*, an *Achaete-Scute*-like *bHLH* gene required for the death of the NSM sister cells (4.3.1.2.2), is located between *dpy-10* and *unc-4*. Since *hlh-3* seems to be an excellent candidate gene for *bc97*, the *hlh-3* locus of *bc97* mutants was sequenced, however, no mutation was found.

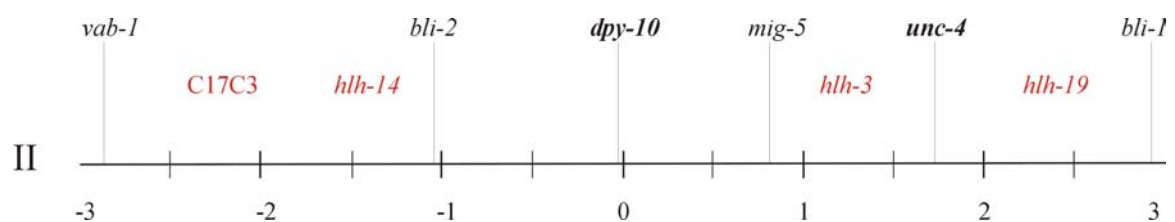


Figure 4-12 Genetic map of the center of Chromosome II. According to a three-factor mapping experiment with *dpy-10* and *unc-4*, *bc97* maps closely to the left and close to *unc-4*.

In order to determine how close *bc97* is located to *dpy-10*, two factor mapping was done with the strain *hlh-2(bx108); bc97 dpy-10(e128); bcIs25* and *hlh-2(bx108); bcIs25*. In the F2, 52 Dpy animals were picked clonally and their progeny was scored for NSM sister cell survival. 26 animals were homozygous for *bc97*, 26 animals, however, had recombined between *bc97* and *dpy-10*. These data exhibit that *bc97* is not, as assumed, closely linked to *dpy-10*, but indeed maps far away (33 m. u.).

Table 4-10 Results of the Two factor mapping of *bc97* with *dpy-10(e128)*.

marker	F2 with parental chromosome: <i>m bc97</i>	F2 with recombinant chromosome: <i>m +</i>
<i>dpy-10</i>	26	26

hlh-2(bx108); bcIs25 males were crossed with *hlh-2(bx108); dpy-10(e128) bc97; bcIs25* hermaphrodites. Dpy F2 animals were isolated, and NSM sister cell survival of their progeny was scored after at least two generations to determine the presence of *bc97*.

4.3.2.3.2 *bc211*

hlh-2(bx108); bcIs25; bc211 animals show an NSM sister cell survival of about 20%, which is not temperature sensitive (4.3.2.1). Linkage analysis was performed as described for *bc97* (4.3.2.3.1). The results shown in Table 4-11 clearly indicated that *bc211* is linked to Chromosome X.

Table 4-11 *bc211* is linked to Chromosome X.

marker	LG	F2 animals homozygous for the phenotypic marker		
		<i>bc211/bc211</i>	<i>bc211/+</i> +/+	and % <i>bc211/bc211</i>
<i>dpy-25</i>	II	6	9	40
<i>dpy-19</i>	III	5	7	42
<i>dpy-20</i>	IV	3	17	15
<i>dpy-11</i>	V	3	7	30
<i>lon-2</i>	X	0	19	0

hlh-2(bx108); bcIs25; bc211 were crossed with *hlh-2(bx108); dpy-25(e817); bcIs25, hlh-2(bx108); dpy-19(e1259); bcIs25, hlh-2(bx108); dpy-20(e1282) bcIs25, hlh-2(bx108); bcIs25; dpy-11(e224), hlh-2(bx108); bcIs2; lon-2(e678)*, respectively. F2s homozygous for the markers were isolated clonally, and their progeny was analysed for the *bc211* phenotype.

This conclusion is further supported by the fact that the NSM sister cells of the male progeny of the cross of (*hlh-2*)*bx108; bcIs25* males with *hlh-2(bx108); bcIs25; bc211* hermaphrodites was 21% (n=80). These males are hemizygous for the X chromosome of their mother, and therefore only have Chromosome X with the *bc211* mutation, and have the *bc211* phenotype.

To determine if the phenotype of *bc211* is dependent on *hlh-2(bx108)*, *hlh-2(bx108); bcIs25; bc211* animals were crossed with *unc-29(e193); bcIs25* (4.3.2.3.1). The progeny of five out of 29 Unc F2s showed the NSM sister cell survival phenotype of *bc211*. Therefore, this phenotype is independent of *hlh-2(bx108)*. In *bcIs25; bc211* animals, at 20°C, the NSM sister cell survive with a frequency of 17% (n=17).

It should also be mentioned that I was not able to obtain males by heat shock, or by *him-14(RNAi)*. Introducing a mutation of *him-5, e1490*, which results in a higher frequency of males (Broverman and Meneely, 1994), leads to the generation of phenotypically normal *bc211* males. These males, however, do not mate, suggesting that the gene affected by *bc211* has other functions other than specifying the NSM sister and I2 sister cell death.

4.3.2.3.3 *bc213* and *bc214* represent new alleles of *ces-2*

The *bc213* and *bc214* mutations are very similar. In an *hlh-2(bx108)* background they result in a rather strong NSM sister cell survival phenotype of 91% and 85%,

respectively. The NSM sister cell survival is not dependent on *hlh-2(bx108)* as in a wild-type background, *bc213* and *bc214* cause 89% or 70% of the NSM sisters to survive (Table 4-12). Linkage analysis mapped both *bc213* and *bc214* to Chromosome I (data not shown). In addition, phenotypically, *bc213* and *bc214* show similarities as both mutations only affect the NSM sister cell death but not the I2 sister cell death. The gene *ces-2* is located on Chromosome I and is required for the NSM sister cell death but not the I2 sister cell death, suggesting that *bc213* and *bc214* are new mutations in *ces-2*. Indeed, complementation analysis showed that *bc213* and *bc214* failed to complement each other, implying that they are mutations in the same gene. In addition, they failed to complement *ces-2(n732)*, indicating that *bc213* and *bc214* are mutations in the *ces-2* gene.

Table 4-12 Complementation Analysis

Genotype	NSM sister cell survival [%]	n
+/+	0	414
<i>ces-2(n732)</i>	38	112
<i>bc213</i>	89	106
<i>bc214</i>	70	546
<i>+/bc213; lon-2/+</i>	11	46
<i>bc213/n732</i>	70	40
<i>n732/bc213</i>	90	20
<i>bc214/n732</i>	53	30

All strains carried *bcIs25*. Experiments were performed at 20°C.

4.3.2.3.3.1 *bc213* results in an early stop codon in the *ces-2* coding region

The coding region of the *ces-2* locus of *bc213* mutants was sequenced, and a T to C transition in position 51 of the coding region was found. This mutation results in a stop codon indicating that no functional protein is transcribed. This strongly suggests that *bc213* results in a null mutation in *ces-2* (see Figure 4-13).

Also, the coding region of the *ces-2* locus of *bc214* mutants was sequenced, however, no mutation was identified. *bc214* might therefore cause a mutation in the regulatory regions of the *ces-2* locus.

```

1  ATGGA CTTTC ATAGAGCACT ATCGGCGCTT TTCACAAATC AAGCAGCCGT
51  TCAACCACTG CTCGGCTCAC TTGGTTTCCC ATTCAACGAC GGAACCTCTA
101 TTCTGACGAC TGCACTTGCT GCACAGTCCG GCGGAAAGAA GTTGGACACT
151 CCGTTGGGGA TTTTACCATT TGACTCACTG CCCACGACAA ATCTTTTAAAC
201 ACCAACCAAG AAGATCAAAC TAGAAGATGA ATTGTGTGCC AGTCCAGTGT
251 CAAGCAGGTC GAGTACGGTT AGCAGTTCAC AC

1  MDFHRALSAL FTNQAAVQPL LGSLGFPFND GTSILTALA AQS GGK KLDLT
51  PLGILPFDSL PTTNLLTPTK KIKLEDELCA SPVSSRSSTV SSSH

```

Figure 4-13 DNA and amino acid sequence of exon 1 of *ces-2*.

bc213 is represented by a T to C transition from in position 51 (shaded in grey). The mutation results in a stop at position 18 of the amino acid sequence (shaded in grey).

4.3.2.3.4 *bc240*

hlh-2(bx108); bcIs25; bc240 animals exhibit a NSM sister cell survival phenotype of 29%, which is not temperature sensitive (4.3.2.1). Linkage analysis (performed as in 4.3.2.3.1) clearly located *bc240* on Chromosome IV as shown in Table 4-13.

Table 4-13 *bc240* links to Chromosome IV.

marker	LG	F2 animals homozygous for the phenotypic marker		
		<i>bc240/bc240</i>	<i>bc240/+</i> +/+	and % <i>bc240/bc240</i>
<i>dpy-5</i>	I	4	12	25
<i>unc-4</i>	II	3	16	25
<i>dpy-19</i>	III	6	12	33
<i>dpy-20</i>	IV	0	13	0
<i>dpy-11</i>	V	4	16	20
<i>lon-2</i>	X	3	17	15

hlh-2(bx108); bcIs25; bc240 were crossed with *dpy-5(e61) hlh-2(bx108); bcIs25*, *hlh-2(bx108); dpy-25(e817); bcIs25, hlh-2(bx108); dpy-19(e1259); bcIs25, hlh-2(bx108); dpy-20(e1282) bcIs25, hlh-2(bx108); bcIs25; dpy-11(e224), hlh-2(bx108); bcIs2*; *lon-2(e678)*, respectively. F2s homozygous for the markers were isolated clonally, and their progeny was analysed for the *bc240* phenotype.

When *hlh-2(bx108); bcIs25 bc242* animals were crossed with *unc-29(e193); bcIs25* animals, 18 Unc F2 were isolated, and none of them exhibited a *bc240* phenotype.

Therefore, the NSM sister cell survival caused by *bc240* is dependent on *hlh-2(bx108)*.

bc240 was mapped on Chromosome IV relatively to *unc-5* and *dpy-20* with a three-factor Mapping experiment. For this experiment, *hlh-2(bx108); bcIs25 bc240* males were crossed with *hlh-2(bx108); bcIs25 unc-5(e53) dpy-20(e1282ts)* hermaphrodites. In the F2 generation, 12 non-Dpy Unc animals and 12 non-Unc Dpy animals recombinants, respectively, were isolated, homozygosed for the recombinant chromosome, and scored for NSM sister cell survival. All Uncs showed the *bc240* phenotype whereas none of the Dpys showed the phenotype (Table 5). This suggests that *bc240* is right to *unc-5*.

Table 4-14 Three-factor mapping data for *bc240* with *dpy-20(e1282ts) unc-5(e53)*.

non-Unc Dpy NSM sister cell survival [%]			Unc non-Dpy NSM sister cell survival [%]		
		n			n
1	2	60	1	13	70
2	4	50	2	19	64
3	0	60	3	15	60
4	3	60	4	20	44
5	6	50	5	21	56
6	3	60	6	22	54
7	5	64	7	23	60
8	2	60	8	20	50
9	0	60	9	26	50
10	0	60	10	23	60
11	2	62	11	20	50
12	10	48	12	22	50

All animals additionally carried *hlh-2(bx108)* and *bcIs25* in their background. In red, the *bc240* phenotype is indicated.

Next, a two-factor-Mapping experiment with *unc-5* was performed to determine the distance between *bc240* and *unc-5*. *hlh-2(bx108); bcIs25* males were crossed with *hlh-2(bx108); unc-5(e53) bcIs25 bc240* hermaphrodites. In the F2 generation, Dpy animals were picked clonally, and their progeny was scored for NSM sister cell survival to determine if recombination had occurred. As shown in Table 4-15, 8 out of 37 Uncs had recombined between *unc-5* and *bc240*. Calculating the distance, this experiment places *bc240* 12 m.u. (m.u., map unit) far from *unc-5*, which is at about 13.8 m.u..

Table 4-15 Results for the Two factor mapping of *bc240* with *dpy-20(e1282ts)*.

Marker	Number of F2 animals with parental chromosome: <i>m bc242</i>	Number of F2 animals with recombinant chromosome: <i>m +</i>
<i>dpy-20</i>	29	8

hlh-2(bx108); bcIs25 males were crossed with *hlh-2(bx108); dpy-20(e1282ts) bcIs25 bc240* hermaphrodites. Dpy F2 animals were isolated, and NSM sister cell survival of their progeny was scored after at least two generations to determine the presence of *bc242*.

A gene already known to be involved in the regulation of the NSM sister cell death also maps into this region, namely *ces-3*. Complementation analysis, however, does not support the hypothesis that *bc240* is a new allele of *ces-3*, since *hlh-2(bx108)/+; bcIs25 bc240/ces-3(n1952)* animals don't show a NSM sister cell survival phenotype (0%, n=100).

Unfortunately, *bcIs25* was mapped to 8.5 m.u. on LGIV (Thellmann, 2002), and therefore is closely linked to *bc240*. This causes problems with further mapping experiments, since all mapping strains need *bcIs25* in their background. Therefore, it was attempted to separate *bc240* from *bcIs25*. For this purpose, *hlh-2(bx108); bcIs25 bc240* males were crossed with *unc-26(e205) dpy-4(e1166)* hermaphrodites. The map position of *unc-26* and *dpy-4* are 8.52 and 12.70, respectively. Recombination events between *unc-26* and *dpy-4* can be easily identified, and are likely to also occur between *bcIs25* and *bc240*, since first results suggest that *bcIs25* is closely linked to *unc-26* whereas *bc240* is closely linked to *dpy-4*. Recombinants were isolated. Unfortunately all of them were also gfp positive, and therefore had not lost *bcIs25*. However, one Unc non-Dpy recombinant was obtained that also showed the *bc240* phenotype. In addition, one Dpy non-Unc recombinant was obtained. Since recombination had occurred both between *bc240* and *unc-26*, and *bc240* and *dpy-4* must be located in between the region spanned by *unc-26* and *dpy-4*. The same applies for *bcIs25* (see Figure 4-14).

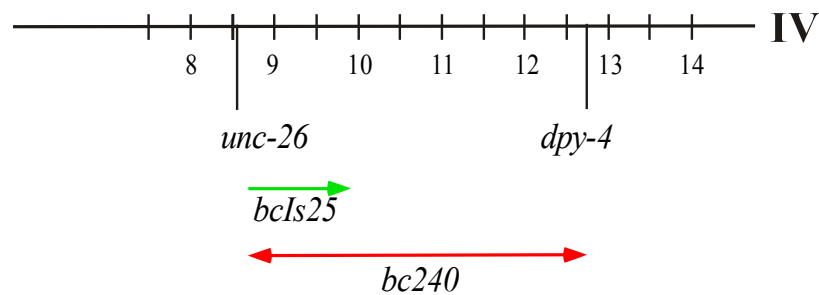


Figure 4-14 *bc240* is located between *unc-26* and *dpy-4* in close vicinity to *bcIs25*.

4.3.2.3.5 *bc241*

bc241 is a temperature-sensitive mutation. Linkage analysis was performed, however, the results obtained were not completely clear, since linkage was observed to both *dpy-5* on Chromosome I and *dpy-11* on Chromosome V (see Table 4-16).

Table 4-16 *bc241* is linked to Chromosome I.

marker	LG	F2 animals homozygous for the phenotypic marker		
		<i>bc241/bc241</i>	<i>bc241/+</i> +/+	and % <i>bc241/bc241</i>
<i>dpy-5</i>	I	1	18	5
<i>unc-4</i>	II	3	17	15
<i>dpy-19</i>	III	n. d.	n. d.	
<i>dpy-20</i>	IV	4	15	21
<i>dpy-11</i>	V	1	19	5
<i>lon-2</i>	X	5	13	27

hlh-2(bx108); bcIs25; bc241 were crossed *dpy-5(e61) hlh-2(bx108); bcIs25, hlh-2(bx108); dpy-25(e817); bcIs25, hlh-2(bx108); dpy-19(e1259); bcIs25, hlh-2(bx108); dpy-20(e1282) bcIs25, hlh-2(bx108); bcIs25; dpy-11(e224), hlh-2(bx108); bcIs2; lon-2(e678)*, respectively. F2s homozygous for the markers were isolated clonally, and their progeny was analysed for the *bc241* phenotype.

A two factor experiment was performed with *dpy-11(e24)* as well as *dpy-5(e61)*. The results from the two factor mapping experiment show that *bc241* is not linked to Chromosome V: only three *dpy-1(e224)* animals out of 20 showed the *bc241* phenotype. *bc241* is weakly linked to *dpy-5* on Chromosome I, though. 17 *dpy-5(e61)* animals out of 35 were homozygous for *bc241* as determined by the NSM sister cell survival phenotype. Therefore, a distance of 35 m.u. away from *dpy-5* (0.00) was calculated. For this reason, *bc241* seems to be located on an arm of Chromosome I.

Interestingly, *ces-2* is also located on a chromosome arm of I (28.96). *ces-2* is required for the NSM sister cell death (Ellis and Horvitz, 1991; Metzstein et al., 1996), and therefore an interesting candidate for *bc241*. Complementation analysis with *ces-2(n732)* and *bc241* was performed. Since both mutations are temperature sensitive, the experiment was performed at 25°C. As shown in Table 4-17, *bc241* complements *ces-2(n732)*, and therefore is most likely not a mutation in *ces-2*. Moreover, *bc241* also affects the cell death of the I2 sister cells, whereas a strong *lf* mutation in *ces-2* only blocks the death of the NSM sister cells (4.3.2.2).

Table 4-17 *bc241* complements *ces-2(n732)*.

Genotype	NSM sister cell survival [%]	n
δ/δ		
<i>hlh-2(bx108) bc241</i>	26	50
<i>ces-2(n732)</i>	73	*
<i>ces-2(n732)/hlh-2(bx108) bc241</i>	5	80
+ <i>ces-2(n732)/hlh-2(bx108)</i> +	1	70
<i>ces-2(n732)/+</i>	3	30
<i>hlh-2(bx108) +/hlh-2(bx108) bc241</i>	7	46

All strains and crosses were kept at 25°C. All animals additionally carried *bcl525*. * (Theilmann, 2002)

4.3.2.3.6 *bc242*

bc242, a mutation that causes a temperature-sensitive NSM sister cell survival phenotype in a *hlh-2(bx108)* background (4.3.2.1), is linked to Chromosome IV as determined by linkage analysis shown in Table 4-18.

Table 4-18 *bc242* is linked to Chromosome IV.

marker	LG	F2 animals homozygous for the phenotypic marker		
		<i>bc242/bc242</i>	<i>bc242/+</i> +/+	and % <i>bc242/bc242</i>
<i>dpy-5</i>	I	3	14	18
<i>unc-4</i>	II	1	12	8
<i>dpy-19</i>	III	3	14	18
<i>dpy-20</i>	IV	0	17	0
<i>dpy-11</i>	V	5	15	25
<i>lon-2</i>	X	5	15	15

hlh-2(bx108); bcIs25; bc242 were crossed with *dpy-5(e61) hlh-2(bx108); bcIs25, hlh-2(bx108); dpy-25(e817); bcIs25, hlh-2(bx108); dpy-19(e1259); bcIs25, hlh-2(bx108); dpy-20(e1282) bcIs25, hlh-2(bx108); bcIs25; dpy-11(e224), hlh-2(bx108); bcIs2; lon-2(e678)*, respectively. F2s homozygous for the markers were isolated clonally, and their progeny was analysed for the *bc242* phenotype.

To determine if the NSM sister cell survival caused by *bc242* is dependent on *hlh-2(bx108)*, *bcIs25* males were crossed with *hlh-2(bx108) dpy-5(e61); bcIs25 bc242* hermaphrodites. Since *dpy-5* is closely linked to *hlh-2*, the *bx108* mutation should segregate with *dpy-5(e61)*. In the F2 generation, 20 non-Dpy hermaphrodites were isolated clonally. One quarter (5 in this case) of the F2 should be homozygous for *bc242*. None of the progenies of the F2s, however, showed the *bc242* phenotype. Therefore, I conclude that the NSM sister cell survival phenotype caused *bc242* is most likely dependent on the presence of *hlh-2(bx108)*.

As shown in Table 4-19, a three-factor experiment with *unc-5* and *dpy-20* on Chromosome IV (Figure 4-15) mapped *bc242* between these two genes, as recombination occurred both between *bc242* and *unc-5*, and between *bc242* and *dpy-20*.

Table 4-19 Three-factor mapping data for *bc242* with *unc-5(e53) dpy-20(e1282ts)*.

non-Unc Dpy			Unc non-Dpy		
	NSM sister cell survival [%]	n		NSM sister cell survival [%]	n
1	20	76	1	23	60
2	6	80	2	7	248
3	15	92	3	16	158
4	4	80	4	20	136
5	0	80	5	18	62
6	0	64	6	17	36
7	6	88	7	5	186
8	4	80	8	17	100
			9	12	58

hlh-2(bx108); bcIs25 bc242 males were crossed with *hlh-2(bx108); unc-5(e53) dpy-20(e1282ts) bcIs25* hermaphrodites. Recombinants between *unc-5* and *dpy-20* were isolated in the F2 generation, homozygosed for the recombinant chromosome, and analyzed for NSM sister cell survival. Red numbers indicate animals that are homozygous for *bc242*.

Two-factor mapping experiments with both *unc-5* and *dpy-20* were performed to obtain more information. Results are shown in Table 3 and 4. These data place *bc242* 5.3 m.u. from *unc-5*, and 8.0 m.u. from *dpy-20*.

Table 4-20 Results of the two-factor mapping of *bc242* with *unc-5(e53)* and *dpy-20(e1282ts)*.

marker	F2 with parental chromosome: <i>m bc242</i>	F2 with recombinant chromosome: <i>m +</i>
<i>unc-5</i>	27	3
<i>dpy-20</i>	23	4

hlh-2(bx108); bcIs25 males were crossed with *hlh-2(bx108); unc-5(e53) bcIs25 bc242* hermaphrodites and *dpy-20(e1282ts) bcIs25 bc242* hermaphrodites, respectively. Unc and Dpy F2 animals were isolated, and NSM sister cell survival of their progeny was scored to determine the presence of *bc242*.

An additional three-factor mapping experiment with *bc242* was performed with two markers located more on the right arm, namely *unc-30* (7.97) and *dpy-4* (12.73). Results are shown in Table 4-21.

Table 4-21 Results of the three-factor mapping of *bc242* with *unc-30(e191)* and *dpy-4(e1166)*.

non-Unc Dpy			Unc non-Dpy		
	NSM sister cell survival [%]	n		NSM sister cell survival [%]	n
1	12	52	1	2	60
2	11	72	2	2	60
3	12	74	3	3	60
4	14	72	4	2	60
5	15	48	5	0	40
6	15	34	6	0	40
7	14	42	7	2	96

hlh-2(bx108); unc-30(e191) bcIs25 dpy-4(e1166) hermaphrodites were crossed with *hlh-2(bx108); bcIs25 bc242* males. Unc non Dpy and Dpy non Unc recombinants were isolated, made homozygous and scored for NSM sister cell survival. Red numbers indicate animals that are homozygous for *bc242*.

These results indicated that *bc242* maps to the left of *unc-30*, and between *unc-5* and *dpy-20* (see Figure 4-15).

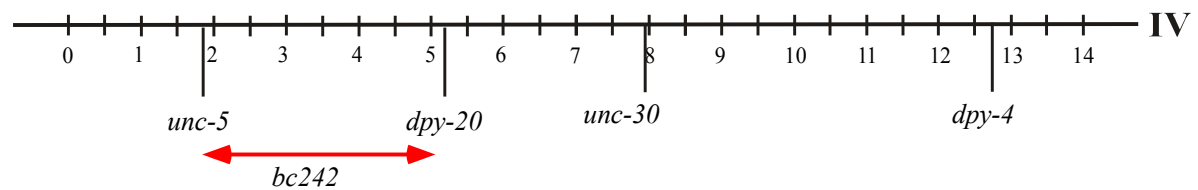


Figure 4-15 *bc242* is located between *unc-5* and *dpy-20* on Chromosome IV.

To further narrow down the region in which *bc242* is located, SNP mapping was performed. SNPs are single nucleotide polymorphism between two divergent populations, e. g., as used here, strains derived from *C. elegans* isolated in Bristol (N2) and Hawaii (CB4856) (Jakubowski and Kornfeld, 1999; Koch et al., 2000; Wicks et al., 2001). These SNPs often result in the absence or presence of specific restriction sites in either N2 or CB4856, and can therefore easily be used to test where a recombination event between a N2 and a CB4856 chromosome had occurred. *hlh-2(bx108); unc-5(e53) bc242 dpy-20(e1282) bcIs25* hermaphrodites (N2 background) were crossed with Hawaii males with the genotype *hlh-2(bx108); bcIs25*. 36 Unc non-Dpys and 43 Dpy non-Uncs were isolated in the F2, made homozygous for the recombinant chromosome, and tested for SNPs between *unc-5* and *dpy-20*. Recombination events were located by testing SNPs in that region for being N2 or CB4856, and the recombinants were tested for *bc242* by scoring NSM sister cell survival. Using this mapping strategy, *bc242* was located relative to a region between the SNP at position 24865 of F20C5 and the SNP at position 7442 of C01F6 (Figure 4-16).

This region is spanned by 11 cosmids and 62 predicted genes. The gene that is mutated by *bc242* should be identified by performing transformation rescue experiments with these cosmids. Alternatively, knocking down the function of the genes in this region by RNAi could identify the gene that is mutated by *bc242*.

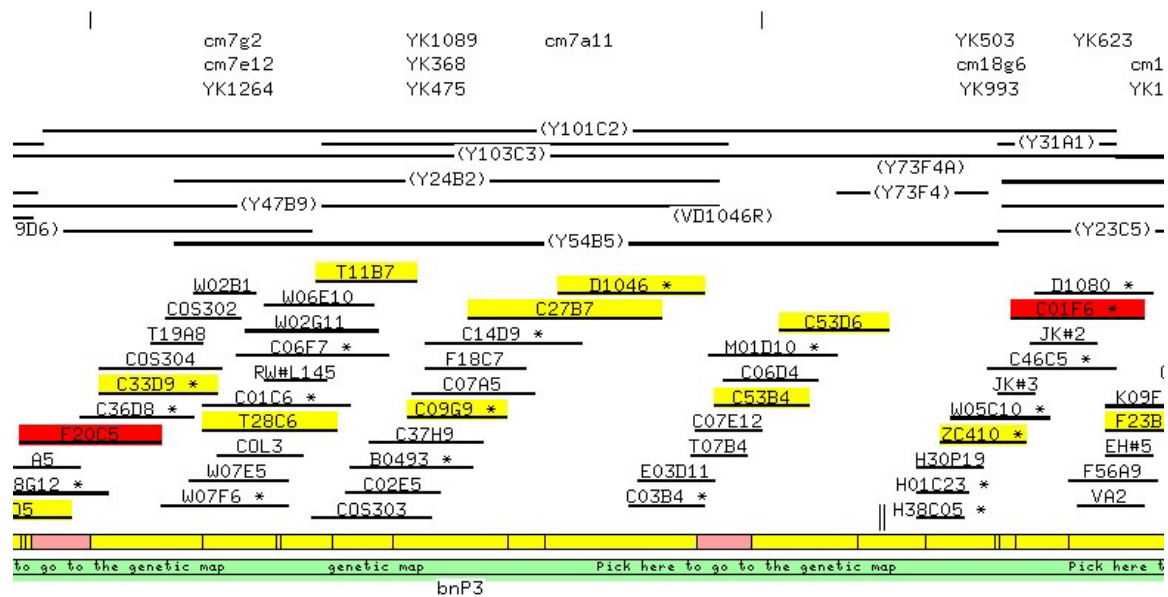


Figure 4-16 Representation of the *bc242* region on Chromosome IV. *bc242* maps between cosmid F20C5 and C01F6 indicated in red. In yellow, available cosmids that span the region are indicated

4.3.2.3.7 *bc252*

bc252 is a temperature-sensitive mutation that causes the NSM sister cells to survive with a frequency of 15% at 25°C in a *hlh-2(bx108)* background but does not cause a phenotype when animals are raised at 20°C. Linkage analysis did not show linkage to any chromosome (see Table 4-22). Two-factor mapping with *dpy-11(e224)*;; *dpy-5*, and *lon-2* revealed that *bc252* does not segregate with any of these markers.

hlh-2(bx108); *bcIs25* males were crossed with *hlh-2(bx108)*; *bcIs25*; *dpy-11(e224)*; *bc252* hermaphrodites (NSM sister cell survival at 25°C 18%, n=82). Only three Dpy F2 animals out of 18 had progeny with more than 10% NSM sister cell survival (11%, 14%, 16%). For *lon-2(e678)*, it was one out of eight (11%), and for *dpy-5(e61)*, seven out of 30 F2s had progeny with the *bc252* NSM sister cell survival phenotype (11%, 13%, 18%, 15%, 16%, 11%, 11%).

Table 4-22 *bc252* does not show linkage to any chromosome.

marker	LG	F2 animals homozygous for the phenotypic marker		
		<i>bc252/bc252</i>	<i>bc240/+</i> and <i>+/+</i>	% <i>bc252/bc252</i>
<i>dpy-5</i>	I	5	15	25
<i>unc-4</i>	II	3	15	17
<i>dpy-19</i>	III	4	4	50
<i>dpy-20</i>	IV	4	9	31
<i>dpy-11</i>	V	1	18	5
<i>lon-2</i>	X	3	17	15

hlh-2(bx108); bcIs25; bc252 were crossed with *dpy-5(e61) hlh-2(bx108); bcIs25, hlh-2(bx108); dpy-25(e817); bcIs25, hlh-2(bx108); dpy-19(e1259); bcIs25, hlh-2(bx108); dpy-20(e1282) bcIs25, hlh-2(bx108); bcIs25; dpy-11(e224), hlh-2(bx108); bcIs2; lon-2(e678)*, respectively. F2s homozygous for the markers were isolated clonally, and their progeny was analysed for the *bc252* phenotype.

bcIs25 males were crossed with *hlh-2(bx108) dpy-5(e61); bcIs25; bc252* hermaphrodites, None out of 18 Dpy F2 animals showed the *bc252* phenotype. Therefore, it is likely that *bc252* results in an NSM sister cell survival phenotype that is dependent on *hlh-2(bx108)*.

4.3.2.3.8 *bc260*

Similar results as for *bc252* were obtained for *bc260*. *bc260* also does not link to any of the markers as shown in Table 4-23.

Table 4-23 *bc260* does not show linkage to any Chromosome.

marker	LG	F2 animals homozygous for the phenotypic marker		
		<i>bc260/bc240</i>	<i>bc260/+</i> and <i>+/+</i>	% <i>bc260/bc260</i>
<i>dpy-5</i>	I	2	2	50
<i>unc-4</i>	II	5	13	28
<i>dpy-19</i>	III	2	6	25
<i>dpy-20</i>	IV	3	15	17
<i>dpy-11</i>	V	3	12	20
<i>lon-2</i>	X	2	14	13

hlh-2(bx108); bcIs25; bc260 were crossed with *dpy-5(e61) hlh-2(bx108); bcIs25, hlh-2(bx108); dpy-25(e817); bcIs25, hlh-2(bx108); dpy-19(e1259); bcIs25, hlh-2(bx108); dpy-20(e1282) bcIs25, hlh-2(bx108); bcIs25; dpy-11(e224), hlh-2(bx108); bcIs2; lon-2(e678)*, respectively. F2s homozygous for the markers were isolated clonally, and their progeny was analysed for the *bc260* phenotype.

Besides the NSM sister cell survival phenotype, *bc260* animals grow very slowly, are non penetrant sterile, have a reduced brood size, and have a Him (Him, high incidence of males) phenotype.

Furthermore, I tried to outcross *hlh-2(bx108) dpy-5(e61). bcIs25* males were crossed with *hlh-2(bx108) dpy-5(e61); bcIs25; bc60* hermaphrodites. However, although several of isolated non-Dpy F2s had very few progeny and appeared like *bc260* animals by their overall appearance, none of them showed NSM sister cell survival. Therefore, also the NSM sister cell survival phenotype of *bc260* mutants might be dependent on *hlh-2(bx108)*, whereas the other phenotypes caused by *bc260* are not dependent on the presence of *hlh-2(bx108)*.

4.4 *dnj-11* is required for the NSM sister cell death

The last candidate isolated in the screen for enhancers of the weak NSM sister cell survival caused by *hlh-2(bx108)* is *bc212*. *bc212* results in cold-sensitive NSM sister cell survival in a *hlh-2(bx108)* background (4.3.2.1). *bc212* animals show additional

phenotypes, like morphological defects, embryonic lethality, and slow growth (see below). Males mate, albeit their mating efficiency is lower compared to wild type.

4.4.1 Cloning of *bc212*: *bc212* is a mutation in *dnj-11*

Using linkage analysis as described above (4.3.2.3.1), *bc212* was linked to Chromosome IV (data not shown). The NSM sister cell survival caused by *bc212* is only partially dependent on *hlh-2(bx108)* (see below), and as *bc212* alone still results in 28% NSM sister cell survival at 20°C, all following experiments were done in a *hlh-2(+)* background.

A three-factor experiment with *unc-5* and *dpy-20* was performed to determine the approximate position of *bc212* on Chromosome IV. *bcIs25 bc212* males were crossed with *bcIs25 dpy-20(e1282ts) unc-5(e53)* hermaphrodites. F2 recombinants, namely non-Dpy Uncs and Dpy non-Uncs, respectively, were isolated and made homozygous for the recombinant chromosome.

As shown in Table 4-24, recombination had occurred between *bc212* and both markers, hence it is likely that *bc212* is located between *unc-5* and *dpy-20*. Since recombination occurred more often between *dpy-20* and *bc212* than between *unc-5* and *bc212*, *bc212* might be located closer to *unc-5*. Taking the distance between *dpy-20* and *unc-5* in account, the calculated position of *bc212* is about 0.5 m.u. to the right side of *unc-5*.

Table 4-24 Results of the three-factor mapping of *bc212* with *unc-5(e53)* and *dpy-20(e1282ts)*.

Recombinants	<i>bc212</i>	+/+
Unc non-Dpy	1	20
Dpy non-Unc	17	5

bc212 bcIs25 males were crossed with *unc-5(e53) dpy-20(e1282ts) bcIs25* hermaphrodites. Unc non-Dpy and Dpy non-Unc F2 animals were isolated, made homozygous for the recombinant chromosome, and the presence of *bc212* was determined by scoring NSM sister cell survival.

To verify the results, two-factor mapping analysis with *unc-5(e53) bc212* was performed. *bcIs25* males were crossed with *bcIs25 bc212 unc-5(e53)* hermaphrodites. In the F2 generation, 34 Unc animals were isolated and checked for NSM sister cell survival after two or three generations. It is easier to distinguish whether *bc212* is heterozygous or homozygous after two or three generations, since *bc212* animals grow very slowly and therefore are overgrown soon. The results are shown in Table

4-25. Two out of 34 Unc F2 animals were recombinant, and therefore, the calculated distance between *bc212* and *unc-5* is 2.9 m.u..

Table 4-25 Results of the Two factor mapping of *bc212* with *unc-5(e53)*.

marker	F2 with parental chromosome: <i>m bc212</i>	F2 with recombinant chromosome: <i>m +</i>
<i>unc-5</i>	32	2

bclIs25 males were crossed with *unc-5(e53) bc212 bclIs25*. Unc F2 animals were isolated, and NSM sister cell survival of their progeny was scored after at least two generations to determine the presence of *bc212*.

To further map *bc212*, SNP mapping (4.3.2.3.6) was performed. *unc-5(e53) bc212 dpy-20(e1282ts) bclIs25* hermaphrodites were crossed with Hawaii males carrying *bclIs25*, and in the F2 generation, recombinants between *unc-5* and *dpy-20* were isolated. In total, 121 Unc non-Dpys and 95 Dpy non-Uncs were isolated. *bc212* mapped between the SNP in C43G2 at position 22057 and the SNP in C17H12 at position 33927 (Figure 4-17).

This region is covered by the YAC Y37B6. Transformation rescue experiments with Y73B6 were performed to test whether an extrachromosomal array containing the wild-type locus of the gene affected by *bc212* can rescue the NSM sister cell survival phenotype caused by *bc212*, and to confirm that the gene defined by *bc212* is in that interval. As shown in Table 4-26, the death of the NSM sisters was rescued in two out of 5 transgenic lines containing Y73B6, confirming that wt copy of the gene affected by *bc212* can rescue the phenotype, and that *bc212* indeed is located in that region. When performing transformation rescue experiments with the single cosmids in this region, it was shown that the cosmid F38A5 rescues the NSM sister cell death (Table 4-26), and therefore, the gene affected by *bc212* must be located on that particular cosmid.

Table 4-26 Transformation rescue experiments reveal that the gene affected by *bc212* is located on Cosmid F38A5.

YAC/Cosmid	line	NSMs [%]	n	rescue
-	-	28	214	-
Y37B6	1	14	102	-
	2	12	78	-
	3	15	48	-
	4	0	12	+++
	5	5	224	++
C43G2	1	21	34	-
	2	14	58	-
	3	20	56	-
	4	26	38	-
	5	34	32	-
F38A5	1	0	42	+++
	2	19	86	-
F15B10	1	47	34	-
	3	42	48	-
	4	28	32	-
C01B10	1	34	70	-
	2	22	138	-
	3	31	98	-

Animals were grown at 20°C. The YAC was injected at a concentration of 50 ng/μl, cosmids were injected at a concentration of 10 ng/ μl. The genotype of the injected animals was *bc212 bcIs25*. As coinjection marker, pPD93.97 (*P_{myo-3}gfp*) was used at a concentration of 50 ng/μl. Transgenic animals were scored for NSM sister cell survival. All experiments were performed at 20°C.

13 genes are present on F38A5, and it was tested whether silencing their function by RNAi could phenocopy *bc212*. The silencing of none of these genes by RNAi resulted in NSM sister cell survival. However, silencing the activity of two of them caused embryonic lethality, and therefore could not be assayed for NSM sister cell survival.

Table 4-27 F38A5 contains 13 genes.

Gene	
<i>F38A5.1</i>	contains similarity to <i>Homo sapiens</i> Hypothetical protein FLJ11200;
<i>F38A5.2</i>	contains similarity to Pfam domain PF01963 (TraB family)
<i>dnj-11</i> , <i>F38A5.13</i>	<i>C. elegans</i> DNJ-11 protein; contains similarity to Pfam domains PF00249 (Myb-like DNA-binding domain), PF00226 (DnaJ domain)
<i>lec-11</i> , <i>F38A5.3b</i>	<i>lec-11</i> encodes a predicted member of the galectin family; can bind sugar in vitro.
<i>F38A5.14</i>	contains similarity to <i>Oryza sativa</i> P0002B05.24 protein
<i>F38A5.12</i>	contains similarity to Pfam domain PF07312 (Protein of unknown function (DUF1459))
<i>F38A5.11</i>	contains similarity to <i>Amsacta moorei</i> entomopoxvirus AMV128.; TR:Q9EMS1
<i>F38A5.5</i>	contains similarity to Pfam domain PF07312 (Protein of unknown function (DUF1459))
<i>F38A5.6</i>	contains similarity to Pfam domain PF03114 (BAR domain)
<i>F38A5.10</i>	contains similarity to Pfam domain PF07312 (Protein of unknown function (DUF1459))
<i>F38A5.9</i>	contains similarity to Pfam domain PF07312 (Protein of unknown function (DUF1459))
<i>F38A5.8</i>	contains similarity to Interpro domain IPR000345 (Cytochrome c heme-binding site)
<i>F38A5.7</i>	contains similarity to <i>Thermoanaerobacter tengcongensis</i> Galactose-1-phosphate uridylyltransferase

The two genes which caused lethality when inactivated by RNAi are highlighted in red.

Since *bc212* also results in partial embryonic lethality (see below), it is not unlikely that one of these two genes is the gene affected by *bc212*. *dnj-11*, a gene which encodes a protein with a DNA-binding domain, is an interesting candidate. The gene was sequenced, and indeed a mutation was found. This mutation results in a C to T transition at position 21 of the coding sequence.

A plasmid that contains the complete *dnj-11* coding sequence and 1773 bp upstream of it (see Figure 4-17) (pBC466) was able to rescue the NSM sister cell survival caused by *bc212* (Table 4-28) indicating that *dnj-11* is the gene defined by *bc212*. pBC466 still contains a significant part of the gene upstream of *dnj-11*, *F38A5.4*. Therefore, a second plasmid was constructed, pBC484, which contains only 996 bp upstream of *dnj-11*. Since the plasmid pBC484 is also able to rescue (Table 4-28, Figure 4-17), it can be excluded that *F38A5.4* is contributing to the rescue.

Table 4-28 The wild-type locus of *dnj-11* can rescue the NSM sister cell survival caused by *bc212*.

Plasmid	line	NSMs [%]	n
-	-	28	214
pBC466	1	3	98
	2	2	50
pBC484	1	0	46

The plasmids were injected at a concentration of 10 ng/μl. The genotype of the injected animals was *bc212 bcIs25*. As coinjection marker for pBC466, pPD93.97 (*P_{myo-3}gfp*) was used at a concentration of 50 ng/μl, as coinjection marker for pBC484, pRF4 (*rol-6*) was used at a concentration of 50 ng/μl. Transgenic animals were scored for NSM sister cell survival. All experiments were performed at 20°C.

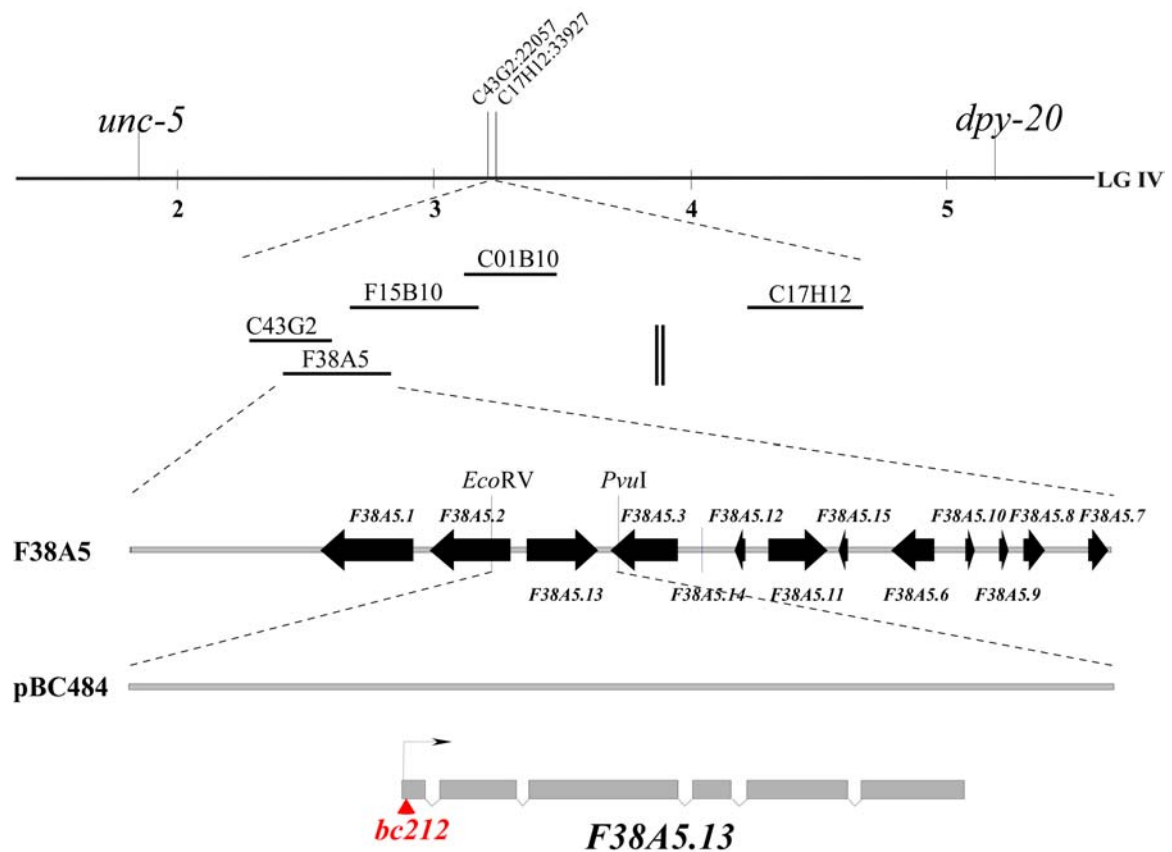


Figure 4-17 The cloning of *bc212*.

bc212 maps between *unc-5* and *dpy-20* on Chromosome IV. SNP mapping narrowed down the region to a region spanned by 5 cosmids and one gap. Transformation rescue experiments revealed that the NSM sister cell survival can be rescued by cosmid F38A5, and further by a *EcoRV PvuI* subclone of F38A5 (pBC484) containing the *dnj-11* locus. In red, the position of *bc212*, a C to T transition, is indicated.

The fact that the wild-type locus of *dnj-11* is able to rescue the NSM sister cell survival caused by *bc212*, and that a mutation in the *dnj-11* coding region was found, strongly suggest that *bc212* is a mutation in *dnj-11*.

Also, RNAi of *dnj-11* could phenocopy the NSM sister cell survival caused *bc212*. *dnj-11* function was silenced using RNAi by feeding in the RNAi-sensitive strain *rrf-3(pk1426)* (Simmer et al., 2002). As previously reported (Piano et al., 2002 and above), *dnj-11(RNAi)* resulted in embryonic lethality. Very few animals escaped the early embryonic lethality and developed to a stage at which the $P_{tph-1}gfp$ reporter is expressed. These “escapers” were scored for NSM sister cell survival, and 22% of the NSM sisters were found to survive (Table 4-30). Taken together, it can be concluded that *bc212* is a mutation that reduces *dnj-11* function.

4.4.2 *dnj-11(bc212)* animals have a pleiotropic phenotype and *bc212* is most likely a missense mutation

The *bc212* mutation results in a C to T transition at position 21 of the coding sequence. This transition causes an early stop codon. For this reason, *bc212* appears to be a null mutation. However, when *dnj-11* gene function was silenced by RNAi, a highly penetrant lethality was observed, implying that *dnj-11* is essential, and that *bc212* is not a null mutation. This hypothesis is confirmed by analyzing the NSM sister cell survival phenotype of animals with the genotype *bc212* over *nDf41*, a deficiency that includes the *dnj-11* locus. *bc212 bcIs25* males were crossed to *nDf41/nT1[unc-?(n754) let-?]* hermaphrodites. Since *bc212* is maternally rescued (see below), the F1 could not be analyzed right away. non-Unc GFP+ F1 animals (with the genotype *bc212 bcIs25/nDf41*) were isolated and their progeny was scored for NSM sister cell survival. The NSM sister cell survival phenotype of the progeny of *dnj-11(bc212)/Df41* showed a strong enhancement from 28% to 61% compared to *bc212/bc212* (see Table 4-29), confirming that *bc212* is not a null mutation.

When investigating the sequence of *dnj-11*, an additional ATG codon is found at position 259 of the nucleotide sequence, which is downstream of the mutation but still upstream of the functional domains (Figure 4-22). A *P_{dnj-11}dnj-11(bc212)::gfp* construct was injected into N2 worms. Five lines were obtained. In some transgenic animals, a very weak GFP signal was observed in a few cells. This result indicates that DNJ-11 protein might still be made in *dnj-11(bc212)* animals, however at a much lower level.

Table 4-29 *bc212/nDf41* results in a stronger NSM sister cell survival phenotype than *bc212/bc212*.

Maternal genotype	NSM sister cell survival [%] (n)
<i>bcIs25</i>	0 (414)
<i>dnj-11(bc212) bcIs25/ dnj-11(bc212) bcIs25</i>	28 (214)
<i>dnj-11(bc212) bcIs25/nDf41</i>	61 (88)

Experiments were performed at 20°C.

4.4.2.1 *dnj-11(bc212)* results in a cold-sensitive NSM sister cell survival phenotype which is suppressed by a loss-of-function mutation in *ces-1*

dnj-11(bc212) causes 50% of the NSM sister cells to survive at 15°C. At 25°C, only 12% NSM sister cells survive in *dnj-11(bc212)* animals (Table 4-30).

The NSM sister cells survive as a result of a block of *egl-1* transcription, as demonstrated by the analysis of $P_{egl-1}his24-gfp$ expression (4.1). $P_{egl-1}his24-gfp$ expression was observed in 100% of NSM sisters in early L1 larvae of *ced-4(n1162); bcIs37* animals (n=15). However, in *ced-4(n1162); unc-5(e53) dnj-11(bc212); bcIs37* L1 larvae, only 31% of the NSM sisters expressed *gfp* (n=17) when animals were grown at 15°C.

Genes known so far in the pathway that specify the cell death of the NSM sister cells are *ces-1*, which negatively regulates *egl-1*, *ces-2*, which negatively regulates *ces-1* (Ellis and Horvitz, 1991; Metzstein et al., 1996; Metzstein and Horvitz, 1999), and *hlh-2* and *hlh-3*, which act downstream of or in parallel to *ces-1* to positively regulate *egl-1* (4.3.1.2, Figure 4-18). To determine genetic interactions of *dnj-11* with these other components of the pathway, double mutants were analyzed for NSM sister cell survival. Interestingly, *hlh-2(bx108)* enhances the NSM sister cell survival phenotype caused by *dnj-11(bc212)* more than in an additive way, suggesting that these genes act synergistically (Table 4-30). In contrast, *hlh-3(bc248)*, which I propose acts with *hlh-2*, does not enhance the *dnj-11(bc212)* phenotype (Table 4-30). It is not clear from these data how *hlh-2*, *hlh-3*, and *dnj-11* interact.

When introducing a *lf* mutation in *ces-1*, *ces-1(n703n1434)*, into *dnj-11(bc212)* animals, I found that *ces-1(n703n1434)* suppresses the NSM sister cell survival (Table 4-30). Hence, *ces-1* is epistatic to *dnj-11*. This result indicates that *dnj-11* acts upstream of and as a negative regulator of *ces-1* (Figure 4-18).

Table 4-30 *bc212* results in a cold-sensitive NSM sister cell survival phenotype that is enhanced by *hlh-2(bx108)* and suppressed by *ces-1(n703n1434)*.

Genotype	NSM sister cell survival [%] (n)					
	15°C		20°C		25°C	
+/+	0	(416)	0	(414)	0	(408)
<i>dnj-11(bc212)</i>	50	(262)	28	(214)	12	(226)
<i>rrf-3(pk1426);control(RNAi)</i>	0	(60)	n.d.		n.d.	
<i>rrf-3(pk1426);dnj-11(RNAi)</i>	22	(218)	n.d.		n.d.	
<i>hlh-2(bx108)</i>	1	(350)	4	(400)	5	(410)
<i>hlh-2(bx108); dnj-11(bc212)</i>	70	(244)	60	(222)	32	(152)
<i>hlh-3(bc248)</i>	n.d.		2	(296)	4	(412)
<i>hlh-3(bc248); dnj-11(bc212)</i>	47	(366)	14	(248)	22	(532)
<i>ces-1(n703n1434)</i>	0	(200)	n.d.		n.d.	
<i>ces-1(n703n1434); dnj-11(bc212)</i>	0	(106)	n.d.		n.d.	

All strains additionally carried *bcIs25*. RNAi was performed by feeding. As a control, *F38A5.1(RNAi)* was performed.

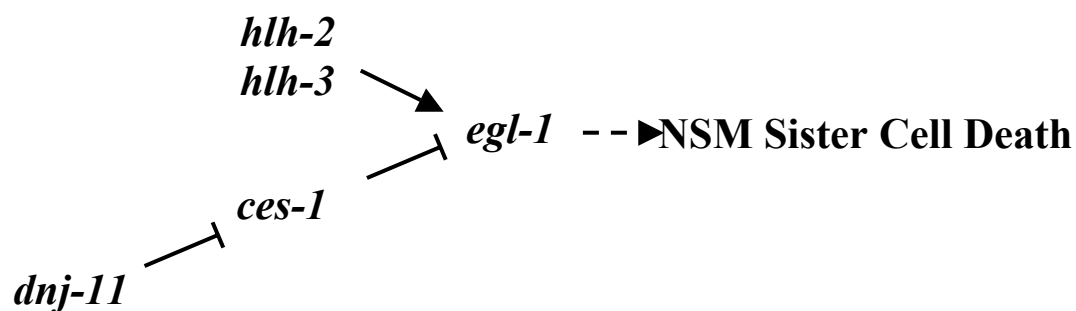


Figure 4-18 Genetic pathway that regulates the NSM sister cell death.

4.4.2.2 *dnj-11* is not required for cell death in general

dnj-11 is required for the NSM sister cell death, however it does not appear to be involved in cell death in general. As shown in Table 4-31, *dnj-11(bc212)* specifically blocks the cell death of the NSM sister cells but not the cell death of other cells in the anterior pharynx (4.2; 4.3.2.2). Moreover, cell death events that take place in the

ventral cord were analyzed. In wild-type animals, 12 Pn.aap are generated, of which six undergo cell death (Sulston and Horvitz, 1977). These cells can be visualized by an integrated $P_{lin-11}gfp$ reporter (*nIs106*) (Reddien et al., 2001); and in mutants in which cell death is blocked e.g. by a *lf* mutation in *ced-3*, all surviving Pn.aap cells express $P_{lin-11}gfp$. However, in *dnj-11(bc212)* mutants, no surviving Pn.aap cells were detected (Table 4-31), which suggest a specific role for *dnj-11* in the death of the NSM sister cells.

Table 4-31 *dnj-11(bc212)* specifically blocks the death of the NSM sister cells.

Genotype	Number of NSM sister cells	Total number of extra cells in the anterior pharynx	range	Number of surviving Pn.aap cells
+/+	0 (19)	0.06	0-1	0 (33)
<i>dnj-11(bc212)</i>	0.89 (19)	1.00	0-3	0 (25)

Extra cells in the anterior pharynx were scored using Nomarski optics. Surviving Pn.aap cells were scored using the $P_{lin-11}gfp$ reporter. The complete genotype of the analysed strains was *bcls25* and *dnj-11(bc212) bcls25* for scoring extra cells in the pharynx, and *nIs106* and *dnj-11(bc212) bcls25; nIs106*, respectively, for scoring surviving Pn.aap cells. All strains were grown at 15°C.

When *hlh-2(bx108); bcls25* males were crossed with *hlh-2(bx108); bcls25 dnj-11(bc212)* hermaphrodites, the heterozygous F1 exhibited the *bc212* phenotype (37% NSM sister cell survival, n=46). This result might hint towards the conclusion that *bc212* is dominant; however, when *bcls25 bc212* males were crossed with *unc-5(e53) dpy-20(e1282ts) bcls25* hermaphrodites, no NSM sister cell survival could be observed (0%, n=70). From this result I conclude that *bc212* exhibits a maternal effect. This conclusion was supported by the following experiment. Wild-type males were crossed with *unc-5(e53) bc212 dpy-20(e1282ts)* hermaphrodites. Unc Dpy animals in the F2 generation did not display a NSM sister cell survival phenotype. These Unc Dpy animals, which are also homozygous for *bc212*, are derived from heterozygous mothers. The NSM sister cell survival phenotype therefore is maternally rescued. The progeny (F3 generation) of the F2 Unc Dpy, the *bc212* phenotype occurred again (Table 4-32).

Even a transgene is able to maternally rescue the phenotype: the non-transgenic progeny of animals carrying an extrachromosomal transgene of the *dnj-11* wild-type locus (pBC466, 4.4.1) displayed a NSM sister cell survival phenotype of only 1.4% (n=74), which is similar to the phenotype observed in transgenic progeny (3%, n=98).

Table 4-32 *dnj-11(bc212)* shows a maternal effect.

Genotype	Maternal Genotype	NSM sister cell survival [%] (n)
<i>unc-5(e53) dnj-11(bc212) dpy-20(e1282)</i>	<i>unc-5(e53) dnj-11(bc212) dpy-20(e1282ts)/</i> +++	1 (136)
<i>unc-5(e53) dnj-11(bc212) dpy-20(e1282)</i>	<i>unc-5(e53) dnj-11(bc212) dpy-20(e1282ts)</i>	15 (104)

bcIs25 males were crossed with *unc-5(e53) bc212 dpy-20(e1282ts) bcIs25* hermaphrodites. F2 and F3 UncDpy animals, which have the genotype *unc-5(e53) dnj-11(bc212) dpy-20(e1282ts)*, were scored for NSM sister cell survival. All strains additionally carried *bcIs25*. Strains were grown at 20°C.

4.4.2.3 Reduction of *dnj-11* function results in morphological defects

Not only the death of the NSM sister cells is affected in *dnj-11(bc212)* animals. As shown above, the inactivation of *dnj-11* by RNAi results in embryonic lethality. Therefore, it is likely that *dnj-11* is an essential gene and its function is required in various processes. *bc212* results in an early stop, and is likely to reduce protein levels. Hence, *bc212* might reduce other functions of *dnj-11* as well. Indeed, morphological defects can be observed at different stages of development in *dnj-11(bc212)* animals (Figure 4-19). However, the majority of surviving animals is not misshaped and does not exhibit visible phenotypes.

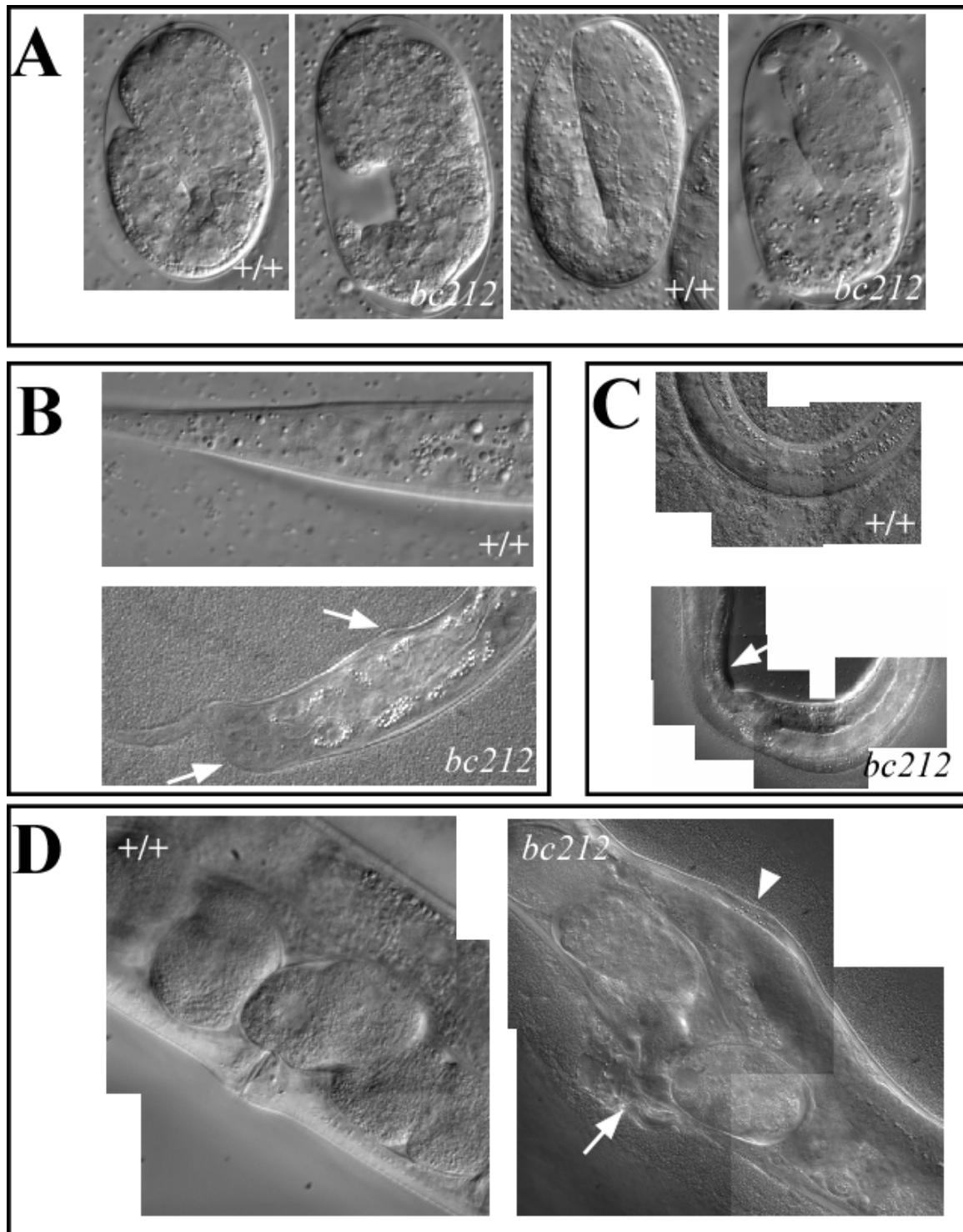


Figure 4-19 *dnj-11(bc212)* animals display various morphological defects.

A. Arrested *bc212* embryos with morphological defects. B. A *bc212* larva has a misshapen tail (arrows point to misshapen structures). C. *bc212* animal with an irregular body shape. D. *bc212* adult with a defective vulva (arrow) and a distorted body area (arrowhead).

4.4.2.4 *dnj-11(bc212)* causes slow growth and embryonic lethality

dnj-11(RNAi) causes highly penetrant embryonic lethality. *dnj-11(bc212)* results in embryonic lethality as well, albeit with a lower penetrance. At 15°C, only 2% of wild-type embryos failed to hatch after three days, whereas 25% of *dnj-11(bc212)* embryos failed to hatch after three days (Table 4-33). For that reason, *dnj-11(bc212)* causes 25% embryonic lethality.

Table 4-33 *bc212* causes embryonic lethality.

Genotype	unhatched eggs on plate [% of laid eggs]		
	after one day	after two days	after 3 days
+/+	85	2	2
<i>dnj-11(bc212)</i>	96	37	24

Each five *bcls25* and five *dnj-11(bc212) bcls25* adults were allowed to lay eggs for 3h. Adults were removed and eggs were counted. Unhatched eggs were counted after 1, 2, and 3 days. The experiment was performed at 15°C.

To estimate the growth rate of *dnj-11(bc212)* animals, I monitored how long individual worms grow until they reach the L4 stage at 15°C. Whereas in wild-type, 70% of the worms reached the L4 stage after 5 days, the earliest *dnj-11(bc212)* L4s were observed after six days (13%). Even after 8 days, only 54% of the animals made it to the L4 stage (Table 4-34). This observation implies that, besides the 25% that arrest as embryos, about 20% of *dnj-11(bc212)* animals arrest as larvae.

Table 4-34 *bc212* causes slow growth.

Genotype	L4s [% of laid eggs]					
	5 days	5 ½ days	6 days	6 ½ days	7 days	8 days
+/+	70	83	89	90	91	92
<i>dnj-11(bc212)</i>	0	0	13	38	52	54

Each five *bcls25* and five *dnj-11(bc212) bcls25* adults were allowed to lay eggs for 3h. Adults were removed and eggs were counted. The earliest L4s were monitored after 5 days. The experiment was performed at 15°C.

4.4.2.5 The broodsize of *dnj-11(bc212)* animals is strongly reduced

Next, the broodsize of *dnj-11(bc212)* animals was determined. As shown in Table 4-35, the broodsize of *dnj-11(bc212)* is only 22% of the wild-type broodsize. Interestingly, the reduced broodsize can be rescued by introducing the wild-type *dnj-11* locus (Table 4-35) as a transgene. A loss-of-function mutation in *ces-1* is able to suppress the NSM sister cell survival phenotype caused by *dnj-11(bc212)* (4.4.2.1), placing *dnj-11* upstream of *ces-1* in specifying the NSM sister cell death. Therefore, it was of interest to determine whether *dnj-11* also acts through *ces-1* in other pathways. However, a *ces-1(lf)* mutation is not able to suppress the small brood size of *dnj-11(bc212)* animals, indicating that the ability of *dnj-11(bc212)* to affect the brood size is not dependent on *ces-1*.

Table 4-35 The broodsize is reduced in *dnj-11(bc212)*.

Genotype	Broodsize	stdev	N
+/+	231	39	10
<i>dnj-11(bc212)</i>	52	13	10
<i>dnj-11(bc212)</i> ; pBC484	199	48	8
<i>ces-1(n703n14340)</i>	193	37	10
<i>ces-1(n703n1434)</i> ; <i>dnj-11(bc212)</i>	36	20	9

Animals were grown at 15°C. L4 larvae were plated on plates individually and replated every day. The progeny was counted as L4s. The standard deviation (stdev) of the broodsize of five different animals is indicated. All animals additionally carried *bcls25*.

4.4.2.6 $P_{dnj-11}dnj-11::gfp$ is Expressed Ubiquitously, and DNJ-11::GFP Localizes to the Cytosol

dnj-11 appears to be a gene involved in many different processes. It is therefore of great interest to determine where *dnj-11* is expressed. In order to determine where *dnj-11* is expressed and where DNJ-11 localizes, a plasmid was constructed containing the *dnj-11* locus with a C-terminal in frame fusion with *gfp* (Figure 4-25). *gfp* was inserted after the sequence encoding the second Myb domain (see below), in

order to create a protein that is still functional. Functionality of this fusion protein was confirmed by the ability of $P_{dnj-11}dnj-11::gfp$ to rescue the NSM sister cell survival phenotype of $dnj-11(bc212)$ mutants (see 4.4.2.9).

$P_{dnj-11}dnj-11::gfp$ expression was observed in embryos, larvae and adults, and in most if not all cells, as shown in Figure 4-20. DNJ-11::GFP localizes to the cytoplasm and is excluded from the nuclei, as shown by α GFP and DAPI staining (Figure 4-21). However, DNJ-11::GFP is not completely soluble and appears grainy.

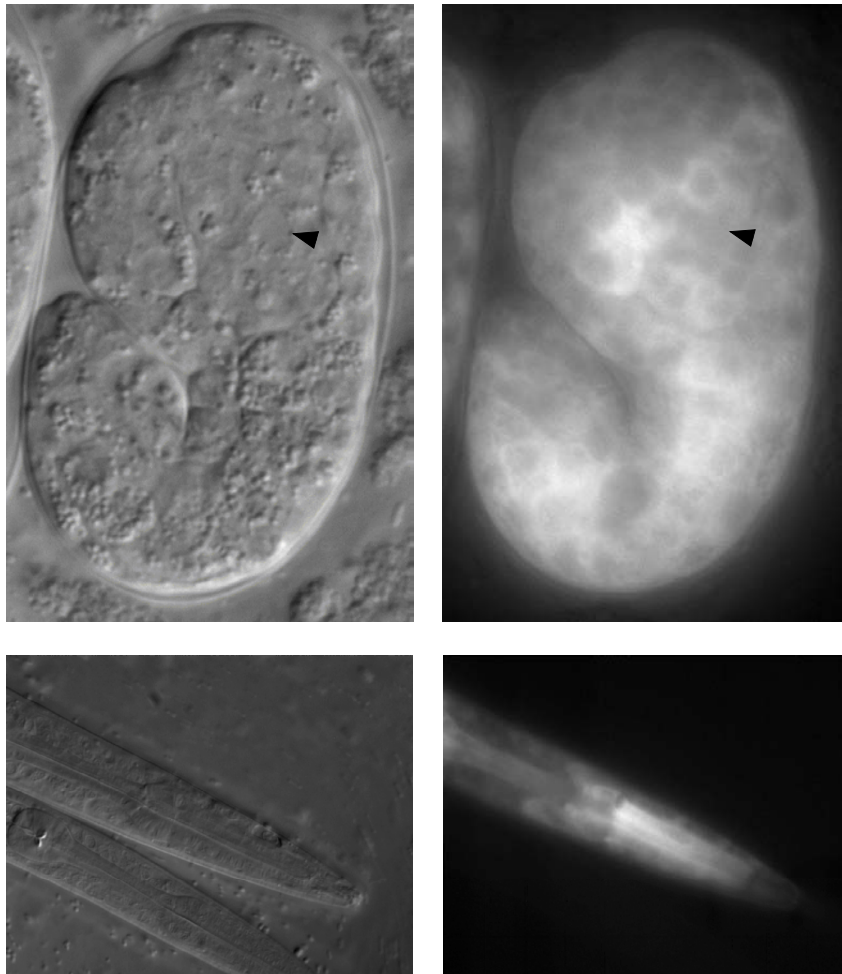


Figure 4-20 $P_{dnj-11}dnj-11::gfp$ is expressed ubiquitously. The upper panel shows an image of an embryo at the 11/2 fold stage (left: Nomarski image, right: epifluorescence image). $dnj-11::gfp$ is expressed in most if not all cells. DNJ-11::GFP localizes to the cytosol. The arrowhead points to the NSM mother cell just before it divides. The lower panel shows the head region of a larva (left: Nomarski image, right: epifluorescence image). $dnj-11::gfp$ is expressed throughout the whole lifespan. The genotype is $bcEx512$.

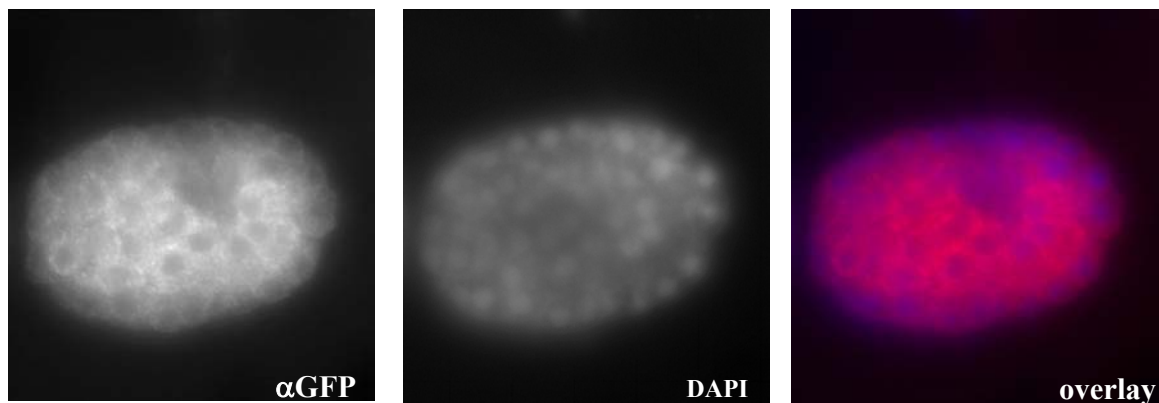


Figure 4-21DNJ-11::GFP localizes to the cytosol.

bcEx512 embryos were stained with an antibody against GFP and with DAPI.

4.4.2.7 *dnj-11* encodes a protein with a DnaJ domain and two Myb-like DNA binding domains and is a member of the MIDA1-like protein family

dnj-11 is predicted to encode a protein with a J domain and two Myb-like DNA binding domains (also known as SANT domains) (www.wormbase.org) (Figure 4-22).

J domains are found in members of the Hsp40 or J-protein family, a family of molecular chaperones, and are thought to regulate the activity of other molecular chaperones, namely Hsp70s (reviewed by (Walsh et al., 2004). Myb-related proteins have two or three tandem repeats of a domain of about 50 amino acid each with three tryptophan residues separated by 18 or 19 amino acids, forming helix-turn-helix motifs. These Myb domains display DNA binding activity (reviewed by (Oh and Reddy, 1999). Myb domains are very similar to SANT domains, domains found in transcriptional regulators and chromatin remodeling enzymes (Aasland et al., 1996).

The protein structure observed in DNJ-11 is found in other eukaryotic proteins. Specifically, DNJ-11 is the ortholog of proteins of the family of MIDA1-like proteins found in animals and plants, which are related to the fungal Zuotin proteins (Figure 4-22).BLAST searches (Altschul et al., 1997) revealed that DNJ-11 is highly similar to the mouse MIDA1 (40% identical, 61% similar), the human MPP11 (38% identical, 54% similar), the *Volvox carterii* GlsA (34% identical, 52% similar), and

the yeast Zuotin (37% identical, 62% similar). Figure 4-22 shows an alignment of DNJ-11 with these members of the family.

The *Saccharomyces cerevisiae* Zuotin was first isolated because of its ability to bind tRNA- and Z DNA (Zhang et al., 1992). Furthermore Zuotin, a component of the fungal translation machinery, has been shown to bind to the Hsp70 Ssz1 and form the ribosome-associated complex (RAC) (Gautschi et al., 2001). Zuotin functions as the DnaJ partner of the Hsp70 Ssb (Huang et al., 2005). A similar role has been established for the human MPP11, which was first identified as a protein that is phosphorylated during M phase, and which was shown to be associated with the mitotic spindle (Matsumoto-Taniura et al., 1996): MPP1 was found to form the mammalian ribosome-associated complex in conjunction with Hsp70L1 (Otto et al., 2005). The mouse homolog MIDA1 was isolated because of its ability to bind Id, a helix-loop-helix protein involved in the regulation of cell differentiation and growth (reviewed by (Norton et al., 1998). MIDA1 has been suggested to function in regulating cell growth (Shoji et al., 1995), and has been shown to exhibit DNA-binding activity (Inoue et al., 1999; Inoue et al., 2000; Yoshida et al., 2004). Mutants of the *Volvox carteri glsA* gene display defects in asymmetric cell division (Miller and Kirk, 1999), and the GlsA protein has been shown to function with Hsp70A (Cheng et al., 2005).

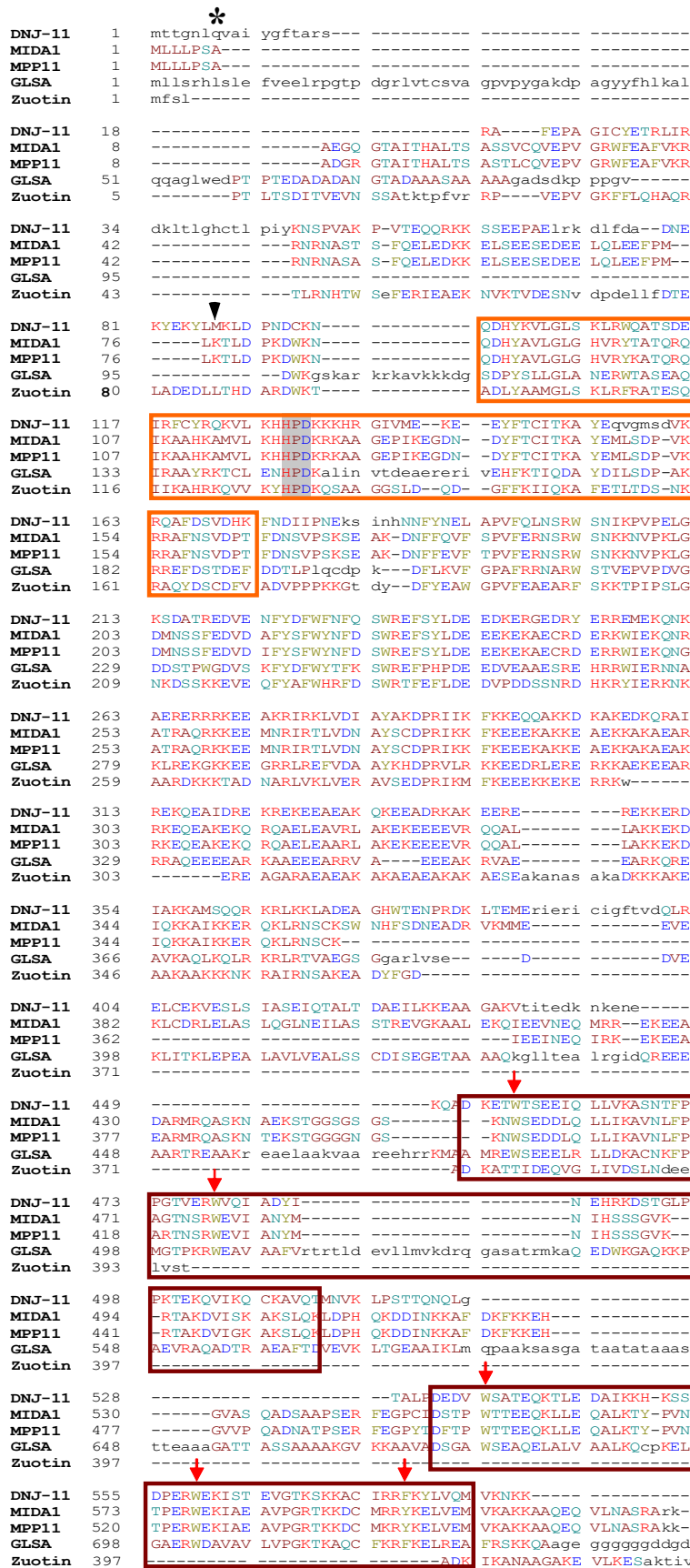


Figure 4-22. Alignment of DNJ-11 with other members of the MIDA1-like protein family.

Amino acids forming the J domain are boxed in orange, whereas the two Myb domains are indicated by red boxes. The tripeptide conserved in all J proteins is shaded in grey.

Conserved aromatic residues in the Myb domains are indicated by red arrows.

bc212 results in a stop in position 7 (*). A second methionine is located before the J domain (black arrow head).

The alignment was done using the DIALIGN algorithm. The color code is basic amino acids, nonpolar amino acids, uncharged polar amino acids, acidic amino acids, and aromatic amino acid.

4.4.2.8 *dnj-11* might be involved in establishing asymmetry during the division of the NSM mother cell.

GlsA, the DNJ-11 ortholog in *Volvox carteri*, has been implicated in establishing asymmetry during cell division. During *Volvox* development, only one specific type of asymmetric cell division occurs. This cell division results in the generation of two daughter cells with different fates, namely a larger reproductive cell and a smaller somatic cell. This cell division is clearly asymmetric with respect to size. There is evidence that it is the amount of cytoplasm rather than asymmetric segregation of fate determining factors that determines the fate of the daughter cells (Kirk et al., 1993). In *glsA* mutants, this cell division occurs symmetrically, resulting in two equally sized cells, which both differentiate into somatic cells (Miller and Kirk, 1999).

The role of GlS A in establishing asymmetry during cell division might be conserved in its *C. elegans* ortholog DNJ-11. The phenotype caused by *dnj-11(bc212)* is similar to the cell division phenotype observed in *glsA* mutants: the asymmetric cell division of the NSM mother cell that gives rise to the NSM that survives and to the NSM sister cell that dies is impaired in *dnj-11(bc212)* mutants. *dnj-11(bc212)* causes the NSM mother cell to divide symmetrically giving rise to two surviving cells. I sought to characterise the asymmetry of the division of the NSM mother cell. At least for early cell death events it is known that the divisions of the progenitor cells are unequal in terms of size. These cell divisions generate a larger cell that survives and a smaller cell that dies (Sulston et al., 1983). As the cell division of the NSM mother cell so far has not been described it was of interest to determine whether the cell division of the NSM mother cell is asymmetric with respect to size. Moreover, if this cell division is asymmetric with respect to size I was interested whether this asymmetry is impaired in *dnj-11(bc212)* mutants.

In order to visualize the size of the NSM and the NSM sister cell, a *gfp* reporter was used that expresses a GFP fusion to the PH domain from PLC1delta (a phospholipase C) driven by the *pie-1* promoter ($P_{pie-1}PM-gfp$, *bcIs57*). The GFP labels all plasma membranes in embryos and therefore can be used to visualize the outline of the NSM and NSM sister cell. In order to estimate the volume of a cell, stacks through the embryo were taken with epifluorescence microscopy. To estimate the size of the whole cell, the cell area in each plane was measured, and the areas were added. To determine the size difference between NSM and NSM sister cell, the ratio of the size

of the NSM sister cell to the size of the NSM was calculated. In Figure 4-23, a stack through a wild-type embryo shortly after the NSM mother cell has divided is shown. The NSM sister cell is significantly smaller than the NSM. On average, the size of a NSM sister cell is about 0.46 times the size of the NSM (n=6) (Table 4-36).

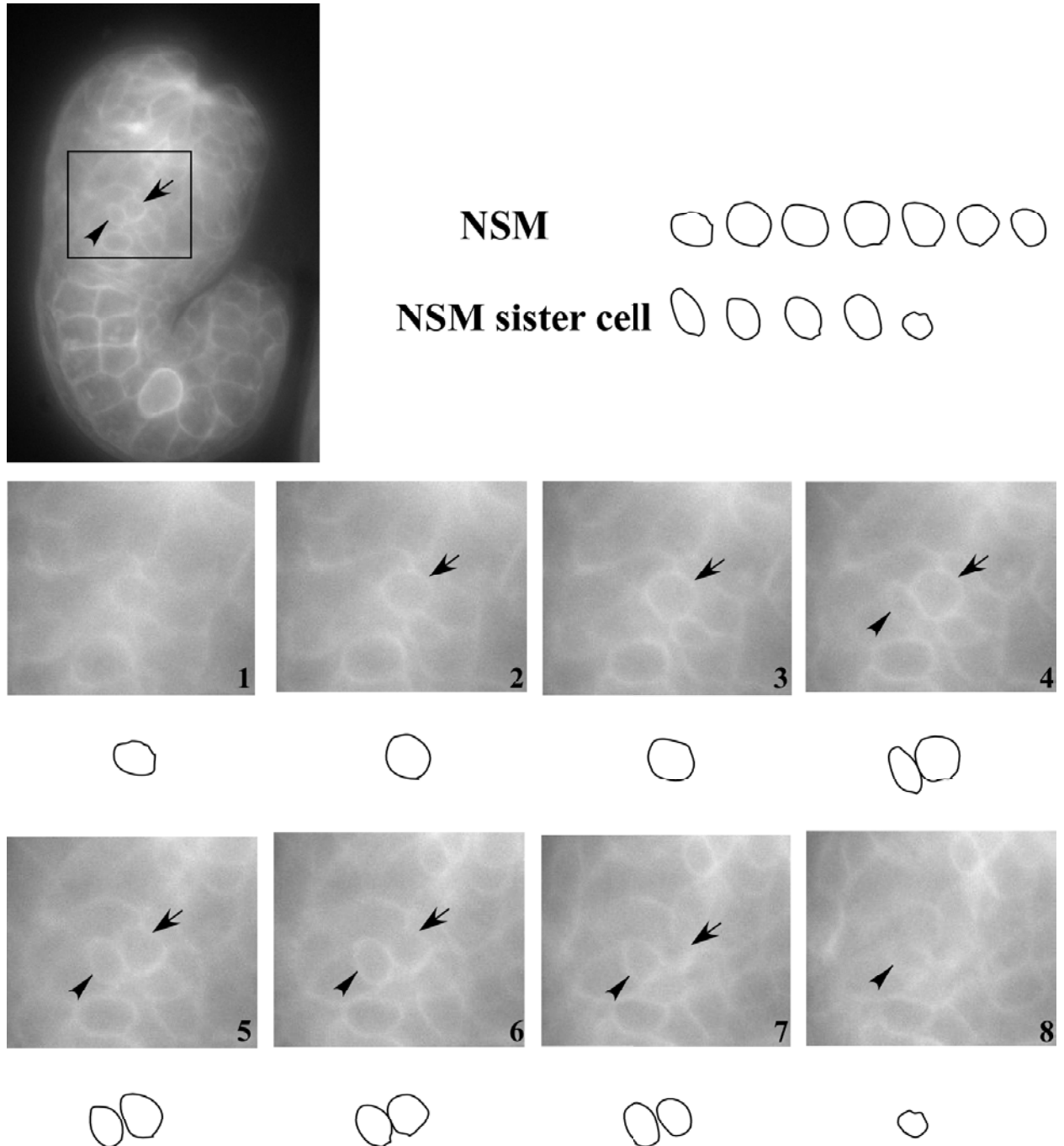


Figure 4-23 The NSM mother divides asymmetrically to give rise to the larger NSM and the smaller NSM sister cell. The Figure shows different focal planes from a stack through an embryo after the NSM mother cell has divided. Black arrows point to the NSM, black arrow heads point to the NSM sister cell. The outline of the cells is indicated below the images.

In *dnj-11(bc212)* mutants, the difference in size between NSM and NSM sister cells is much more variable, ranging from two cells of different size seen as in wild-type to two cells of equal size. On average the NSM sister is 0.68 times the size of the NSM, which is significantly different from wild-type. The greater range might reflect the incomplete penetrance of the *dnj-11(bc212)* phenotype, and it remains to be determined if the size of the NSM sister cell correlates with its fate.

It is not clear though, whether the NSM sister cells survive as a result of a symmetric cell division in *dnj-11(bc212)* mutants, or whether the NSM and NSM sister cell are of similar size as a result of a block in cell death. To distinguish between these two possibilities I analyzed the cell division of the NSM mother cell in other mutants, namely in *ces-1(gf)* and *egl-1(lf)* mutants. A *ces-1(gf)* mutation has been shown to block the death of the NSM sister cell (Ellis and Horvitz, 1991), and previous data suggested that the NSM sister cell survives in *ces-1(gf)* mutants because excessive amounts of CES-1 directly block *egl-1* transcription (Thellmann et al., 2003). In addition, *ces-1* acts downstream of *dnj-11*. Therefore, I expected that the NSM mother cell in *ces-1(gf)* animals still would divide asymmetrically if the difference in size is not caused by simply blocking cell death. However, as shown in Table 4-36, the NSM sister is of almost the same size as the NSM in *ces-1(gf)* mutants. On the other hand, the NSM mother cell still divides asymmetrically in *egl-1(lf)* mutants, in which cell death is blocked in general (Table 4-36, Figure 4-24). This result suggests that a *lf* mutation in *dnj-11* and a *gf* mutation in *ces-1* result in a defect in the asymmetric division of the NSM mother cell. Moreover, this defect is not caused by a block in cell death.

Table 4-36 The asymmetric division of the NSM mother cell is impaired in *dnj-11(bc212)* and *ces-1(n703gf)* mutants but not in *egl-1(n1048n3082)* mutants.

Genotype	size of NSM sister cell/ size of NSM	stdev	range	n
+/+	0.46	0.10	0.30 - 0.59	6
<i>dnj-11(bc212)</i>	0.68	0.27	0.25 – 1.06	9
<i>ces-1(n703)</i>	0.94	0.15	0.72 -1.22	8
<i>egl-(n1048n3082)</i>	0.52	0.08	0.37-0.59	7

Shown is the average ratio of the of the NSM sister cell to the size of the NSM. The cell size was determined as described in the text. The standard deviation (stdev) of the different values as well as the range is indicated. The complete genotype was *bcIs57, dnj-11(bc212) bcIs25; bcIs57, ces-1(n703); bcIs57*, and *egl-(n1048n3082); bcIs57*.

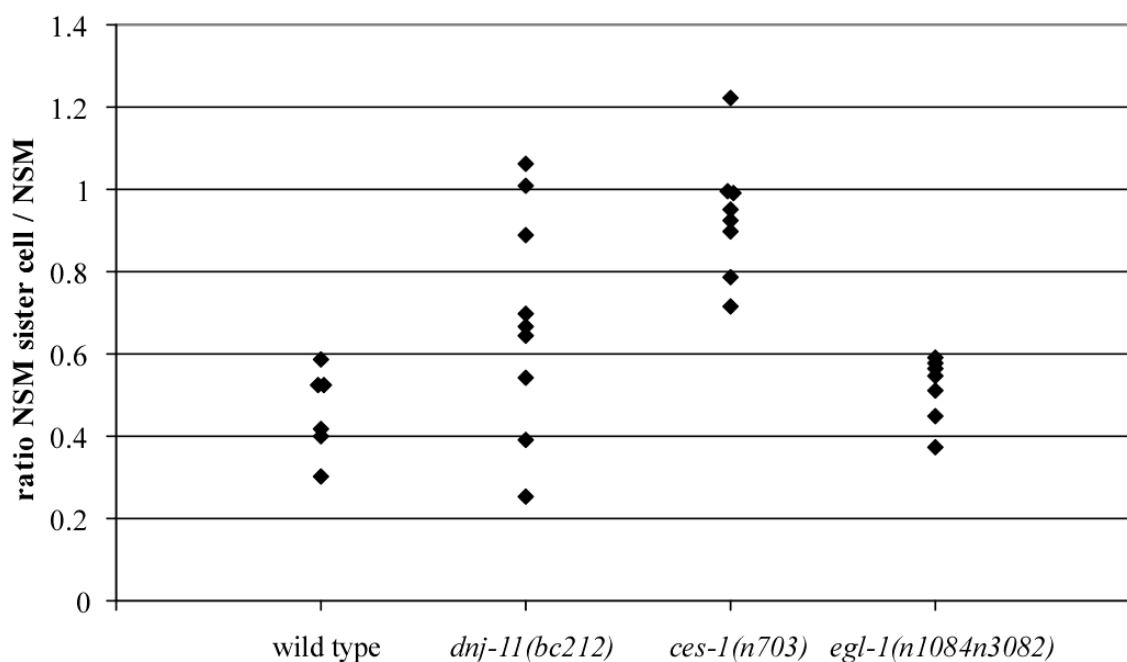


Figure 4-24 Graphic representation of the data shown in Table 4-36. Each diamond represents the ratio of the size of the NSM sister cell to the size of the NSM observed in one particular embryo. The cell size was determined as described in the text.

4.4.2.9 Analysis of the domains of DNJ-11 for their functional relevance in the NSM sister cell death

As shown above, DNJ-11 is related to the MIDA1-like proteins, which are characterised by the presence of a N-terminal DnaJ domain, and C-terminal Myb-like domains. MIDA1-like proteins also share another region of similarity, the so-called M region, the biological function of which remains to be investigated.

The family of DnaJ-like proteins is structurally very diverse, however, they all share one conserved domain, the J domain. The J domain has been proposed to mediate the interaction with their chaperone partners, which are members of the Hsp70 protein family. Moreover, the J domain functions also in stimulating the ATPase activity of Hsp70 proteins (Cyr et al., 1994). Three amino acids are conserved among all DnaJ-like proteins, and are indispensable for their function, namely a His-Pro-Asp tripeptide (Miller and Kirk, 1999; Sell et al., 1990; Tsai and Douglas, 1996). I sought to determine the functional relevance of the J domain of DNJ-11 with respect to the specification of the NSM sister cell death. For that purpose, a mutation was introduced in a plasmid containing the *dnj-11* locus that changes the histidine of this tripeptide to a glutamine (H129Q). This plasmid was tested for its ability to rescue the NSM sister cell survival phenotype caused by *dnj-11(bc212)*. *dnj-11* was fused to *gfp* to visualize the protein and therefore to be able to exclude the possibility that this mutation results in the failure to produce a stable protein.

A similar approach was undertaken to determine the functional relevance of the two Myb-like domains. Myb domains can bind DNA, and their conserved tryptophan residues are essential for this function. It has also been shown for the Myb-related SANT domains that substitution of these highly conserved aromatic residues impairs their function (Boyer et al., 2002; Kroczyńska et al., 2004).

Substitution of a single tryptophan by a glycine in the second or third Myb-domain of c-Myb, the Myb-domains that are essential for DNA binding, abolished the ability of c-Myb to bind DNA *in vitro* (Saikumar et al., 1990). Therefore, I sought to identify the role of the Myb-like domains of DNJ-11 by testing whether proteins in which the Myb-domains have been mutated could rescue the *dnj-11(bc212)* phenotype. Two different mutations were introduced into the $P_{dnj-11}dnj-11::gfp$ rescuing plasmid, one

resulting in the substitution of Trp 456 to Gly (pBC529), the other one resulting in the substitution of Phe 578 with Gly (pBC530) (Figure 4-25).

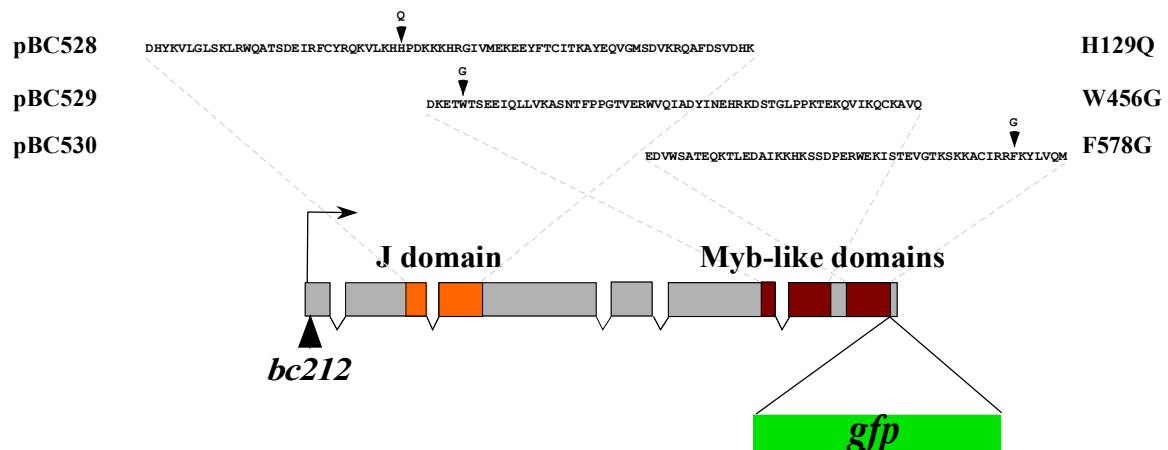


Figure 4-25 Schematic representation of the *dnj-11* locus. In orange, the region coding for the J domain is indicated, the Myb-like domains are displayed in red. The amino acid sequence for each domain is shown with arrowheads indicating amino acids that have been mutated in the plasmids pBC528, pBC529, and pBC530. All plasmids also contain an in frame fusion with *gfp* at the end of the second Myb-like domain.

These plasmids were introduced into *dnj-11(bc212); bcIs25* animals and tested for their ability to rescue the NSM sister cell death. Importantly, all point mutations did not alter protein production or localization as assayed by the presence of GFP. Preliminary results are shown in Table 4-37.

Table 4-37 Analysis of the role of the domains of DNJ-11 for the cell death of the NSM sister cells.

Transgene	affected domain	NSM sister cell survival [%] (n)				rescue
		15°C		20°C		
-	-	60	(92)	28	(214)	-
<i>P_{dnj-11}dnj-11::gfp</i>		48	(42)	5	(114)	++
		58	(50)	28	(110)	-
		25	(24)	11	(28)	+
<i>P_{dnj-11}dnj-11(bc212)::gfp</i>	early stop	71	(56)	27	(98)	-
		78	(58)	n.d.		-
		73	(48)	41	(68)	-
		40	(40)	20	(60)	-
<i>P_{dnj-11}dnj-11 (H129Q)::gfp</i>	DnaJ	65	(48)	32	(120)	-
				44	(106)	-
<i>P_{dnj-11}dnj-11(W456D)::gfp</i>	Myb 1	n.d.		13	(48)	+
				13	(136)	+
		73	(44)	58	(76)	-
<i>P_{dnj-11}dnj-11(F578G)::gfp</i>	Myb 2			39	(64)	-
				12	(68)	+

The genotype of the injected animals was *dnj-11(bc212) bcIs25*. pRF4 (*rol-6(su1006)*) was used as co-injection marker at a concentration of 50 ng/μl. Plasmids were injected at a concentration of 10 ng/μl.

4.4.2.10 Are Hsp70 proteins involved in establishing the cell death fate of the NSM sister cell?

DNJ-11, a class III J protein, is required for the NSM sister cell death. It is not known, however, how DNJ-11 functions in this process. J proteins are reported to act with members of the Hsp70 protein family as their necessary functional partners. Hsp70 proteins bind and release their substrates in a reversible way, coupled to an ATP hydrolysis cycle. Hsp70s have a low intrinsic ATPase activity, which can be stimulated by members of the Hsp40 family of co-chaperones (defined by the presence of the J domain). The stimulation of the ATPase activity is important for the

binding of Hsp70 to their substrates, since it is the ADP-bound form of Hsp70 that has a high affinity to substrates (Kelley, 1999). High selectivity is observed in the interactions between J domains and isoforms of Hsp70; e.g. two of three Hsp70 classes, Ssz1 and Ssb1/2 interact exclusively with the DNJ-11 homolog in yeast Zuo1, whereas the third class does not show any interaction with Zuo (reviewed by (Walsh et al., 2004). In *Volvox*, Hsp70A and GlsA function as chaperone partners in regulating asymmetric division (Cheng et al., 2005).

Therefore, the question arises whether DNJ-11 acts with a specific Hsp70 partner to cause the death of the NSM sister cells. According to wormbase, the *C. elegans* genome encodes 15 proteins with Hsp70 domains (Table 4-38). To determine a possible role of any of these Hsp70s in regulating the death of the NSM sister cells, RNAi by feeding was performed to silence their gene function. The resulting RNAi animals were analysed with respect to NSM sister cell survival.

Table 4-38 *hsp70* genes in the *C. elegans* genome

Gene	Chromosome	map position	name	allele
C12C8.1	I	3.75	<i>hsp-70</i>	
C15H9.6	X	-3.71	<i>hsp-3</i>	<i>tm0832</i>
C30C11.4	III	-0.27		
C37H5.8	V	0.00	<i>hsp-6</i>	<i>tm515</i>
C49H3.8	IV	3.49		
F11F1.1	III	21.21		
F26D10.3	IV	16.35	<i>hsp-1</i>	
F43E2.8	II	0.50	<i>hsp-4</i>	
F44E5.4	II	4.05		
F46F5.1	II	-15.60		
F54C9.2	II	0.81	<i>stc-1</i>	
T14G8.3	X	8.84		<i>ok502</i>
T24H7.2	II	-0.39		
Y113G7B17	V	25.00		
Y17G7B.3	II	5.37		

Two different strains were used for the RNAi experiment that are hypersensitive for RNAi, namely *rrf-3(pk14260)* animals, and *lin-35(n745)* animals. RNAi was

performed at 15°C and 20°C. Most of the genes showed a more or less penetrant embryonic lethal phenotype, which was more prominent at 15°C. Therefore, escapers were scored. As shown in Table 4-39, RNAi of none of the *hsp70* genes resulted in an obvious NSM sister cell survival phenotype. I cannot conclude from the data that Hsp70 proteins are not required for the NSM sister cell death, because it is highly possible that an effect on the NSM sister cells is masked by early embryonic lethality.

Table 4-39 Effect of RNAi of the *C. elegans hsp70* genes on the death of the NSM sister cells.

gene	NSM sister cell survival [%] (n)							
	15°C				20°C			
	<i>rrf-3</i>		<i>lin-35</i>		<i>rrf-3</i>		<i>lin-35</i>	
<i>C12C8.1</i>	0	(8)	2.6	(76)	0	(64)	0	(46)
<i>C15H9.6</i>	3.8	(26)	0	(36)	0	(42)	0	(42)
<i>C30C11.4</i>	4.1	(122)	0	(124)	3.5	(86)	0	(110)
<i>C37H5.8</i>	lethal		lethal		lethal		lethal	
<i>C49H3.8</i>	lethal		3.3	(30)	0	(70)	0	(44)
<i>F11F1.1</i>	0	(16)	0	(44)	0	(76)	0	(48)
<i>F26D10.3</i>	lethal		lethal		1.6	(62)	lethal	
<i>F43E2.8</i>	lethal		0	(42)	0	(14)	0	(26)
<i>F44E5.4</i>	0	(32)	0	(60)	0	(182)	0	(52)
<i>F46F5.1</i>	lethal		0	(54)	0	(64)	0	(72)
<i>F54C9.2</i>	0	(36)	0	(48)	0	(56)	0	(50)
<i>T14G8.3</i>	0	(66)	1.8	(56)	0	(50)	0.8	(126)
<i>T24H7.2</i>	0	(48)	0	(56)	0	(60)	0	(40)
<i>Y113G7B.17</i>	3.6	(28)	0	(44)	0	(62)	0	(76)
<i>Y17G7B.3</i>	0	(62)	2	(48)	0	(62)	0	(70)

RNAi was performed by feeding, NSM sister cells were scored using the $P_{tph-1}::gfp$ reporter. The genotype of the strain was *rrf-3(pk1426); bcIs25* and *lin-35(n745); bcIs25*.

4.5 Identification of factors that repress *egl-1* expression in the NSMs

So far, experiments were set up to gain insights into the mechanisms through which the asymmetric cell division of the NSM mother cells is established and which result in the activation of *egl-1* expression in the NSM sister cell. However, it is not clear whether *egl-1* expression is actively regulated in the NSM as well, e.g. repressed by survival factors. A forward genetic screen for mutants lacking NSMs has not led to the identification of factors required for the survival of the NSMs (Hatzold, 2001). A candidate is the Snail-like protein CES-1, as it has been shown that a *gf* mutation in *ces-1* represses *egl-1* expression in the NSM sister cell. Therefore, in wild-type animals, CES-1 might function in repressing *egl-1* transcription in the NSMs. However, a *ces-1(lf)* mutation does not cause a phenotype, as the NSMs survive like in wild-type (Metzstein and Horvitz, 1999). Therefore, *ces-1* might act redundantly with other factors. For this reason, I used a candidate approach in order to identify factors that act redundantly with CES-1 to cause the survival of the NSMs.

4.5.1 The *C. elegans* genome encodes two homologs of *ces-1*, which are candidates factors for acting redundantly with *ces-1*

In *Drosophila*, it has been shown that members of the Snail family function redundantly in certain processes. In addition, *Xenopus Snail* and the related *Slug* can act redundantly (reviewed by (Hemavathy et al., 2000) For that reason it is possible that the function of CES-1 in the repression of *egl-1* transcription in the NSM is redundant with the function of other Snail-like proteins.

The K02D7.2 protein is most similar to CES-1, and is therefore an interesting candidate. So far, no mutation of *K02D7.2* was available. To identify a possible role of this gene in the survival of the NSMs I isolated a deletion mutant. The deletion *bc366* removes bp 24491 to 25439 of cosmid K02D7, and as shown in Figure 4-26, results in the deletion of 949 bp of the *K02D7.2* locus. This mutation causes a frame shift with a subsequent early stop. therefore, *bc266* is likely to be a strong *lf* mutation, since it codes for a truncated protein missing a part of the second, and the complete third and forth zinc finger domain. The animals are homozygous viable, and they do not show any obvious phenotypes.

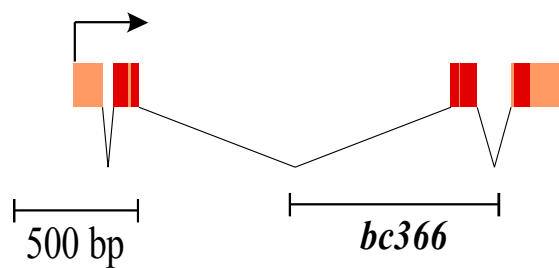


Figure 4-26 Schematic representation of the *K02D7.2* locus. The regions coding for the four zinc fingers are indicated in red. *bc366* is a deletion that removes exon 3 and subsequently causes a frame shift and early stop.

Another protein related to CES-1 is the gene product of *C55C2.1* (Nieto, 2002). A deletion mutant for *C55C2.1*, *ok1228*, was obtained from the knockout consortium, and further back crossed and analysed. It was found that the deletion spans 1116 bp, removing 11064 to 12179 of cosmid C55C2. The deletion results in the loss of exon 3 and 4, and a subsequent frameshift (Figure 4-27). Since this truncated protein does not have any zinc fingers, *ok1228* is thought to represent a strong *lf* allele. Like *K02D7.2(lf)* and *ces-1(lf)* animals, *C55C2.1(lf)* are viable and don't exhibit visible phenotypes.

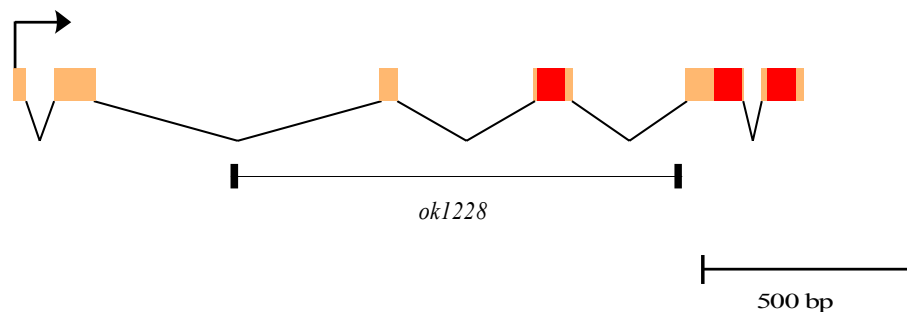


Figure 4-27 Schematic representation of the *C55C2.1* locus. The regions coding for the three zinc fingers are indicated in red. *ok1228* is a deletion that removes exon 3 and 4 and subsequently causes a frame shift and early stop resulting in a truncated protein with no Zinc fingers.

Subsequently, the NSMs in these mutants were analyzed for their possible absence, however, as shown in Table 4-40, none of the mutation caused the inappropriate death of the NSMs. Furthermore, double mutants with *ces-1* as well as the triple mutant did not show a phenotype. Therefore, the three *snail*-like genes *ces-1*, *C55C2.2*, and *K02D7.2* are not required for the survival of the NSMs. From these results I conclude that *ces-1*, *K02D7.2*, and *C55C2.1* do not act redundantly to repress *egl-1* expression in the NSM.

Table 4-40 Lf mutations in the *snail*-like genes *ces-1*, *C55C2.1*, and *K02D7.2*, do not result in the ectopic death of the NSMs.

Genotype	NSMs [%]
+/+	100 (many)
<i>ces-1(n703n1434)</i>	100 (many)
<i>K02D7.2(bc366)</i>	100 (80)
<i>C55C2.1(ok1228)</i>	100 (102)
<i>ces-1(n703n1434); K02D7.2(bc366)</i>	100 (100)
<i>ces-1(n703n1434) C55C2.1(ok1228)</i>	100 (358)
<i>ces-1(n703n1434) C55C2.1(ok1228); K02D7.2(bc366)</i>	100 (74)

Experiments were performed at 20°C. All strains additionally carried *bcIs25*. The presence of the NSMs was assayed using the expression of the $P_{iph-1}gfp$ reporter.

4.5.2 *ces-1* might act in conjunction with *lin-22*, a hairy homolog

Another possible mechanism to prevent the NSM from dying would be that *ces-1* acts redundantly together with another type of transcription factor. A candidate gene is *lin-22*, a gene that exhibits homology to the *Drosophila* gene *hairy* (Wrischnik and Kenyon, 1997). In *Drosophila*, it has been shown that a loss of function of the *scratch* (*scrt*) gene, coding for a zinc finger transcription factor of the Snail family, like *ces-1*, results in a reduced number of photoreceptors in the eye. This phenotype is strongly enhanced in embryos lacking the function of both *scrt* and the gene *deadpan*, which encodes a Hairy homolog. Loss of function of *deadpan* alone, however, does not cause a significant phenotype, indicating that the genes act redundantly (Roark et al., 1995). Therefore, it might be possible that *ces-1* and *lin-22* act together in a similar way. *lin-22(lf)* itself does not cause any NSM death (Hatzold, 2001). Several attempts were made to construct a strain that is homozygous for lf mutations in both *ces-1* and *lin-22*. Since the single mutations do not cause an obvious phenotype, two marker mutations were used to balance the *ces-1(lf)* and *lin-22(lf)* mutations. The strains *ces-1(n703n1434); lin-1(e1275); bcIs30* ($P_{iph-1}gfp$ integrated on X) and *unc-29(e193); lin-22(n372); bcIs30* were used for the crossing. *lin-1(e1275)* causes a Muv phenotype, and is located on Chromosome IV at -8.44, close to *lin-22* (-6.67). *unc-29* is located on Chromosome I at 3.29, close to *ces-1* at 2.96. However, I did not succeed in obtaining a strain homozygous for both *ces-1(lf)* and *lin-22(lf)*, since all

wild-type animals isolated always had some Unc or Muv progeny. A strain was obtained that was 100% non Muv, and therefore most probably homozygous for *lin-22*, but still had Unc progeny, and therefore was most likely heterozygous for *ces-1*. Strikingly, in the progeny of *ces-1(lf)/unc-29(lf); lin-22* animals, dead embryos were observed (Figure 4-28). Therefore, it is possible that *ces-1(lf); lin-22(lf)* animals are embryonic lethal. Unfortunately, the effect on the survival of NSMs could not be analyzed. However, from this experiment I conclude that *ces-1* and *lin-22* act redundantly in an essential process, as depletion of both causes embryonic arrest. This lethality is probably not due to increased cell death, as these embryos do not display an excessive amount of cell corpses. *ces-1* and *lin-22* might function together in an essential process that is distinct from promoting survival.

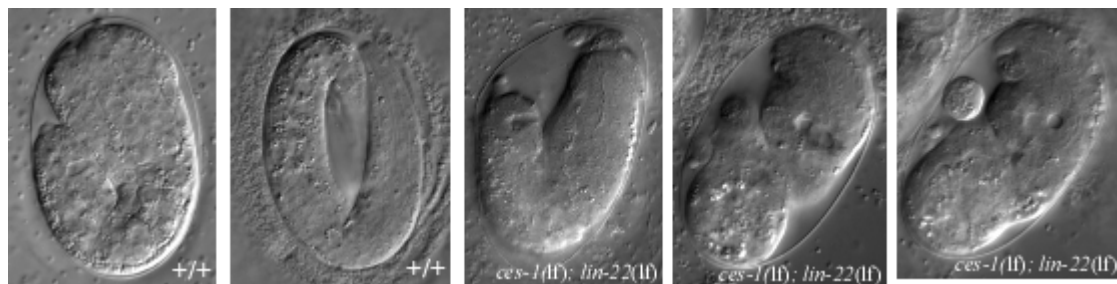


Figure 4-28 *ces-1(n703n1434); lin-22(n372)* double mutants might be embryonic lethal. The images show different arrested embryos from *ces-1(n703n1434)/unc-29(e193); lin-22(n372)* mothers that are most likely homozygous for *ces-1(n703n1434)* and *lin-22(n372)*, compared to wild-type embryos.

5 Discussion

5.1 *egl-1* is regulated at the transcriptional level, a mechanism that is conserved

egl-1 is the most upstream gene of the central cell-death pathway required for all developmental cell deaths in *C. elegans*. Its regulation is crucial for the activation of the cell-death program specifically in the 131 cells destined to die.

The analysis of the expression of *gfp* under the control of the *egl-1* promoter in the NSMs and NSM sister cells suggests that *egl-1* is transcriptionally active in the NSM sister cell but not in the NSM. The activity of EGL-1 thus is regulated at the transcriptional level. At least one additional neuronal cell death in *C. elegans*, the death of the HSNs, which die specifically in males is dependent on the transcriptional activation of the *egl-1* gene (Conradt and Horvitz, 1999). Transcriptional regulation might therefore be an important mechanism through which the activity of EGL-1 is regulated.

EGL-1 is a BH3-only protein, and the function of BH3-only proteins as initiators of programmed cell death has been conserved between *C. elegans* and mammals. To date, at least 10 mammalian BH3-only proteins have been identified. Interestingly, it was shown for four of them that their activity is regulated at the transcriptional level (reviewed by Puthalakath and Strasser, 2002). It has been reported that the *BH3-only* genes *Noxa* and *Puma/Bbc3* are transcriptionally upregulated in thymocytes and fibroblasts after DNA damage, and that this upregulation is dependent on p53 (Han et al., 2001; Nakano and Vousden, 2001; Oda et al., 2000; Yu et al., 2001). The activity of the BH3-only genes *Bim* and *Hrk/DP5* also appears to be regulated at the transcriptional level. *Bim* and *Hrk/DP5* have been found to be upregulated in cultured neurons after NGF withdrawal (Harris and Johnson, 2001; Putcha et al., 2001; Whitfield et al., 2001). This transcriptional upregulation of *Bim* is required for the death of cultured sympathetic neurons after NGF withdrawal. Therefore, the regulation of *BH3-only* genes by transcriptional activation might be a common mechanism conserved throughout evolution.

5.2 *hlh-2* and *hlh-3* are required for the NSM sister cell death

hlh-2 and *hlh-3* appear to be at least partially required for the NSM sister cell death since reducing their function can result in the survival of the NSM sister cells. A weak hypomorphic mutation in *hlh-2*, *bx108*, causes 5% NSM sister cells to survive. This weak incompletely penetrant phenotype can be explained by the nature of the mutation. *bx108* is a missense mutation in the sequence coding for the first helix, and it results in the change of R to H at position 316 of the amino acid sequence (Portman and Emmons, 2000). Since this mutation does not dramatically change the character of the amino acid residue, *bx108* has been suggested to only reduce the dimerization affinity of HLH-2 or alter its dimerization specificity (Portman and Emmons, 2000). HLH-2 is a member of the Daughterless-like protein family and is likely to act as a necessary dimerization partner for other bHLH proteins. Based on the following observation, it is highly possible that HLH-2 functions together with the Achaete-Scute-like protein HLH-3 to promote the NSM sister cell death. Reducing the activity of *hlh-3* by RNAi results in a weak NSM sister cell survival phenotype of 7%. Additionally, a deletion mutation in *hlh-3* that is a potential null mutation (*bc248*) causes a similar phenotype. This phenotype indicates that *hlh-3* is partially required for the death of the NSM sister cells. In a *hlh-2(bx108); hlh-3(bc248)* double mutant, the NSM sister cell survival is strongly enhanced to 31%. This synergistic effect of *hlh-2(bx108)* and *hlh-3(bc248)* on the survival of the NSM sister cells not only suggests that both genes are required for their deaths but indicates that *hlh-2* and *hlh-3* are functioning together to promote their deaths. It has already been shown that HLH-2 and HLH-3 can form a heterodimer that binds DNA in a sequence-specific manner (Krause et al., 1997). In this work I showed that a HLH-2/HLH-3 heterodimer can bind to Snail-binding sites/E-boxes in Region B of the *egl-1* locus *in vitro*. The Snail-binding sites/E-boxes in Region B are required for the death of the NSM sister cells *in vivo* (Thellmann et al., 2003). As both HLH-2 and HLH-3 are present in the NSM sister cells at the time they are dying, it is very likely that the HLH-2/HLH-3 heterodimer acts as a direct activator of *egl-1* transcription in the NSM sister cells. I propose that HLH-2 and HLH-3 activate *egl-1* expression in the NSM sister cells by binding to the Snail-binding sites/E-boxes in Region B of the *egl-1* locus, and that *egl-1* expression in the NSM sister cells promotes their death (Figure 5-1).

The Snail-binding sites/E-boxes are also required for the ability of CES-1 to repress *egl-1* transcription (Thellmann et al., 2003). Therefore, in *ces-1(gf)* mutants, ectopic CES-1 is likely to bind to the Snail-binding sites/E-boxes and thereby prevents HLH-2/HLH-3 from binding. As a consequence, *egl-1* is not expressed, and the NSM sister cells survive (Figure 5-1).

In *hlh-2(bx108); hlh-3(bc248)* mutant animals, the NSM sister cells survive with a frequency of only 31%, compared to 96% in *egl-1(lf)* mutants. The incompletely penetrant NSM sister cell survival phenotype caused by *hlh-2(bx108); hlh-3(bc248)* may have various reasons. First of all, it is not clear what effect an *hlh-2* null mutation would have on the cell death of the NSM sister cells. *hlh-2(RNAi)* results in highly penetrant early embryonic lethality (Krause et al., 1997). Therefore, the effect of a complete elimination of *hlh-2* function on the death of the NSM sister cells cannot be studied. Additionally, several attempts to isolate a *hlh-2* deletion mutant have failed so far (data not shown). Since also no deficiencies are available that cover the *hlh-2* locus, it is possible that *hlh-2* is haploinsufficient for viability.

bc248 is a potential null mutation in *hlh-3*, based on the fact that *bc248* removes most of the functional domain, and that the NSM sister cell survival phenotype is not enhanced in animals with *hlh-3(bc248)* in *trans* to a deficiency, or *hlh-3(bc248)* animals treated with *hlh-3(RNAi)*. However, it only results in a weak NSM sister cell survival phenotype. Therefore, HLH-3 is likely to function redundantly with other factors, possibly other bHLH proteins that form heterodimers with HLH-2.

As the deletion of Region B of the *egl-1* locus also does not result in the complete block of NSM sister cell death, other regulatory regions of the *egl-1* locus are still able to drive *egl-1* expression in the NSM sister cells. However, it is not clear if the residual expression of *egl-1* is dependent on *hlh-2* and *hlh-3*. It is possible that HLH-2 and HLH-3 can activate *egl-1* expression via regions other than Region B, as E-boxes are present in other parts of the *egl-1* promoter. Interestingly, a *ces-1(gf)* mutation blocks NSM sister cell death completely. Our current model suggests that in a *ces-1(gf)* mutant *egl-1* expression in the NSM sister cells is repressed by ectopic amounts of CES-1, which directly bind to the Snail-binding sites/E-boxes in Region B and thereby prevent HLH-2/HLH-3 from binding (Figure 5-10). Two possibilities could explain that the *ces-1(gf)* phenotype is more penetrant than the phenotype caused by the deletion of Region B. First, CES-1 binding to Region B might not only block the activator from binding to the same sites but might also affect factors acting

in cis on other regions of the *egl-1* locus. Alternatively, CES-1 itself might bind to different Snail sites in regions other than Region B and directly block activators from binding (Figure 5-1). To distinguish between these two possibilities, it remains to be tested if the completely penetrant NSM sister cell survival phenotype caused by *ces-1(gf)* is dependent on Region B.

The function of CES-1 in wild-type embryos is less obvious. Preliminary results show that a functional CES-1::YFP fusion protein driven by the *ces-1* promoter in some cases can be detected in the NSM but never in the NSM sister cell (J. Hatzold and B. Conradt, unpublished). This localization of CES-1::YFP suggests that CES-1 is localized asymmetrically to the NSM. CES-1 therefore might repress *egl-1* expression in the NSM resulting in its survival. However, since a *ces-1(lf)* mutation does not result in a phenotype, CES-1 is proposed to function redundantly with another factor (see below).

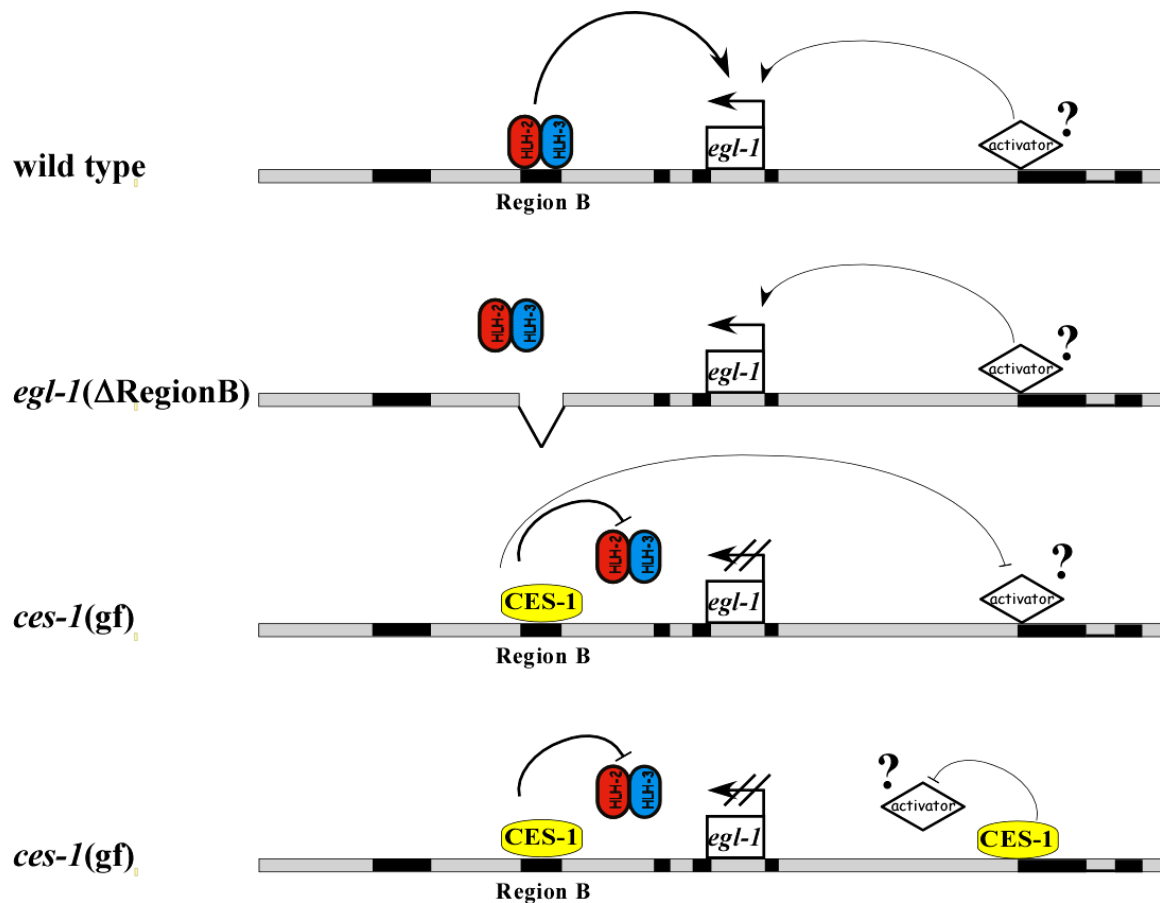


Figure 5-1 A HLH-2/HLH-3 heterodimer activates *egl-1* expression in the NSM sister cell through binding to the E-boxes in Region B.

In wild-type embryos, *egl-1* expression in the NSM sister cells is mainly activated by HLH-2/HLH-3 binding to the E-boxes in Region B of the *egl-1* locus. Additionally, an activator can activate *egl-1* expression through a regulatory region distinct from Region B.

In Region B deletion mutants, HLH-2/HLH-3 is not able to activate *egl-1* expression through binding to the E-boxes in Region B, resulting in survival of the NSM sister cells. Since *egl-1* expression can be activated partially by an additional activator functioning independent from Region B, the NSM sister cell survival phenotype is not completely penetrant.

In *ces-1*(gf) mutants, *egl-1* expression in the NSM sister cells is repressed by ectopic CES-1 occupying the E-boxes in Region B, thereby preventing HLH-2/HLH-3 from binding. CES-1 additionally represses the activity of the activator acting through a Region distinct from Region B, either by binding to a different site, or by binding to Region B.

5.3 A forward genetic screen resulted in the isolation of at least six new genes involved in the cell-death fate of NSM sister cells

Previous screens for mutations that cause the NSM sister cells to survive resulted in the identification of three different genes, *ces-1*, *ces-2*, and *ces-3* (Ellis and Horvitz, 1991). These screens failed to identify mutations in *hlh-2* and *hlh-3*. However, since *ces-2* and *ces-3* have so far only been defined by one *lf* allele each, these screens were not saturating. Moreover, *hlh-2(RNAi)* results in embryonic lethality. Thus only weak *lf* mutations in *hlh-2*, which do not result in lethality, can be isolated by screening viable animals. Weak mutations also are likely to cause only a weak NSM sister cell survival phenotype, decreasing the likelihood of isolating a *hlh-2* mutation.

Since a strong *lf* mutation in *hlh-3* results in a NSM sister cell survival phenotype with a very low penetrance, the likelihood of identifying *hlh-3* mutations by screening for animals with surviving NSM sister cells is accordingly low.

In this work, an additional screen for mutants was performed in a sensitized background. Only about 2000 haploid genomes were screened, however, 10 *ces* mutations were identified that resulted in an NSM sister cell survival phenotype. Compared to previous screens the number of isolated mutations appears rather high. For example, a screen performed in a wild-type background led to the identification of only three *ces* mutation when screening 9700 haploid genomes (Ellis and Horvitz, 1991). Several facts might account for the high efficiency of the *hlh-2* enhancer screen. First, since the screen was performed in an *hlh-2(bx108)* background, mutations were isolated that did not show a phenotype in an otherwise wild-type background. Second, the screening of the F3 generation, as opposed to screening the F2 generation as done before, allowed the identification of mutations that are maternally rescued. For example, the *bc212* homozygous progeny from heterozygous mothers does not exhibit a phenotype, and therefore, *bc212* would have been missed when screening the F2 generation. Screening the F3 generation also increased the probability of identifying mutations that result in an incomplete penetrant phenotype. In fact, eight out of ten isolated mutations exhibit a NSM sister cell survival phenotype of less than 50%.

At least six new genes involved in the NSM sister cell death were identified in this screen. Most of the mutations cause a low frequency of NSM sister cell survival. This fact either suggests that these mutations are hypomorphic alleles rather than null

alleles or that many genes that regulate the NSM sister cell death function at least partially redundantly. Several genes that regulate NSM sister cell survival appear to be involved in additional processes. For example, both *hlh-2* and *dnj-11* are essential genes, and loss of their function results in pleiotropic phenotypes. *bc212*, a mutation in *dnj-11* isolated in the *hlh-2* enhancer screen, is likely to be a hypomorphic allele. On the other hand, *hlh-3* is proposed to act redundantly, and a potential null mutation, *bc248*, only results in a weak phenotype. Therefore, it is very likely that some mutations isolated in the *hlh-2* enhancer screen affect redundant genes, whereas others are hypomorphic alleles. The cloning and characterization of these genes might elucidate new factors and mechanisms participating in the NSM sister cell death, such as direct or indirect regulators of *egl-1* expression or factors involved in establishing asymmetry in the NSM mother cell.

5.4 *dnj-11* might be required to establish asymmetry during the division of the NSM mother cell

bc212 was identified in the *hlh-2* enhancer screen as a mutation that caused the NSM sister cells to survive. I showed that *bc212* is a mutation in the gene *dnj-11*. *bc212* most likely diminishes but not completely abolishes *dnj-11* function, since *dnj-11(bc212)* mutants exhibit a milder phenotype than *dnj-11(RNAi)* mutants or *dnj-11(bc212)* animals *in trans* to a deficiency. *dnj-11* is required for the death of the NSM sister cells but additionally has functions in a variety of processes. Reducing the function of *dnj-11* by either RNAi or *bc212* can cause embryonic lethality, suggesting that *dnj-11* is an essential gene. Amongst other phenotypes, slow growth, morphological defects, and a small broodsize are observed in *dnj-11(bc212)* animals. In specifying the death of the NSM sister cells, *dnj-11* appears to function in establishing polarity in the NSM mother cell. As shown in this work, in wild-type animals, the NSM mother cell divides asymmetrically. The division generates two cells of different size, the larger NSM, which survives, and the smaller NSM sister cell, which dies. *dnj-11* is required for the asymmetric cell division: in some *dnj-11(bc212)* mutants, the division of the NSM mother cell results in two daughter cells of equal size. The phenotype of *dnj-11(bc212)* mutants is not completely penetrant, for example only 25% of the embryos die, and only 50% of the NSM sister

cells survive. Also the defect in the asymmetric cell division of the NSM mother cell is not seen in each individual, as only a fraction of embryos have a NSM mother cell that divides symmetrically. Interestingly, preliminary results suggest that symmetric divisions appear to correlate with the survival of the NSM sister cell (J. Hatzold and B. Conradt, unpublished). This correlation suggests that a symmetric cell division of the NSM mother cell causes the NSM sister cell to survive, and accordingly, that the size of the daughter cell determines its fate. Therefore, I propose that *dnj-11* is required for establishing asymmetry during the division of the NSM mother cell. Moreover, the asymmetry of the cell division, which results in the generation of a larger cell destined to survive and a smaller cell destined to die, determines the fate of the daughter cells.

5.5 CES-1 is involved in establishing asymmetry during the division of the NSM mother cell

However, the mechanism of how DNJ-11 functions to establish polarity in the NSM mother cell is currently rather unclear. It is likely that DNJ-11 functions indirectly. One reason is that, genetically, *dnj-11* negatively regulates the *snail*-like gene *ces-1* in the NSM sister cell death pathway, and altered *ces-1* function also impairs the asymmetric division of the NSM mother cell. In *ces-1(gf)* animals, in which *ces-1* is proposed to be upregulated, the NSM sister cell and the NSM are of equal size. This observation shed new light on our model of the mechanism that regulates the NSM sister cell death. So far, CES-1 was proposed to be able to act as a direct transcriptional repressor of *egl-1* in the NSM sister cell. However, *ces-1* might have a second, distinct function, which is in establishing polarity in the NSM mother cell. Evidence that Snail-like proteins function in asymmetric cell division, comes from studies in *Drosophila*. The loss of *snail* family genes has been shown to cause defects in the asymmetric division of neuroblasts. During the development of the *Drosophila* central nervous system (CNS), neuroblasts delaminate from the neuroectoderm. These neuroblasts are polarized and divide asymmetrically resulting in two daughter cells of different size. As the large apical daughter cell retains neuroblast identity, and repeatedly undergoes asymmetric divisions, these neuroblasts exhibit stem cell property. The small basal/lateral daughter cell, on the other hand, becomes the

ganglion mother cell (Lu et al., 2000). Mutants simultaneously lacking the function of three *snail* family genes, *snail*, *escargot*, and *worniu*, are severely defective in the neuroblast asymmetry (Cai et al., 2001). *sna/esg/wor*-deficient embryos have delayed and decreased expression of *inscutable* (*insc*), as well as Insc translation is inhibited. Insc is required for the correct localization of proteins and mRNA of cell fate determinants like Pros and Numb, and also required for the proper orientation of the spindle (Lu et al., 2000). It was suggested that Snail family proteins regulated Insc at the transcriptional level as well as at the translational level, and that this regulation most likely occurs indirectly. Consequently, the disruption of neuroblast polarity in *sna/esg/wor*-deficient embryos is caused by the lack of Insc. However, *insc* mutants display a less severe phenotype than *sna/esg/wor*-deficient mutants. Therefore, it has been proposed that the *snail* family of genes acts in two distinct pathways, a *insc*-dependent and an *insc*-independent pathway. A different study suggested that Snail, Esg, and Wor are required for both the expression of *insc* and the expression of *string*, a gene encoding a *cdc25* phosphatase, in the neuroblasts. Both pathways are necessary for the asymmetric cell division of these neuroblasts (Ashraf and Ip, 2001). Based on these studies in *Drosophila*, it is possible that *ces-1* function is required for establishing polarity in *C. elegans*. One can speculate that CES-1 has two distinct roles in the death of the NSM sister cells. First, it is likely that CES-1 can directly repress *egl-1* expression, as discussed above. Additionally, CES-1 might function already in the NSM mother cell. Possibly, CES-1 regulates genes that are required to establish polarity in the NSM mother cell, similar to Snail family proteins in *Drosophila*. Excess amounts of CES-1 caused by a *gf* mutation result in the failure of the NSM mother cell to divide unequally, whereas a similar phenotype is observed in *Drosophila* neuroblasts lacking the function of certain Snail family proteins. However, these phenotypes are not necessarily contradictory. Elevated levels of CES-1 might cause an upregulation of a factor functionally homologous to the *Drosophila* Insc, which is required for the proper localization of fate-determining factors to one side of the cell. Elevated levels of this factor can cause a disruption of the localization of these fate-determining factors, similar to a disruption caused by the lack of that factor. Therefore, loss-of-function as well as gain-of-function mutations in *snail*-like genes might cause a disruption of polarity, and consequently result in a symmetric cell division. A similar observation was made in a study investigating the role of *C. elegans dsh-2* (dishevelled) in asymmetric neuroblast division. Here, it was

shown that the loss as well as the overexpression of DSH-2 results in a defect in asymmetric cell division causing a duplication of PHA neurons (Hawkins et al., 2005).

A *lf* mutation in *ces-1(lf)* does not result in a NSM sister cell survival phenotype nor does it result in the inappropriate death of the NSM. It remains to be determined, however, whether in *ces-1(lf)* mutants the NSM mother cell still divides asymmetrically as in wild-type. It is very likely that CES-1 functions redundantly with other factors. As shown in *Drosophila*, eliminating the function of the *snail*-family genes *snail*, *wor*, or *esg* does not result in a polarity defect in neuroblasts, however, eliminating the function of all three genes simultaneously causes symmetric divisions (Ashraf and Ip, 2001; Cai et al., 2001). The *C. elegans* genome encodes three proteins belonging to the Snail superfamily of zinc finger transcription factors, which are CES-1, K02D7.2 and C55C2.1 (Nieto, 2002). However, in triple *lf* mutants the NSMs survive and the NSM sister cells die like in wild type. It remains to be tested whether the division of the NSM mother cell is asymmetric with respect to size in the triple *lf* mutant.

However, it also might be possible that CES-1 acts together with proteins of other families. A candidate is the Hairy-like bHLH transcription factor LIN-22, as it has been shown that the *Drosophila* orthologs of CES-1 and LIN-22, Scratch and Deadpan, act together. A null mutation in *scratch* results in a reduced number of photoreceptors in the eye, which is significantly enhanced in embryos lacking the function of both *scratch* and *deadpan*. *lf* mutations of *deadpan* alone, however, do not cause a significant phenotype, indicating that both genes act redundantly (Roark et al., 1995). A *ces-1; lin-22* double mutant most likely is embryonic lethal, which impedes the analysis of the role of *ces-1* and *lin-22* in the regulation of the NSM sister cell death.

5.6 DNJ-11 might establish asymmetry in the NSM mother cell by regulating CES-1 activity

CES-1 function in the NSM mother cell is likely to be regulated by *dnj-11*. It remains to be determined how this regulation is achieved. One possibility is that DNJ-11 directly regulates *ces-1* transcription. DNJ-11 is a member of the MIDA1 family of proteins, like the *Volvox carteri* GlsA. Like DNJ-11, GlsA has been shown to be

required for asymmetric cell division (Miller and Kirk, 1999), and GlsA interacts with Hsp70A to establish asymmetry (Cheng et al., 2005). It is not clear how GlsA and Hsp70A function in this process; however, they have been proposed not to act directly with the division apparatus. GlsA and Hsp70A have been shown to co-localize with histones during interphase. GlsA, like DNJ-11, has two C-terminal SANT domains, domains implicated in transcription and chromatin modification (Aasland et al., 1996). Therefore, it was suggested that GlsA, together with Hsp70A, regulates the expression of a gene required for the shift in the division plane by chromatin modifications. However, a function of the GlsA SANT domains has not been established so far, leaving the role of GlsA in gene regulation rather speculative. The mouse homolog MIDA1 has been shown to bind DNA, and also be able to stimulate the expression of reporter genes, and therefore was suggested to function as a transcriptional activator (Inoue et al., 1999; Inoue et al., 2000; Shoji et al., 1995; Yoshida et al., 2004). However, the physiological relevance of the MIDA1 function as a transcriptional stimulator remains elusive. Different studies have shown that a major role of members of the MIDA1 protein family in the cell is functioning with the translational apparatus. The yeast Zuotin and mammalian MPP11 have been shown to associate with ribosomes, and form the ribosome-associated complex (RAC) in conjunction with HSP70 proteins (Gautschi et al., 2001; Huang et al., 2005; Hundley et al., 2005; Otto et al., 2005). DNJ-11 primarily localizes to the cytoplasm, and therefore might function in translation, similar to its mammalian and yeast homologs. Thus, DNJ-11 might regulate CES-1 at the translational level. It remains to be determined if *ces-1* mRNA or CES-1 protein levels are altered in *dnj-11(bc212)* mutants, which can be done for example by analyzing transcriptional and translational reporters.

The following model provides a proposal of how DNJ-11 and CES-1 could contribute to the asymmetric division of the NSM mother cell, and the subsequent cell death of the NSM sister cell. In the wild type NSM mother cell, DNJ-11 is required to keep CES-1 levels low by a mechanism not yet known. DNJ-11 might function directly or indirectly, and either transcriptionally, translationally, or post-translationally. However, enough CES-1 is present to promote a so far unknown polarity-determining factor, most likely indirectly through transcriptional regulation. This factor establishes polarity in the NSM mother cell by inducing a shift of the division plane, and by the

asymmetric localization of cell-fate determinants such as CES-1 (Figure 5-2). The shift in the division plane results in an asymmetric cell division generating two daughter cells of unequal size (Figure 5-3). CES-1 preferentially gets distributed to the larger NSM. Here, it binds to the *egl-1* locus preventing the activator HLH-2/HLH-3 from activating *egl-1* transcription. As a consequence, *egl-1* transcription is kept off and the NSM survives.

In *dnj-11* mutant animals, as well as in *ces-1(gf)* mutants, elevated CES-1 levels are present in the NSM mother cell. Elevated CES-1 levels cause an excess amount of the polarity-determining factor, resulting in the abolishment of polarity. As a result, the NSM mother cell divides equally, and CES-1 gets distributed to both daughter cells. CES-1 therefore can prevent HLH-2/HLH-3 from binding to the *egl-1* locus in both daughter cells resulting in the repression of *egl-1* expression. Consequently, the NSM and the NSM sister cell survive.

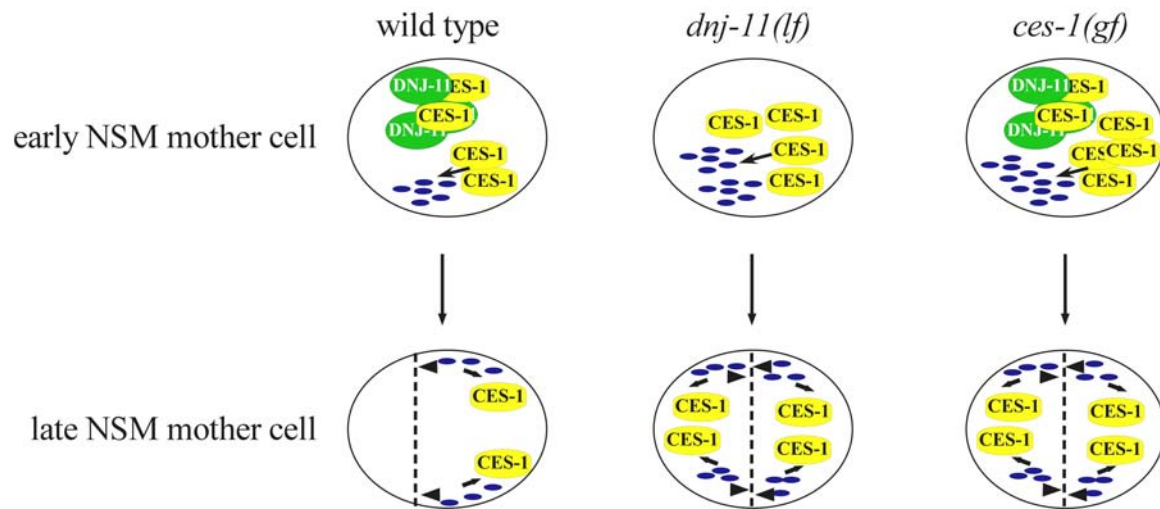


Figure 5-2 DNJ-11 and CES-1 are required to establish polarity in the NSM mother cell.

In the early NSM mother cell in wild-type embryos, DNJ-11 represses the generation of active CES-1 by an yet unknown mechanism. CES-1 levels therefore are low in the NSM mother cell. CES-1 is required for the activity of the polarity-determining factor X (blue), probably in a indirect way acting through transcriptional control. Factor X establishes polarity in the late NSM mother cell by localizing CES-1 to one side (indicated by black arrows) and by shifting the division plane (indicated by arrowheads).

In *dnj-11(lf)* embryos, the lack of DNJ-11 activity results in elevated levels of active CES-1. Consequently, ectopic amounts of factor X are generated. An imbalance of Factor X results in disruption of polarity as the correct localization of CES-1 is disturbed and the division plane is not correctly shifted. A similar phenotype is observed in *ces-1(gf)* embryos.

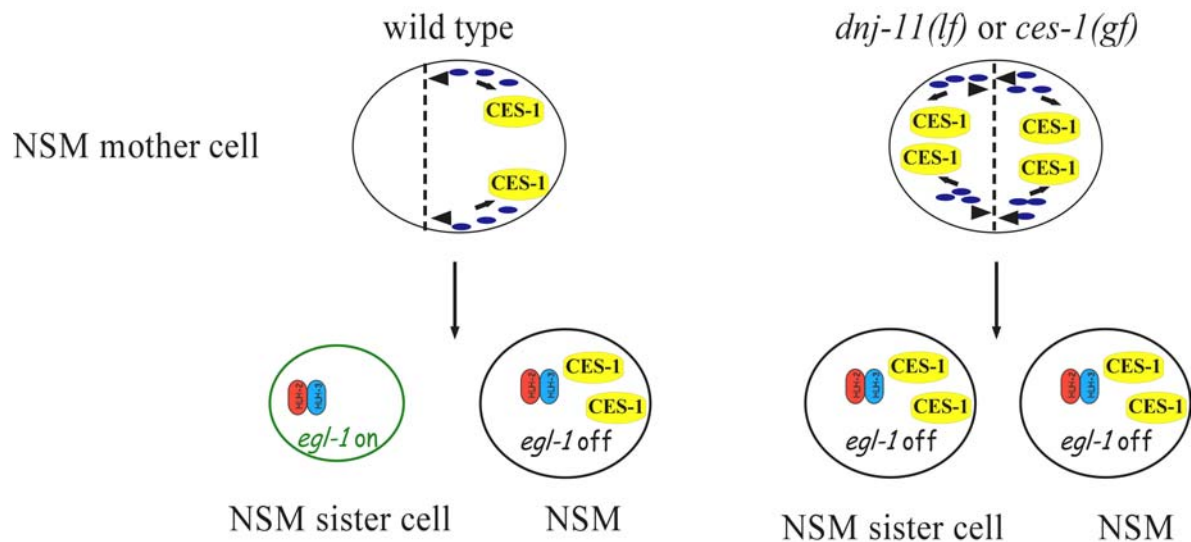


Figure 5-3 The polarization of the NSM mother cell mediated by DNJ-11 and CES-1 results in the generation of two daughter cells of different fate.

In wild-type embryos, the NSM mother cell is polarized, which results in the asymmetric localization of CES-1 and a shift in the division plane (see Figure 5-2). The division of the NSM mother cell results in the generation of a larger and a smaller daughter cell. The larger cell, the NSM, inherits higher amounts of CES-1, which prevents HLH-2/HLH-3 from activating *egl-1* expression. As a consequence, the NSM survives. Since CES-1 does not get distributed to the smaller cell, the NSM sister cell, HLH-2/HLH-3 activates *egl-1* expression, resulting in programmed cell death.

As polarity of the NSM mother cell is disrupted in *dnj-11(lf)* and *ces-1(gf)* mutant embryos (see Figure 5-2), a symmetric division generates two daughter cells of equal size. Elevated amounts of CES-1 get distributed to both the NSM and the NSM sister cell, preventing HLH-2/HLH-3 from activating *egl-1* expression and therefore resulting in the survival of both NSM and NSM sister cell.

6 References

- Aasland, R., Stewart, A. F., and Gibson, T. (1996). The SANT domain: a putative DNA-binding domain in the SWI-SNF and ADA complexes, the transcriptional co-repressor N-CoR and TFIIB. *Trends Biochem Sci* *21*, 87-88.
- Altschul, S. F., Madden, T. L., Schaffer, A. A., Zhang, J., Zhang, Z., Miller, W., and Lipman, D. J. (1997). Gapped BLAST and PSI-BLAST: a new generation of protein database search programs. *Nucleic Acids Res* *25*, 3389-3402.
- Ashraf, S. I., and Ip, Y. T. (2001). The Snail protein family regulates neuroblast expression of *inscuteable* and *string*, genes involved in asymmetry and cell division in *Drosophila*. *Development* *128*, 4757-4767.
- Boyer, L. A., Langer, M. R., Crowley, K. A., Tan, S., Denu, J. M., and Peterson, C. L. (2002). Essential role for the SANT domain in the functioning of multiple chromatin remodeling enzymes. *Mol Cell* *10*, 935-942.
- Brenner, S. (1974). The Genetics of *Caenorhabditis elegans*. *Genetics* *77*, 71-94.
- Broverman, S. A., and Meneely, P. M. (1994). Meiotic Mutants That Cause a Polar Decrease in Recombination on the X Chromosome in *Caenorhabditis elegans*. *Genetics* *136*, 119-127.
- Cai, Y., Chia, W., and Yang, X. (2001). A family of snail-related zinc finger proteins regulates two distinct and parallel mechanisms that mediate *Drosophila* neuroblast asymmetric divisions. *Embo J* *20*, 1704-1714.
- Chen, F., Hersh, B. M., Conradt, B., Zhou, Z., Riemer, D., Gruenbaum, Y., and Horvitz, H. R. (2000). Translocation of *C. elegans* CED-4 to nuclear membranes during programmed cell death. *Science* *287*, 1485-1489.
- Cheng, Q., Pappas, V., Hallmann, A., and Miller, S. M. (2005). Hsp70A and GlsA interact as partner chaperones to regulate asymmetric division in *Volvox*. *Dev Biol* *286*, 537-548.
- Conradt, B., and Horvitz, H. R. (1998). The *C. elegans* protein EGL-1 is required for programmed cell death and interacts with the Bcl-2-like protein CED-9. *Cell* *93*, 519-529.
- Conradt, B., and Horvitz, H. R. (1999). The TRA-1A sex determination protein of *C. elegans* regulates sexually dimorphic cell deaths by repressing the *egl-1* cell death activator gene [see comments]. *Cell* *98*, 317-327.
- Cyr, D. M., Langer, T., and Douglas, M. G. (1994). DnaJ-like proteins: molecular chaperones and specific regulators of Hsp70. *Trends Biochem Sci* *19*, 176-181.
- del Peso, L., Gonzalez, V. M., and Nunez, G. (1998). *Caenorhabditis elegans* EGL-1 disrupts the interaction of CED-9 with CED-4 and promotes CED-3 activation. *J Biol Chem* *273*, 33495-33500.

- Ellis, H. M., and Horvitz, H. R. (1986). Genetic Control of Programmed Cell Death in the Nematode *C. elegans*. *Cell* 44, 817-826.
- Ellis, R. E., and Horvitz, H. R. (1991). Two *C. elegans* genes control the programmed deaths of specific cells in the pharynx. *Development* 112, 591-603.
- Frank, C. A., Baum, P. D., and Garriga, G. (2003). HLH-14 is a *C. elegans* Achaete-Scute protein that promotes neurogenesis through asymmetric cell division. *Development* 130, 6507-6518.
- Fuse, N., Hirose, S., and Hayashi, S. (1994). Diploidy of *Drosophila* imaginal cells is maintained by a transcriptional repressor encoded by *escargot*. *Genes Dev* 8, 2270-2281.
- Gautschi, M., Lilie, H., Funfschilling, U., Mun, A., Ross, S., Lithgow, T., Rucknagel, P., and Rospert, S. (2001). RAC, a stable ribosome-associated complex in yeast formed by the DnaK-DnaJ homologs Ssz1p and zuotin. *Proc Natl Acad Sci U S A* 98, 3762-3767.
- Goodwin, E. B., and Ellis, R. E. (2002). Turning clustering loops: sex determination in *Caenorhabditis elegans*. *Curr Biol* 12, R111-120.
- Han, J., Flemington, C., Houghton, A. B., Gu, Z., Zambetti, G. P., Lutz, R. J., Zhu, L., and Chittenden, T. (2001). Expression of *bbc3*, a pro-apoptotic BH3-only gene, is regulated by diverse cell death and survival signals. *Proc Natl Acad Sci U S A* 98, 11318-11323.
- Hanahan, D. (1985). Techniques for transforming *E. coli*.
- Harris, C. A., and Johnson, E. M., Jr. (2001). BH3-only Bcl-2 family members are coordinately regulated by the JNK pathway and require Bax to induce apoptosis in neurons. *J Biol Chem* 276, 37754-37760.
- Hassan, B. A., and Bellen, H. J. (2000). Doing the MATH: is the mouse a good model for fly development? *Genes Dev* 14, 1852-1865.
- Hatzold, J. (2001) Untersuchungen zur Zelltodregulation in den NSMs und den NSM-Schwesterzellen im Nervensystem von *C. elegans*, TU München, München.
- Hawkins, N. C., Ellis, G. C., Bowerman, B., and Garriga, G. (2005). MOM-5 frizzled regulates the distribution of DSH-2 to control *C. elegans* asymmetric neuroblast divisions. *Dev Biol* 284, 246-259.
- Hemavathy, K., Ashraf, S. I., and Ip, Y. T. (2000). Snail/slug family of repressors: slowly going into the fast lane of development and cancer. *Gene* 257, 1-12.
- Hengartner, M. O., Ellis, R. E., and Horvitz, H. R. (1992). *Caenorhabditis elegans* gene *ced-9* protects cells from programmed cell death. *Nature* 356, 494-499.
- Heschl, M. F., and Baillie, D. L. (1990). Functional elements and domains inferred from sequence comparisons of a heat shock gene in two nematodes. *J Mol Evol* 31, 3-9.

- Horvitz, H. R. (1999). Genetic control of programmed cell death in the nematode *Caenorhabditis elegans*. *Cancer Res* 59, 1701s-1706s.
- Huang, P., Gautschi, M., Walter, W., Rospert, S., and Craig, E. A. (2005). The Hsp70 Ssz1 modulates the function of the ribosome-associated J-protein Zuo1. *Nat Struct Mol Biol* 12, 497-504.
- Hundley, H. A., Walter, W., Bairstow, S., and Craig, E. A. (2005). Human Mpp11 J protein: ribosome-tethered molecular chaperones are ubiquitous. *Science* 308, 1032-1034.
- Inoue, T., Shoji, W., and Obinata, M. (1999). MIDA1, an Id-associating protein, has two distinct DNA binding activities that are converted by the association with Id1: a novel function of Id protein. *Biochem Biophys Res Commun* 266, 147-151.
- Inoue, T., Shoji, W., and Obinata, M. (2000). MIDA1 is a sequence specific DNA binding protein with novel DNA binding properties. *Genes Cells* 5, 699-709.
- Jagasia, R., Grote, P., Westermann, B., and Conradt, B. (2005). DRP-1-mediated mitochondrial fragmentation during EGL-1-induced cell death in *C. elegans*. *Nature* 433, 754-760.
- Jakubowski, J., and Kornfeld, K. (1999). A local, high-density, single-nucleotide polymorphism map used to clone *Caenorhabditis elegans* *cdf-1*. *Genetics* 153, 743-752.
- Jansen, G., Hazendonk, E., Thijssen, K. L., and Plasterk, R. H. A. (1997). Reverse genetics by chemical mutagenesis in *Caenorhabditis elegans*. *Nat Genetics* 17, 119-121.
- Kataoka, H., Murayama, T., Yokode, M., Mori, S., Sano, H., Ozaki, H., Yokota, Y., Nishikawa, S., and Kita, T. (2000). A novel snail-related transcription factor Smuc regulates basic helix- loop-helix transcription factor activities via specific E-box motifs. *Nucleic Acids Res* 28, 626-633.
- Kelley, W. L. (1999). Molecular chaperones: How J domains turn on Hsp70s. *Curr Biol* 9, R305-308.
- Kirk, M. M., Ransick, A., McRae, S. E., and Kirk, D. L. (1993). The relationship between cell size and cell fate in *Volvox carteri*. *J Cell Biol* 123, 191-208.
- Koch, R., van Luenen, H. G., van der Horst, M., Thijssen, K. L., and Plasterk, R. H. (2000). Single nucleotide polymorphisms in wild isolates of *Caenorhabditis elegans*. *Genome Res* 10, 1690-1696.
- Krause, M., Park, M., Zhang, J. M., Yuan, J., Harfe, B., Xu, S. Q., Greenwald, I., Cole, M., Paterson, B., and Fire, A. (1997). A *C. elegans* E/Daughterless bHLH protein marks neuronal but not striated muscle development. *Development* 124, 2179-2189.
- Kroczyńska, B., Evangelista, C. M., Samant, S. S., Elguindi, E. C., and Blond, S. Y. (2004). The SANT2 domain of the murine tumor cell DnaJ-like protein 1 human

- homologue interacts with alpha1-antichymotrypsin and kinetically interferes with its serpin inhibitory activity. *J Biol Chem* 279, 11432-11443.
- Lee, J. E. (1997). Basic helix-loop-helix genes in neural development. *Curr Opin Neurobiol* 7, 13-20.
- Lu, B., Jan, L., and Jan, Y. N. (2000). Control of cell divisions in the nervous system: symmetry and asymmetry. *Annu Rev Neurosci* 23, 531-556.
- Massari, M. E., and Murre, C. (2000). Helix-loop-helix proteins: regulators of transcription in eucaryotic organisms. *Mol Cell Biol* 20, 429-440.
- Matsumoto-Taniura, N., Pirollet, F., Monroe, R., Gerace, L., and Westendorf, J. M. (1996). Identification of novel M phase phosphoproteins by expression cloning. *Mol Biol Cell* 7, 1455-1469.
- Mello, C., and Fire, A. (1995). DNA transformation. *Methods Cell Biol* 48, 451-482.
- Metzstein, M. M., Hengartner, M. O., Tsung, N., Ellis, R. E., and Horvitz, H. R. (1996). Transcriptional regulator of programmed cell death encoded by *Caenorhabditis elegans* gene *ces-2*. *Nature* 382, 545-547.
- Metzstein, M. M., and Horvitz, H. R. (1999). The *C. elegans* cell death specification gene *ces-1* encodes a snail family zinc finger protein. *Mol Cell* 4, 309-319.
- Miller, S. M., and Kirk, D. L. (1999). *glsA*, a *Volvox* gene required for asymmetric division and germ cell specification, encodes a chaperone-like protein. *Development* 126, 649-658.
- Nakano, K., and Vousden, K. H. (2001). PUMA, a novel proapoptotic gene, is induced by p53. *Mol Cell* 7, 683-694.
- Nakayama, H., Scott, I. C., and Cross, J. C. (1998). The transition to endoreduplication in trophoblast giant cells is regulated by the mSNA zinc finger transcription factor. *Dev Biol* 199, 150-163.
- Nieto, M. A. (2002). The snail superfamily of zinc-finger transcription factors. *Nat Rev Mol Cell Biol* 3, 155-166.
- Norton, J. D., Deed, R. W., Craggs, G., and Sablitzky, F. (1998). Id helix-loop-helix proteins in cell growth and differentiation. *Trends Cell Biol* 8, 58-65.
- Oda, E., Ohki, R., Murasawa, H., Nemoto, J., Shibue, T., Yamashita, T., Tokino, T., Taniguchi, T., and Tanaka, N. (2000). Noxa, a BH3-only member of the Bcl-2 family and candidate mediator of p53-induced apoptosis. *Science* 288, 1053-1058.
- Oh, I. H., and Reddy, E. P. (1999). The myb gene family in cell growth, differentiation and apoptosis. *Oncogene* 18, 3017-3033.
- Oppenheim, R. W. (1991). Cell death during development of the nervous system. *Annu Rev Neurosci* 14, 453-501.

- Otto, H., Conz, C., Maier, P., Wolfle, T., Suzuki, C. K., Jenö, P., Rucknagel, P., Stahl, J., and Rospert, S. (2005). The chaperones MPP11 and Hsp70L1 form the mammalian ribosome-associated complex. *Proc Natl Acad Sci U S A* *102*, 10064-10069.
- Parrish, J., Metters, H., Chen, L., and Xue, D. (2000). Demonstration of the in vivo interaction of key cell death regulators by structure-based design of second-site suppressors. *Proc Natl Acad Sci U S A* *97*, 11916-11921.
- Piano, F., Schetter, A. J., Morton, D. G., Gunsalus, K. C., Reinke, V., Kim, S. K., and Kempthues, K. J. (2002). Gene clustering based on RNAi phenotypes of ovary-enriched genes in *C. elegans*. *Curr Biol* *12*, 1959-1964.
- Portman, D. S., and Emmons, S. W. (2000). The basic helix-loop-helix transcription factors LIN-32 and HLH-2 function together in multiple steps of a *C. elegans* neuronal sublineage. *Development* *127*, 5415-5426.
- Putcha, G. V., Moulder, K. L., Golden, J. P., Bouillet, P., Adams, J. A., Strasser, A., and Johnson, E. M. (2001). Induction of BIM, a proapoptotic BH3-only BCL-2 family member, is critical for neuronal apoptosis. *Neuron* *29*, 615-628.
- Puthalakath, H., and Strasser, A. (2002). Keeping killers on a tight leash: transcriptional and post-translational control of the pro-apoptotic activity of BH3-only proteins. *Cell Death Differ* *9*, 505-512.
- Reddien, P. W., Cameron, S., and Horvitz, H. R. (2001). Phagocytosis promotes programmed cell death in *C. elegans*. *Nature* *412*, 198-202.
- Riddle, D. L., Blumenthal, T., Meyer, B., and Priess, J. R., eds. (1997). *C. elegans II* (Cold Spring Harbor Laboratory Press).
- Roark, M., Sturtevant, M. A., Emery, J., Vaessin, H., Grell, E., and Bier, E. (1995). *scratch*, a pan-neural gene encoding a zinc finger protein related to *snail*, promotes neuronal development. *Genes Dev* *9*, 2384-2398.
- Saikumar, P., Murali, R., and Reddy, E. P. (1990). Role of tryptophan repeats and flanking amino acids in Myb-DNA interactions. *Proc Natl Acad Sci U S A* *87*, 8452-8456.
- Sambrook, J., Fritsch, E. F., and Maniatis, T. (1989). *Molecular cloning. A laboratory manual, Second Edition* edn (New York, Cold Spring Harbor Laboratory, Cold Spring Harbor, NY).
- Sell, S. M., Eisen, C., Ang, D., Zylicz, M., and Georgopoulos, C. (1990). Isolation and characterization of dnaJ null mutants of *Escherichia coli*. *J Bacteriol* *172*, 4827-4835.
- Shoji, W., Inoue, T., Yamamoto, T., and Obinata, M. (1995). MIDA1, a protein associated with Id, regulates cell growth. *J Biol Chem* *270*, 24818-24825.
- Simmer, F., Tijsterman, M., Parrish, S., Koushika, S., Nonet, M., Fire, A., Ahringer, J., and Plasterk, R. (2002). Loss of the Putative RNA-Directed RNA Polymerase RRF-3 Makes *C. elegans* Hypersensitive to RNAi. *Curr Biol* *12*, 1317.

- Sulston, J. E., and Horvitz, H. R. (1977). Post-embryonic cell lineages of the nematode, *Caenorhabditis elegans*. *Dev Biol* 56, 110-156.
- Sulston, J. E., Schierenberg, E., White, J. G., and Thomson, J. N. (1983). The Embryonic Cell Lineage of the Nematode *Caenorhabditis elegans*. *Dev Biol* 100, 64-119.
- Sze, J. Y., Victor, M., Loer, C., Shi, Y., and Ruvkun, G. (2000). Food and metabolic signalling defects in a *Caenorhabditis elegans* serotonin-synthesis mutant. *Nature* 403, 560-564.
- Thellmann, M. (2002) Regulation von Programmierterem Zelltod in den NSM-Schwesterzellen im Nervensystem von *Caenorhabditis elegans*, Muenchen.
- Thellmann, M., Hatzold, J., and Conradt, B. (2003). The Snail-like CES-1 protein of *C. elegans* can block the expression of the BH3-only cell-death activator gene *egl-1* by antagonizing the function of bHLH proteins. *Development* 130, 4057-4071.
- Thompson, C. B. (1995). Apoptosis in the pathogenesis and treatment of disease. *Science* 267, 1456-1462.
- Timmons, L., Court, D. L., and Fire, A. (2001). Ingestion of bacterially expressed dsRNAs can produce specific and potent genetic interference in *Caenorhabditis elegans*. *Gene* 263, 103-112.
- Timmons, L., and Fire, A. (1998). Specific interference by ingested dsRNA. *Nature* 395, 854.
- Tsai, J., and Douglas, M. G. (1996). A conserved HPD sequence of the J-domain is necessary for YDJ1 stimulation of Hsp70 ATPase activity at a site distinct from substrate binding. *J Biol Chem* 271, 9347-9354.
- Vaux, D. L. (1993). Toward an understanding of the molecular mechanisms of physiological cell death. *Proc Natl Acad Sci U S A* 90, 786-789.
- Walsh, P., Bursac, D., Law, Y. C., Cyr, D., and Lithgow, T. (2004). The J-protein family: modulating protein assembly, disassembly and translocation. *EMBO Rep* 5, 567-571.
- Whitfield, J., Neame, S. J., Paquet, L., Bernard, O., and Ham, J. (2001). Dominant-negative c-Jun promotes neuronal survival by reducing BIM expression and inhibiting mitochondrial cytochrome c release. *Neuron* 29, 629-643.
- Wicks, S. R., Yeh, R. T., Gish, W. R., Waterston, R. H., and Plasterk, R. H. (2001). Rapid gene mapping in *Caenorhabditis elegans* using a high density polymorphism map. *Nat Genet* 28, 160-164.
- Wood, W. B. (1988). The nematode *C. elegans*, Cold Spring Harbor Laboratory, Cold Spring Harbor, NY).

- Wrischnik, L. A., and Kenyon, C. J. (1997). The role of *lin-22*, a hairy/Enhancer of split homolog, in patterning the peripheral nervous system of *C. elegans*. *Development* *124*, 2875-2888.
- Yan, N., Gu, L., Kokel, D., Chai, J., Li, W., Han, A., Chen, L., Xue, D., and Shi, Y. (2004). Structural, biochemical, and functional analyses of CED-9 recognition by the proapoptotic proteins EGL-1 and CED-4. *Mol Cell* *15*, 999-1006.
- Yoshida, M., Inoue, T., Shoji, W., Ikawa, S., and Obinata, M. (2004). Reporter gene stimulation by MIDA1 through its DnaJ homology region. *Biochem Biophys Res Commun* *324*, 326-332.
- Yu, J., Zhang, L., Hwang, P. M., Kinzler, K. W., and Vogelstein, B. (2001). PUMA induces the rapid apoptosis of colorectal cancer cells. *Mol Cell* *7*, 673-682.
- Zhang, S., Lockshin, C., Herbert, A., Winter, E., and Rich, A. (1992). Zuotin, a putative Z-DNA binding protein in *Saccharomyces cerevisiae*. *Embo J* *11*, 3787-3796.

Abbreviations

Amp	Ampicillin
Apaf	apoptotic protease-activating factor
AS	Achaete-Scute
Bcl	B cell lymphoma
BH3	Bcl-2 Homology region 3
bHLH	basic helix-loop-helix
bp	base pair
bZIP	basic leucine zipper
<i>C. briggsae</i>	<i>Caenorhabditis briggsae</i>
<i>C. elegans</i>	<i>Caenorhabditis elegans</i>
Ced	cell-death defective
Ces	cell death specification
cs	cold sensitive
DIC	Differential Interference Contrast
Dpy	Dumpy
Drp	dynamain-related protein
dsRNA	double strand RNA
<i>E. coli</i>	<i>Escherichia coli</i>
Egl	egg-laying defective
EMS	ethyl methanesulfonate
EMSA	electro mobility shift assay
gf	gain-of-function
GFP	green fluorescence protein
Him	high incidence of males
HSN	hermaphrodite-specific neuron
kb	kilo base pair
lf	loss-of-function
Lin	lineage abnormal
Lon	long
m.u	map units
Muv	multi vulvae
NSM	neurosecretory motoneurons
PCR	polymerase chain reaction
RAC	ribosome-associated complex
RNAi	RNA-mediated interference
Rol	roller
RT	room temperature
stdev	standard deviation
Tra	transformer
ts	temperature sensitive
Unc	uncoordinated

Acknowledgements

First of all, I want to thank Dr. Barbara Conradt for giving me the opportunity to do my PhD thesis work in her lab on this very exciting project. I want to thank you for the great supervision, the support, the trust, and the inspiration, from which I learned a lot, and which made me enjoy science.

I am very grateful to Prof. Dr. Charles David for being my supervisor, and with that making it possible for me to pursue my thesis in Dr. Conradt's lab.

I want to thank all past and current lab members for creating an excellent work atmosphere, where I found all sorts of help, support, motivation, and above all, friends. Special thanks go to Marion Thellmann, who help me a lot in the initial phase of this work, for all the discussions about this project, and also for becoming a really good friend. Many thanks go to Cornelia Schmutz, Franziska Boettger, and Elke Stenvers for their helping hands with this project. I want to thank Phillip Grote especially for his never-ending willingness to discuss anything and to help with anything. I also want to thank him and Claudia Huber and Tatiana Tomasi for making me feel home when I first arrived to the lab in Hanover. Many thanks go also to Ralda Nehme, for her never-ending willingness to listen, and, not at least, for carrying on this project.

Many thanks go to all my friends also outside the lab, who gave me trust, patience, and support during those years, with very special thanks to Marcus Steiner. I want to thank especially my parents, who always supported me in my plans, and who help me a lot in this final phase of my thesis.

Erklärung

Hiermit versichere ich, Julia Hatzold, geboren am 11. August 1976 in München, dass ich die vorliegende Arbeit selbständig verfasst und keine anderen als die angegebenen Quellen und Hilfsmittel verwendet habe.

München, 21. April 2006